NATIONAL ADVISORY COMMITTEE FOR AERONAUTICS

TECHNICAL NOTE 2503

HYDRODYNAMIC INVESTIGATION OF A SERIES OF HULL MODELS SUITABLE FOR SMALL FLYING BOATS AND AMPHIBIANS

By W. C. Hugli, Jr., and W. C. Axt

Stevens Institute of Technology

Washington

November 1951

NATIONAL ADVISORY COMMITTEE FOR AERONAUTICS

TECHNICAL NOTE 2503

HYDRODYNAMIC INVESTIGATION OF A SERIES OF HULL MODELS SUITABLE FOR SMALL FLYING BOATS AND AMPHIBIANS

By W. C. Hugli, Jr., and W. C. Axt

SUMMARY

This report presents the results of an investigation made at the Experimental Towing Tank, Stevens Institute of Technology, to obtain hydrodynamic information on a series of hull models suitable for small flying boats or amphibians of from 2000 to 5000 pounds gross weight. The series of hulls consisted of a basic hull with simple lines, and of plus and minus variations to this design in which the beam, sternpost angle, and afterbody length were altered. Modifications were also investigated to determine the advantage of refining the hull lines.

The hulls were tested for hydrodynamic resistance and main spray. On the basis of these characteristics, the best beam and sternpost angle were selected for each of the three afterbody lengths investigated. The resulting three hulls were further tested for landing and porpoising characteristics.

The results show that it is possible to design a hull with simple lines that will be suitable for small flying boats or amphibians. Refining the hull lines will improve the hydrodynamic characteristics slightly but will also increase the construction cost.

INTRODUCTION

In recent years, the extensive development activity in flying boats has been directed toward large military designs almost to the exclusion of work on design problems peculiar to small flying boats in the personal-owner class. The last comprehensive work on small flying boats was that undertaken by the National Advisory Committee for Aeronautics in 1934 on the model 40 series (reference 1). The significant advances in hydrodynamic research since that time made it appear timely to make a new and more detailed investigation of a series of hull models suitable for small flying boats and amphibians ranging from 2000 to 5000 pounds in gross weight. Such an investigation was carried out at the Experimental

Towing Tank, Stevens Institute of Technology, under the sponsorship and with the financial assistance of the National Advisory Committee for Aeronautics.

The hull design problems of large flying boats are different from those of small flying boats. The larger hulls, generally having lower power loadings and lower take-off-speed coefficients, are less sensitive to the hydrodynamic resistance characteristics than the smaller hulls. Furthermore, while it is feasible to incorporate into the lines of the larger hulls such refinements as chine flare and dead-rise warping, the lines of the smaller hulls must be as simple as possible in order to keep construction costs within reasonable limits.

In an investigation such as this, where the goal of satisfactory hydrodynamic characteristics must be attained with a simple form, the hull design on which the study is based greatly influences the ultimate value of the work. To this end, the basic hull used in this investigation was designed with simple lines on the basis of previous model tests and general experience. The series of hulls consisted of the basic hull and of variations to this design in which the hull width, afterbody length, and angle between forebody and afterbody were altered. In order to determine the possible advantages to be gained by refining the hull lines, two alterations to the forebody and one alteration to the afterbody of the basic hull were tested.

The investigation was carried out in four phases. First, brief tests were made to determine a longitudinal position of the center of gravity which could be used for all of the hulls. Second, because of the importance of resistance and main spray with respect to small flying boats, these characteristics were determined for all hulls. Third, on the basis of these tests, the best beam and sternpost angle for each afterbody length were selected. The resulting three hulls, each of different afterbody length, were then tested for landing and longitudinal stability. Finally, forebody and afterbody modifications were investigated to determine their advantages, if any, over the simplified hull lines.

DEFINITIONS AND SYMBOLS

The terms and symbols used in this report are defined as follows:

C_{Δ} load coefficient $\left(\Delta/wb^3\right)$

C_V speed coefficient $\left(V/\sqrt{gb}\right)$

C_R	resistance coefficient $\left(R/wb^3\right)$
C_D	air-drag coefficient $\left(D/\frac{1}{2}\rho_a AV^2\right)$
C_M	trimming-moment coefficient $\left(M/wb^4\right)$
C_X	longitudinal-spray coefficient $\left(X/b\right)$
C_Z	vertical-spray coefficient $\left(Z/b\right)$
C_L	lift coefficient
L_f/b	ratio of forebody length to beam
L_a/b	ratio of afterbody length to beam
k/L	pitching "gyradius" constant
$M_q/V\frac{1}{2}\rho_w b^4$	aerodynamic pitch-damping constant
Δ	load on water, pounds
w	specific weight of water; 62.3 pounds per cubic foot
b	maximum beam of hull at chine, feet
V	speed, feet per second
g	acceleration due to gravity; 32.2 feet per second per second
R	resistance, pounds
D	air drag, pounds
A	maximum cross-sectional area of model, square feet; 0.186 square feet for models with 6-inch beam
ρ_a	mass density of air, pound-seconds squared per foot^4
ρ_w	mass density of water, pound-seconds squared per foot^4

M	trimming moment, pounds
X	longitudinal position of main-spray point of tangency, measured fore (positive) or aft (negative) of the step, feet
Z	vertical position of main-spray point of tangency, measured from tangent to forebody keel at main step, feet
L_f	forebody length, measured from intersection of chine and keel to step along a line parallel to tangent to forebody keel at main step, feet
L_a	afterbody length, measured from step to sternpost, feet
L	total length, forebody plus afterbody, feet
k	pitching radius of gyration, feet
M_q	aerodynamic tail-damping derivative (see section entitled "Apparatus and Procedure" for complete definition)
s	full scale, used as a subscript
m	model, used as a subscript
h	step height at main step, percent of maximum beam
σ	sternpost angle, angle between tangent to forebody keel at main step and line joining tip of step and the sternpost, degrees
β_f	forebody dead rise at keel and main step, degrees
τ	trim, angle between tangent to forebody keel at main step and free-water surface

Moment data are referred to the center of gravity, and water trimming moments which tend to raise the bow are considered positive. The coordinates of the center of gravity are measured above the tangent to the forebody keel at the main step and forward of a plane perpendicular to the keel and passing through the step.

The following combinations of the coefficients defined above are used:

Coefficient	Symbol	Taken from reference -
Planing range		
Lift	$\sqrt{C_\Delta}/C_V$	2
Resistance	$\sqrt{C_R}/C_V$	3
Displacement range		
Speed	$C_V{}^2/C_\Delta{}^{1/3}$	3
Resistance	$C_R/C_V{}^2C_\Delta{}^{2/3}$	3
Longitudinal spray	$C_X/C_\Delta{}^{1/3}$	4
Vertical spray	C_Z/C_Δ	4

The numerical designation of each model (shown on the summary charts) describes the principal hull proportions. Thus, if a model has the designation

3.25 - 1.04 - 20

it means that $L_f/b = 3.25$, $h/\sigma = 1.04$, and $\beta_f = 20$. The basis for this numerical model designation is explained in reference 5.

DESCRIPTION OF MODELS

Over-All Design

This investigation was undertaken to provide design information on hulls for amphibians of from 2000 to 5000 pounds gross weight. By making hydrodynamic tests over sufficiently wide ranges of get-away speed and

loading, it was feasible to form the series around a single prototype having an intermediate gross weight of 3000 pounds. The general proportions for a hull of this size were based to some extent on published design information given in reference 6. Hull dimensions of various small amphibians, scaled to a gross weight of 3000 pounds, are given in table I. On the basis of modern trends, a forebody length of 156 inches was chosen in preference to the average value given in table I. The normal beam was selected as 48 inches, with alternate values of 42 and 54 inches.

Afterbodies of varying length were included in the investigation. The values of tail length given in table I were used as a guide in selecting the longest length of afterbody which was 216 inches. The shortest afterbody length of 108 inches was selected as comparable with that used in previous designs. The normal afterbody length for the series was taken halfway between the long and short afterbody lengths. Consequently, as will be noted in the tabulation of main dimensions below, the basic hull of the family has an afterbody length somewhat greater than the average of afterbody lengths obtained from table I.

The following full-size prototype main dimensions were incorporated in the basic hull. The average design dimensions obtained from table I are also presented for comparison.

Dimension	Basic hull E.T.T. model 1024-01	Average given in table I
Gross weight, pounds	3000	3000
Forebody length, inches	156.0	140.7
Afterbody length, inches	162.0	111.8
Beam, maximum, inches	48.0	-----
Beam at step, inches	47.72	47.2
Dead rise at step, degrees	20.0	19.8
Step height, inches	4.0	3.2
Afterbody angle, degrees	6.6	-----
Sternpost angle, degrees	8.0	9.4
Model scale	8.0	-----

Table II gives additional particulars of the basic hull.

Hull Design

Forebody.- Wherever practical, the hull lines chosen were made up from readily computable curves - a process which permits convenient scaling of the lines up or down. In addition, this procedure has construction advantages because it facilitates the accurate joining of component portions.

The "forebody flat" - the region in which the dead rise increases linearly with the distance forward of the step - is 34.6 percent of the forebody length. It is sufficiently long to satisfy the need of planing area at the hump, and yet short enough to obtain easy buttock lines. The variation in dead-rise angle with forebody length is shown in figure 1. The dead rise at the bow of the amphibian is 45°. It was not deemed necessary to make the bow dead rise as high as is customary on military flying boats since the whole forward portion of the basic forebody was lifted relatively higher above the base line. Because of the higher-placed bow sections, the basic design should be able to operate in waves of greater height than previously built flying boats of the size contemplated.

The keel curvature, starting at the forward end of the flat, is of essentially elliptical form, as shown in figure 2.

Beam.- A maximum beam of 48 inches, occurring 24 inches forward of the main step, was selected for the basic hull. Placing the maximum beam forward of the step yields the maximum wetted area for a given wetted length, a condition desired at hump speeds. As the speed increases and the wetted area diminishes, the wetted length becomes excessively short for a given beam; it is therefore advantageous to have a smaller beam at the step. This expedient provides both a greater area forward and a greater space for the cockpit. In addition, it provides for finer lines aft, thus reducing afterbody interference with spray from the forebody at high speeds, and also reducing the skin area of the hull which would tend to reduce both weight and cost.

The plan of the forebody chine line from the bow to the maximum beam at station 132 is, essentially, of elliptical form. From station 132 to the sternpost of the afterbody, the plan form is a modified parabola, as indicated in figure 3.

Main step.- The depth of the step influences landing stability and resistance at high speeds. A step depth of 4 inches (8.3 percent of maximum beam) was selected for the basic hull. The 4-inch step height appears to be adequate when compared with the information on the influence of various hull parameters upon skipping (see reference 7). A

later report (reference 8) not available at the time these hulls were designed gives additional design information on step depth.

Afterbody.- The dead-rise angle of the afterbody was maintained at 20° throughout the length of the afterbody.

Tail cones were not included. Afterbody-roach profile measurements for the short afterbodies at prehump speeds were included in the test program to aid the designer.

Spray strips.- Simple spray strips of the type shown in figure 4 were attached to the forebodies in order to control the spray.

Lines.- The lines thus derived for the parent model with variations of afterbody length are shown in figure 5.

Hull Series

The block grid, figure 6, shows the basic model and the plus and minus variations in beam, sternpost angle, and afterbody length of the basic design making up the hull series.

In deriving the hulls of wider or narrower beam, the forebody-keel profile and the dead-rise angles of the basic hull were unaltered. Thus, the chine heights above the forebody keel varied for hulls of different beam, but the lateral and longitudinal angles of the planing bottom remained constant. The forebody plan form was altered with change in beam, because the value of the beam b enters the forebody-plan-form equation given in figure 3. The afterbody plan form was altered with change in length and beam by changing the values of the constants in the equation of afterbody plan form. The value of the constant p was determined by the beam and afterbody length. The exponent was taken as 2.25 for the long afterbody, 2.50 for the medium-length afterbody (parent), and 2.75 for the short afterbody.

The change in sternpost angle was accomplished by rotating the afterbody about the intersection of the afterbody keel with the vertical plane of the main step.

The lines of the other models in the series are shown in figures 7 and 8.

Hull Modifications to Parent

The hull series was designed with the object of obtaining satisfactory hydrodynamic characteristics with "simplified" lines. Since oversimplification could result in hydrodynamic penalties, two refinements of the parent forebody and one of the parent afterbody were investigated.

Concave forebody bottom (model no. 1220-01).- The chine and keel lines of the parent hull (model no. 1024-01) were retained but the bottom was made concave and no chine strips were used (fig. 9).

Increased forebody dead-rise warping (model no. 1222-01). The dead rise of the parent forebody was increased forward of station 102 to the bow. The increase was obtained by dropping the parent keel line and raising the chine line equal amounts at each station (figs. 1 and 9).

Afterbody dead-rise warping (model no. 1221-01).- The constant afterbody dead rise of 20° was altered to have a maximum dead rise of 33° at station 237 (figs. 1 and 9).

APPARATUS AND PROCEDURE

The test facilities of tank 3 of the Experimental Towing Tank are described in reference 9. The apparatus employed in conducting general tests for resistance, main-spray, and porpoising characteristics of flying-boat hulls is shown in figure 10.

With but two exceptions, all tests were conducted in smooth water at a series of constant speeds; bow-spray tests were made in waves, and landings were made as the towing carriage was decelerated.

The parabolic unloading curves given in figure 11 show the upper and lower limits of the loading range used in the resistance, spray, and porpoising tests.

The resistance investigation was made with the models free to trim in the displacement speed range and at a series of fixed trim angles in the planing speed range over a wide range of load. In all of the resistance tests, a 0.040-inch-diameter strut was towed ahead of the model to induce turbulence in the model boundary layer. It has been found from past testing experience at this tank that a definite improvement in the uniformity and reliability of the data can be obtained with induced turbulence. The resistance includes the air drag of the model, but does not include the air drag of the apparatus.

The main-spray tests were made in the displacement speed range with the models free to trim over a wide range of load. The dimensions of the main-spray blister were obtained by means of three-view photographs. With the aid of mirrors, a camera mounted above the model simultaneously recorded top, front, and side views of the spray blister. This photographic technique is described in reference 10.

General porpoising tests were run at a number of fixed speeds, the choice of speeds depending on the load. At each speed, moments were applied to cover a range of trims sufficient to embrace the upper and lower stability limits. At each speed and applied moment a test was made with damping in pitch obtained by means of a calibrated dashpot and piston. The aerodynamic pitch-damping rate M_q for the horizontal tail alone was determined from the equation given in reference 2:

$$M_q = K\frac{\rho a}{2} S_t L_t^2 V\left(\frac{dC_L}{d\alpha}\right)_t \text{ pounds feet seconds/radian}$$

The value of K was taken as 1.00. The values of tail area S_t and tail length L_t were taken from the averages given in table I. The ratio $\left(dC_L/d\alpha\right)_t$ was calculated from unpublished curves of wind-tunnel tests furnished by one of the aircraft manufacturers. For this investigation, a pitch-damping rate corresponding to $M_q = 7.53 \times 10^{-3} V_m$ was used.

The specific porpoising apparatus shown in figure 12 and described in reference 11 was used in conducting the landing tests. This apparatus is equipped with a hydrofoil which is calibrated to provide the scale aerodynamic lift forces and force derivatives. An attempt was made to duplicate the full-size landing maneuver as closely as possible. While in the air, the model was accelerated to well over the landing speed with enough applied moment to hold it at some predetermined landing trim. The model was then decelerated at the rate of 2 feet per second per second until it landed. From the instant that deceleration began and until after the model landed the model heave and trim were recorded. The number of skips can be determined from such records.

The landing tests were made at one gross weight and two wing loadings. The landing trim angle was determined by the wing characteristics as a function of wing loading and speed. Curves of landing trim against landing speed for the two values of wing loading investigated are shown in figure 13.

There were 27 possible hull combinations of variations in beam, sternpost angle, and afterbody length, as shown in figure 6. It was thought best to select the afterbody length as the independent variable, thus narrowing the problem to the selection of the proper beam and sternpost angle for a given length of afterbody. At the outset of the program, it was anticipated that the 8 extreme combinations of beam, sternpost angle, and afterbody length could be omitted, thereby reducing the number of combinations to 19. However, test results on some of the other models indicated that 4 of the extreme combinations should be tested but that 2 of the 19 combinations could be omitted, so that 21 of the possible 27 combinations were investigated (see fig. 6).

The investigation was carried out in four phases. In phase 1, preliminary porpoising tests were undertaken to select a suitable value for the design position of the center of gravity to be used in all of the tests. By making brief porpoising tests on the hull having the widest beam and largest sternpost angle (shortest forebody wetted length), with various longitudinal positions of the center of gravity, it was possible to select a center-of-gravity location sufficiently close to the step to prevent lower-limit porpoising near hump speed. By making brief porpoising tests on the hull having the narrowest beam and lowest sternpost angle (longest forebody wetted length), with various longitudinal positions of the center of gravity, it was possible to select a center-of-gravity location sufficiently far forward of the step to prevent upper-limit porpoising. Thus, a center-of-gravity location deemed satisfactory in these two extreme cases was selected for the entire series.

The resistance and main-spray characteristics are the two most important hydrodynamic characteristics in a study of this type. In phase 2, therefore, all 21 hull combinations were tested for resistance and main-spray characteristics.

On the basis of the tests in phase 2, three hull combinations - one for each afterbody length - were selected for further testing. Two of these three hulls were investigated for landing characteristics. Since it was known that the depth of step influences the landing stability, one of these hulls was tested with normal and decreased depth of step. Porpoising tests were then made on each of the three hull combinations at the best step depth. This portion of the work was designated phase 3.

Phase 4 was planned in order to determine the possible advantages of using tested design refinements. The refinements and characteristics investigated were as follows:

Refinement	Characteristics investigated
Concave forebody bottom	Low-speed resistance and main spray
Increased forebody dead-rise warping	Low-speed resistance, main spray, bow spray, and lower-limit porpoising
Afterbody dead-rise warping	Landing and high-speed resistance

RESULTS

Center-of-Gravity-Location Test Data

The results of the preliminary porpoising tests made on the hulls with the widest beam and largest sternpost angle (shortest forebody wetted length) and with narrowest beam and lowest sternpost angle (longest forebody wetted length) to determine a longitudinal location for the center of gravity which could be used for all of the hulls are given in figure 14. Although the changes in center-of-gravity location do not affect the trim limits of stability, they do affect the free-to-trim track. The center-of-gravity location used in all subsequent tests - 1.50 inches forward of the step and 6.50 inches above the forebody keel - gave a free-to-trim track which was above the lower and below the upper trim limits of stability for the two extreme models investigated.

General Test Data

The data obtained from the tests of all hulls investigated are given in collapsed form on summary charts (figs. 15 to 35). This form of presentation, developed by Locke (see reference 5), enables the results of resistance, spray, and porpoising tests for any one model to be presented on a single summary chart which is divided into three parts and shows:

(1) At the top - dimensions of the spray blister envelopes for free-to-trim tests at displacement speeds, in accordance with the method of presentation developed in reference 4.

(2) In the middle - resistance and trim angle for free-to-trim tests at displacement speeds, in accordance with the method of presentation developed in reference 3. A curve is shown for each C_{Δ}, since no basis has been found for collapsing the trim tracks in this speed range.

(3) At the bottom - resistance and stability characteristics at planing speeds, in accordance with the methods of presentation developed in references 2 and 3. The curves represent the data for all values of C_{Δ} and trim covered by the tests.

The summary charts can be used to make either specific or general comparisons using the method outlined in reference 12.

Static Properties

The trim angles and the draft at the main step obtained at various loadings with the models at rest in the tank are given in figures 36 and 37. The center-of-gravity location used in these tests was the same as that used throughout the entire investigation. Static properties of all hull combinations were not obtained, but those that have been obtained represent the more important hull combinations.

Landing Test Data

Specific landing tests were to be made on three hulls - one for each afterbody length. Unfortunately, it was impossible to test the hull with the longest afterbody length without a costly revision of the apparatus. The other models were tested at various depths of step, and the results, which are in the form of charts of number of skips against trim angle at contact, are given in figures 38 and 39. The variation of trim angle with speed used in the landing tests is given in figure 13.

Hull-Modification Test Data

The various hull modifications were made to show the improvements that could be gained by refining the hull lines. Since the modifications would not change all the hydrodynamic characteristics, the modified hulls were tested only for those characteristics where changes could be anticipated. The data obtained from the tests of the modified hulls are given in collapsed form on summary charts, figures 40 to 43. Figure 44 shows the influence of step depth on the skipping characteristics of the hull with the warped afterbody.

Afterbody-Roach Profile Measurements

With a boom-supported tail assembly it is important that the tail clear the afterbody roach occurring at speeds just below the hump. Afterbody-roach profiles for the short and medium afterbody lengths are given in figures 45, 46, and 47.

Air-Drag Tests

The air drag of the models was determined with the model in air, supported just above the water surface, and run at a number of speeds and various trim angles. Two models with a 6.00-inch beam - one with a short afterbody and a 6° sternpost angle, the other with a long afterbody and a 10° sternpost angle - were used in these tests. The average drag coefficient C_D was found to be substantially independent of model, speed, and trim angle and to have a value of about 0.80. The high value of this coefficient can be explained only by the fact that the model had an open deck. It is of similar order to many other models that have been tested in this tank.

Bow-Spray Tests

A few rough-water tests were made on the basic hull (model no. 1024-01) and the hull with increased forebody warping (model no. 1222-01) at speeds ranging from 4 to 10 feet per second $\left(C_V = 1.0 \text{ to } 2.5\right)$ with a load of 5.45 pounds $\left(C_\Delta = 0.70\right)$ in waves 3 by 60 inches (2 by 40 feet full scale) and 4.5 by 90 inches (3 by 60 feet full scale). The results, which are based on visual observations, are given below:

Model no.	Wave size	
	3 in. high by 60 in. long	4.5 in. high by 90 in. long
1024-01 (basic hull)	Slight spray over bow at 6 ft/sec; above and below this speed bow clear	Much spray over bow from 8 to 10 ft/sec
1222-01 (increased forebody warping)	Slight spray over bow at 6 ft/sec; above and below this speed bow clear	Much spray over bow at 7 ft/sec, diminishing until bow is clear at 10 ft/sec

There was a slight improvement in the bow spray with increased forebody warping.

ANALYSIS AND DISCUSSION

Resistance and Main-Spray Tests

To select the best beam and sternpost angle for a given length of afterbody on the basis of resistance and main-spray characteristics requires means for making comparisons of the various hulls. A comparison between different hulls, however, is not easy to make, since no nondimensional form of presenting test data has yet been devised to represent satisfactorily the transition between the displacement and planing stages. Even if this problem were solved, a direct comparison would be possible only if one curve were to lie above another throughout the entire speed range.

It might be imagined that a satisfactory criterion for comparison would be the resistance when the model carries a definite load at a definite speed. However, a difficulty arises in this method. If, for a given variation of load with speed, the beam of the hull is altered while the length is held constant, the water resistance also changes. This is shown in figures 48 to 54, wherein the specific resistance characteristics are worked out for a large number of cases for one take-off speed and one weight. In nearly all of the cases it will be seen that as the beam is decreased the hump resistance increases while the resistance at high speed decreases. This is in agreement with previous investigations (see, e.g., references 13 and 14).

Now even these charts cannot be used directly to determine the optimum configuration because of the interrelated effects of the available margin of thrust at the main hump and at the second hump near get-away speed. Thus, in general, a large excess thrust and a high take-off speed favor a narrow hull. There are limitations, however, on how narrow a hull can be made, since overloading a hull causes it to throw up a large spray blister at low speeds. Figure 55 illustrates this, for it shows that the spray heights increase with decrease in beam.

In view of the above considerations, it was apparent that take-off calculations under specified design conditions would afford the one sure means of assessing the merits of the various hulls. Calculations were therefore undertaken, with the following full-scale factors taken as being common to all:

Gross weight, pounds	3000
Take-off speed, miles per hour	60, 68.7, 77.4
Wing loading, pounds per square foot of wing area	11.03, 14.5, 18.4
Take-off lift coefficient (C_L)	1.2

The objective of the take-off calculations is to enable the selection of the best beam and sternpost angle for a given length of afterbody. For this comparison to be effective, the spray characteristics of all

hulls with a given afterbody length should be approximately the same. This can be accomplished by selecting the displacement for each of the model hulls on a constant forebody plan-form area basis, as originally suggested in reference 15. The displacements for constant forebody plan-form area and the corresponding scale of models are given in the accompanying table:

Model			Scale	Full scale (3,000-lb displacement)		
b (in.)	L_f (in.)	Δ (lb)		b (ft)	L_f (ft)	$L_f \times b$ (sq ft)
5.25	19.50	4.80	8.55	3.74	13.89	52
6.00	19.50	5.86	8.00	4.00	13.00	52
6.75	19.50	6.99	7.54	4.24	12.25	52

Several simplifying assumptions were made to reduce the labor involved in the calculations. The most important was that the lift was not a function of trim angle, which permitted the use of a parabolic unloading curve. The air drag of the airplane was not included in the total resistance, and, in an effort to compensate for this, no correction was made to the model frictional resistance.

In the calculations, the hulls were trimmed to the zero-moment trim track up to just beyond the hump speed. From hump speed to get-away, the trim track selected was a smooth transition from the free-to-trim track to the trim for minimum resistance at 90 percent of get-away speed.

The thrust curves used in obtaining the take-off times are the same as those used and discussed later on in the report. Charts of the variation of resistance with speed for the middle take-off speed (68.7 mph) are given in figures 56 to 58.

The height of spray at three longitudinal locations along the hulls - 6 feet forward of the step, at the step, and 6 feet behind the step - for the middle take-off speed is given in figure 59. This constant forebody plan-form area comparison shows some variations in spray height as the beam is changed within an afterbody length group. The variation of spray height is, however, much less than that obtained on a constant load basis, as shown in figure 55.

The take-off times (full scale) obtained from the calculations are given in figure 60. It should be borne in mind that these take-off times are only relative because of the aforementioned short cuts taken in making the calculations. The take-off-time comparison shows that, for hulls with the short afterbody, the optimum beam may be somewhat greater than the widest beam investigated, and the optimum sternpost angle appears to be about 6° or possibly a little lower. For hulls with the medium afterbody, the optimum beam is 4.0 feet, and the optimum sternpost angle is about 8°. For hulls with the long afterbody, the optimum beam again is 4.0 feet, and at this beam there is very little difference in take-off time with change in sternpost angle, although the higher sternpost angles show a slight advantage as the take-off speed is increased.

The main-spray comparison for the take-off speed of 68.7 miles per hour, figure 59, gives about the same results as does the take-off-time comparison.

On the basis of take-off times and spray heights, the best beam and sternpost angle for each length of afterbody were selected for further testing. The beam selected for all three afterbody lengths was the middle, or 4.0-foot, beam. The sternpost angles selected were 6° for the short afterbody, 8° for the middle afterbody, and 10° for the long afterbody. The 10° sternpost angle for the long afterbody was deemed best, since at this sternpost angle the high-speed resistances are not only lower at best trim but are considerably lower at trims above best trim, as shown in figure 61.

Landing Tests

After the best beam and sternpost angle for each of the three afterbody lengths were selected on the basis of resistance and spray, two of these three models were further investigated for landing and porpoising characteristics. The 4-inch full-scale depth of step used in this series was selected, as discussed earlier in this report, to avoid instability on water landings. The results of the landing tests (figs. 38 and 39) give no indication of skipping at the design step depth of 4 inches (8.3 percent of the beam). The parent hull did encounter some skipping on landing when the step depth was reduced to 2 inches (4.2 percent of the beam), as shown in figure 39. The landing tests indicated, therefore, that the design step depth should not be altered with the basic afterbody.

Full-Scale Resistances and Take-Off Times

To make the study more complete, and to illustrate the more detailed application of model data, the results of the resistance tests for the three hulls have been expanded to full scale. The following conditions were assumed for additional calculations:

	Hull 1	Hull 2	Hull 3
Gross weight, lb	3000	3000	3000
Take-off speed, mph	60	68.7	77.4
Wing area, sq ft	272	207	163
Wing loading, lb/sq ft	11.03	14.5	18.4
Aspect ratio	6	7.89	10
Horsepower	185	215	245

The best three model hulls previously determined were used in this study. Again, the free-to-trim track was followed to just beyond hump speed. From hump speed to get-away, the trim track followed a faired curve from the free-to-trim track to the trim for minimum resistance at 90 percent of get-away speed. Model air drags were subtracted from the model resistance data to give hydrodynamic drag.

It will be remembered that in these resistance tests an effort was made to insure the existence of turbulence in the boundary layer by means of a strut towed ahead of the model. This results in somewhat higher model resistances but makes it possible to correct the frictional resistance when expanding from model to full scale.

Since the frictional resistance is a small part of the total hydrodynamic resistance at speeds lower than hump speed, no correction of the frictional resistance was made in this speed range, and the model resistance was expanded to full scale by multiplying the model resistance by the cube of the scale ratio (see reference 16). At speeds beyond hump speed, where the frictional resistance is a large part of the total resistance, the model resistances were expanded to full size by a method (see appendix A) similar to that used in expanding surface-ship model data. This method of expansion is important only in the

region of the secondary peak of resistance (or minimum available margin of thrust) which occurs at approximately 90 percent of get-away, and which is associated with the phenomenon often referred to as "sticking." At this particular point of the speed range, all of the corrections can be lumped together and approximated by using the ratio of model to full-scale expansion of $\lambda^{2.80}$ instead of λ^3 which would result if the Reynolds number effect were neglected.

The calculated air drag of the airplane and hull was added to the expanded water resistances. The air drag at take-off was computed from the drag components corrected for change in angle and ground effect.

The drag coefficients used for the component parts of the airplane are given in table III and the curves of power available and power required are given in figure 62. From this information, the propeller characteristics were selected (given in table III) and the thrust curves computed by the methods outlined in reference 17.

The take-off times of each of the three hulls were computed for each of the three take-off speeds. The curves of water resistance plus air drag together with the thrust curves given in figures 63 to 65 were used to compute the take-off times.

The take-off times of the hulls under the various conditions are approximately the same. This should not be surprising because the best beam and sternpost angle were selected for each length of afterbody.

Porpoising Tests

The upper and lower trim limits of stability for the three hulls - each of different afterbody length - under the various take-off conditions are given in figures 66 to 68. A comparison of these charts shows that the stable trim range increases with the length of the afterbody.

Hull Modifications

The effect of the spray strips used on the models can be seen in figure 69, where a comparison of the main-spray heights of the parent model with and without spray strips is given. This chart shows that the spray strips are extremely effective in reducing the height of the main spray.

The effect of the spray strips on the low-speed resistance and trim characteristics is given in figure 70, where the resistances and trims

of the parent model with and without spray strips are compared. The spray strips generally increase the trim a little and reduce the resistance a little at the hump.

Although the use of concave forebody sections instead of straight forebody sections is effective in reducing the spray heights, it is not quite so effective as the use of spray strips (see fig. 69). The resistances and trim angles of the concave-forebody model are slightly lower than those of the parent hull, as shown in figure 71.

Increasing the forebody dead-rise warping has negligible effects on the main-spray characteristics (see fig. 69) and on the displacement-speed-range resistance and trim characteristics (see fig. 71). The lower trim limit of stability of the hull with increased forebody dead-rise warping is only slightly lower than that of the parent hull at the lower speeds, and slightly higher at speeds near take-off, as shown in figure 72. Since the model with the increased forebody dead-rise warping was identical to the parent model for a beam length forward of the step (see fig. 1), it is not surprising that there are only small differences in the lower trim limits of stability at the higher speeds. Increasing the forebody dead-rise warping improves the bow spray slightly.

Warping the afterbody dead rise decreases the high-speed resistances appreciably, as shown in figure 73, even though the sternpost angle of the warped afterbody hull had to be $\frac{1}{2}^{\circ}$ lower than that of the parent model in order to obtain the same hump trim as the parent hull. Warping the afterbody enables the step depth to be reduced from 8.3 percent of beam (4 in., full size) to at least 4.2 percent of beam (2 in.) without encountering skipping on landing (see fig. 74).

In general, the modifications improve the hydrodynamic characteristics of the parent hull. Warping the afterbody would permit a lower depth of step and concave forebody sections would permit a reduction in spray-strip size. These improvements, however, are not great and would probably not be justified since the complication of the hull lines would entail increased costs.

Physical Picture of Two-Step Planing

In the region of the hump speed, a flying-boat hull planes on both the forebody bottom and the afterbody bottom. It is believed instructive to construct a physical picture of this phenomenon and of the forces and moments involved in the process. For this purpose, underwater photographs of the parent hull without spray strips were taken to show the

forebody and afterbody wetted areas. One such photograph is shown in figure 75, together with the forces resulting from these wetted areas as estimated by the methods given in reference 18. A force diagram, together with calculations of the forebody and afterbody hydrodynamic pitching moments, is given in figure 76.

An understanding of the physical picture of two-step planing in the vicinity of the hump was utilized in designing the parent hull of the series. Prior to the actual layout of the hull lines, values of hump speed, hump trim, and water-borne load at hump speed were assigned for the basic hull on the basis of previous experience. By means of the methods given in reference 18, the forebody wetted length was estimated; this, in turn, enabled an estimation of the center of pressure and of the pitching moment due to the resultant hydrodynamic force on the forebody to be made.

The required moment generated by the afterbody must balance the moment produced by the forebody. To determine the moment produced by the afterbody, the wave profile in the wake of the forebody was plotted. A location of the afterbody was chosen by trial and error so that the resulting position of the center of pressure - determined from the wetted length of the afterbody - produced the moment required to balance that due to the hydrodynamic force acting on the forebody. In this manner, the sternpost angle was determined.

In order to use the information given in reference 18, it is necessary to know the hump trim and the speed at which it occurs. The prediction of hump trim is not easy and to date is based on previous model tests. In order to calculate the hump trim, a relationship between the sternpost angle, the ratio of afterbody length to beam, and the load coefficient has to be determined. For the present series, an empirical relationship between these quantities is given by the following equation:

$$\tau_{\text{at hump, calculated}} = -0.8 + 1.2\sigma + \left(\frac{6}{L_a/b}\right)^2 C_\Delta$$

A comparison of the measured hump trims and the calculated hump trims is given in figure 77.

Similarly, the speed at which the hump trim occurs can be calculated from an empirical relationship between the ratio of afterbody length to beam and the sternpost angle as follows:

$$C_{V_{\text{at hump trim, calculated}}} = 1.14 + 0.60\left(\frac{L_a}{b}\right) - 0.023(\sigma - 7.5)^2$$

A comparison of the measured speed coefficient at hump trim and the calculated speed coefficient at hump trim is given in figure 78.

CONCLUSIONS

The following conclusions were reached from the hydrodynamic investigation of a series of hull models suitable for small flying boats and amphibians:

1. It is possible to design a hull with simplified lines suitable for small flying boats or amphibians.

2. Refinements in the hull lines such as concave forebody sections, increased forebody dead-rise warping, and afterbody dead-rise warping improve the hydrodynamic characteristics, but the gains may not be worth the additional construction cost in personal-owner-type flying boats.

3. The beam and sternpost angle selected to give the best spray and resistance characteristics for a particular length of hull also give satisfactory landing and porpoising characteristics.

4. Comparison of hulls of the same length, but varying beam, on a constant-load basis shows, in general, that the narrow hulls have less resistance, being better in the displacement and planing speed ranges, though worse in the vicinity of hump speed. The narrower hulls, however, are more deeply immersed and consequently throw more spray.

5. Comparison of these hulls on a basis of constant forebody planform area shows, in general, little variation in spray height with beam. In this type of comparison, narrowness must be accompanied by increased length if hulls of different length-beam ratio are to carry the same load. The increased length partially offsets the advantage in resistance of the narrow hull.

Stevens Institute of Technology
Hoboken, N. J., December 29, 1949

APPENDIX A

EXPANSION OF MODEL RESISTANCE DATA

It has been known for many years that flying-boat-hull model resistance is subject to scale effect. The scale effect is the result of differences in the model and full-scale frictional resistance coefficients caused by the different model and full-scale Reynolds numbers when model and prototype are run at equal Froude numbers. The problem has been complicated by the lack of knowledge of full-scale roughness resistance. In the past, it has been the practice, whenever practicable, to compare the resistance of models of equal size, thereby canceling scale effects. For full-size predictions, resistance was expanded by the cube of the scale ratio, reliance being placed on large models to reduce scale effect. It was tacitly assumed that the increased roughness drag of the full-size flying boat would compensate for the decreased frictional resistance. As the scale ratio became greater because of the increased size of flying boats and because of the use of smaller models, it became apparent that this assumption was too conservative. The need for a model-to-full-scale resistance expansion similar to that used in surface-ship resistance testing thus became apparent. No standard procedure for expansion of flying-boat model resistance, however, has achieved wide acceptance because of the lack of knowledge concerning full-scale roughness resistance and the many arithmetical difficulties in the computations.

The procedure for expansion of model test data to full size (reference 19), widely used in surface-ship resistance testing, utilizes the Schoenherr friction formulation. A similar method used in Germany in model-seaplane resistance testing is given in reference 20. Both of these procedures, however, require wetted-area measurements which are not often recorded in seaplane tests. The method suggested in this appendix is simpler than those given in references 19 or 20 inasmuch as wetted-area measurements are not needed.

The Schoenherr friction formula, which is of an awkward form, can be approximated by an exponential formula for any particular arrangement of Reynolds numbers desired. In particular, if the Reynolds number does not exceed about 2×10^7, the well-known formula of Prandtl and von Kármán can be used. This formula for the coefficient of frictional resistance C_f is:

$$C_f = 0.074 \, (Re)^{-0.2}$$

from reference 21 where the Reynolds number Re is equal to VL/ν.

For model tests such as these, where the Froude numbers of model and full-scale are equal, the following relationships exist:

λ linear scale ratio, $\frac{\text{full scale}}{\text{model}}$

$\lambda^{1/2}$ speed scale ratio

At equal Froude numbers, the trim angles of model and full-size hulls are equal, the wave formation of the model is identical to that of the prototype, and the distribution of wetted areas is the same. The frictional resistance is therefore proportional to the frictional-resistance coefficient. Using the exponential form of expression for the frictional-resistance coefficient gives the following equation for the correction factor, where subscripts m and s are used to denote model and full scale, respectively:

$$\frac{C_{f_s}}{C_{f_m}} = \left(\frac{Re_s}{Re_m}\right)^{-0.2}$$

$$= \left(\frac{V_s L_s}{V_m L_m}\right)^{-0.2}$$

$$= \left(\lambda^{1/2}\lambda\right)^{-0.2}$$

$$= \lambda^{-0.3}$$

The conversion of model frictional resistance to full-size frictional resistance is then

$$R_{f_s} = R_{f_m} \lambda^3 \lambda^{-0.3}$$

$$= R_{f_m} \lambda^{2.7}$$

The hydrodynamic resistance is considered to be composed of the resistance component of the force normal to the planing bottom and the frictional force tangential to the planing bottom. This frictional force includes that of the afterbody as well as that of the forebody. The lift

force of the afterbody, if any exists, is neglected. Trim is here defined as the true mean inclination of the planing area and not as a nominal figure referred to an arbitrary reference line. Thus, in computing full-scale resistances, the following steps were taken:

(1) Total model water resistance = Model dynamic resistance + model frictional resistance (where model dynamic resistance = $\Delta_m \tan \tau$)

(2) Model dynamic resistance $\times \lambda^3$ = Full-scale dynamic resistance

(3) Model frictional resistance $\times \lambda^{2.7}$ = Full-scale frictional resistance

(4) Total full-scale water resistance = Item (2) + item (3)

The above method of expansion was used in the speed range from 60 percent of get-away to get-away, where the frictional resistance is a large part of the total resistance. When these resistances are plotted against speed, the resulting curve is similar to curve A in figure 79. The low-speed end of this curve is joined to the resistance curve from zero to hump speed, labeled B in figure 79, by a smooth curve labeled C.

APPENDIX B

COMPARISON OF NACA 40BE DESIGN AND E.T.T. MODEL NO. 1057

INTRODUCTION

The series of hulls described in the body of this report was designed on the basis of present-day hydrodynamic knowledge and was tested for longitudinal stability and main-spray characteristics as well as for resistance characteristics. The last comprehensive work on small flying boats was that undertaken by the NACA in 1934 on the model 40 series in which the only characteristic of the above three investigated was the resistance. Since the present study can be considered to be a continuation of the model 40 series study, it was thought desirable to make a comparison of the longitudinal stability, spray, and resistance characteristics of the two hull series. In order to do so, one of the designs in the model 40 series was built to the same beam as the models in the E.T.T. series, and tested in the same manner.

This appendix presents a comparison of the resistance, main spray, and longitudinal stability characteristics between two models - one in each series - that have approximately the same hull proportions.

MODELS

The design selected from the NACA model 40 series was model 40BE. This design, built to a 6-inch beam, is designated model no. 1290-01. Model no. 1057-04 (having a sternpost angle of 9°) was selected from the E.T.T. series.

These two designs had practically the same ratios of forebody and afterbody length to beam, and the sternpost angle of the model selected from the E.T.T. series was taken to be the same as that of the 40BE model.

The center-of-gravity locations for the two models were slightly different, as can be seen from the following table:

Model no.	Center of gravity above forebody load, (in.)	Center of gravity forward of step, (in.)
1057-04 (E.T.T.)	6.50	1.50
1290-01 (NACA 40BE)	7.18	1.85

Model no. 1290-01 was set up with the same center-of-gravity location as had been used in the earlier NACA tests, while model no. 1057-04 had the same center-of-gravity location used for all models in the E.T.T. series.

The pertinent particulars of both models are given in table IV, and the hull lines are presented in figure 80.

RESULTS

The data obtained from the tests on the 6-inch-beam model of the 40BE design - model no. 1290-01 - are presented in collapsed form on a summary chart in figure 81. The data for the corresponding design in the E.T.T. series - model no. 1057-04 - were obtained by interpolation from the data obtained on models nos. 1057-01 and 1057-03, which are presented in summary-chart form in figures 25 and 22, respectively.

Specific comparisons of the two designs were obtained from the summary charts by using the load-fall-off curve given in figure 82.

ANALYSIS AND DISCUSSION

The two designs were compared on the basis of a full-scale gross weight of 3000 pounds and a take-off speed of 68.7 miles per hour. As in the body of the report, the model resistances were expanded to full scale by the method outlined in appendix A.

The longitudinal stability characteristics of the 40BE design (model no. 1290-01) are presented in figure 83, which shows three trim tracks labeled A, B, and C. Trim track A is that for best trim and is based on the NACA data reported in reference 1. Trim track B is the free-to-trim track $\left(C_M = 0.0\right)$ as obtained in the porpoising tests of model no. 1290-01. Trim track C follows a faired curve from the free-to-trim track in the vicinity of the hump toward the trim for minimum resistance at 90 percent of get-away speed but rises at the high-speed end to avoid the lower trim limit of stability.

A comparison of the longitudinal stability characteristics of both designs is presented in figure 84. The trim track shown in this figure for model no. 1290-01 is the same as that labeled C in figure 83. The trim track for model no. 1057-04 follows, from hump speed to get-away, a faired curve from the free-to-trim track to the trim for minimum resistance at 90 percent of get-away speed.

The lower trim limit of stability for model no. 1057-04 is lower than that for the 40BE design, and the upper trim limit of stability for model no. 1057-04 is higher than that for the 40BE design. The spread between the upper and lower trim limits of stability at 50 miles per hour is approximatley $8\frac{1}{2}^{\circ}$ for model no. 1057-04 and is only 4° for the 40BE design. This increase in the range of stable trims can be accounted for by the differences in the design of the two hulls.

Previous investigations, reported in references 11 and 22, have indicated that warping of the forebody bottom of flying boats lowered the lower trim limit of stability. The warping of the forebody bottom was accomplished by maintaining the same keel profile and increasing the dead-rise angles. This method is approximately equivalent to an upward rotation of the original bottom with respect to the design reference line. Consequently, any modification which is equivalent to an upward rotation of the original bottom with respect to the design reference line should lower the lower trim limit when the trim angles are referred to the original design reference line.

One of the differences between model no. 1057-04 and the 40BE design is the higher profile of the 1/4-beam widths for model no. 1057-04, as shown in figure 85. This difference is approximately equivalent to an upward rotation of the 40BE design with respect to the design reference line. Since the design reference line is the same for both hulls, the lower trim limit of stability should be lower for the upward-rotated forebody, namely that of model no. 1057-04.

The higher upper trim limit of stability of model no. 1057-04 is primarily due to the increased depth of step; model no. 1057-04 has more than twice the step depth of model no. 1290-01.

The resistances of the two models are compared in figure 86. The trim tracks up to hump speed are the zero-moment trim tracks. The differences in the zero-moment trim tracks are primarily due to the difference in center-of-gravity location. From hump speed to get-away speed, the trim tracks are those shown in figure 84.

Model no. 1057-04 has higher resistances than model no. 1290-01 in the vicinity of the hump, but lower resistances at higher speeds. The take-off times for a 68.7-mile-per-hour take-off speed are the same for both models. At higher take-off speeds, model no. 1057-04 has somewhat lower take-off times, while at lower take-off speeds, model no. 1290-01 has somewhat lower take-off times.

The spray heights of the two models are compared in figure 87. It can be seen from this comparison that model no. 1290-01 has slightly lower spray than model no. 1057-04. This is probably due to the fact that the spray strips used on model no. 1290-01 increase the beam, and hence the load per unit area of wetted bottom is somewhat less than that of model no. 1057-04.

CONCLUDING REMARKS

The E.T.T. design (model no. 1057-04) has a greater range of stable trims, lower high-speed resistances, and probably better landing stability than the NACA 40BE design (model no. 1290-01). The NACA 40BE design has lower low-speed resistances and somewhat lower spray heights.

REFERENCES

1. Parkinson, John B., and Dawson, John R.: Tank Tests of N.A.C.A. Model 40 Series of Hulls for Small Flying Boats and Amphibians. NACA Rep. 543, 1936.

2. Locke, F. W. S., Jr.: General Porpoising Tests of Flying-Boat-Hull Models. NACA ARR 3I17, 1943.

3. Locke, F. W. S., Jr.: General Resistance Tests on Flying-Boat Hull Models. NACA ARR 4B19, 1944.

4. Locke, F. W. S., Jr.: "General" Main-Spray Tests of Flying-Boat Models in the Displacement Range. NACA ARR 5A02, 1945.

5. Locke, F. W. S., Jr.: A Collection of the Collapsed Results of General Tank Tests of Miscellaneous Flying-Boat-Hull Models. NACA TN 1182, 1947.

6. Locke, Fred W. S., Jr.: A Correlation of the Dimensions, Proportions, and Loadings of Existing Seaplane Floats and Flying-Boat Hulls. NACA ARR, March 1943.

7. Locke, F. W. S., Jr.: An Analysis of the Skipping Characteristics of Some Full-Size Flying Boats. NACA ARR 5J24, 1946.

8. Olsen, Roland E., and Land, Norman S.: Effect of Afterbody Length and Keel Angle on Minimum Depth of Step for Landing Stability and on Take-Off Stability of a Flying Boat. NACA TN 1571, 1948.

9. Fried, Walter: The No. 3 Tank for Model Seaplane Tests. Rep. No. 289, Exp. Towing Tank, Stevens Inst. Technology, Oct. 1945.

10. Locke, F. W. S., Jr., and Bott, Helen L.: A Method for Making Quantitative Studies of the Main Spray Characteristics of Flying-Boat Hull Models. NACA ARR 3K11, 1943.

11. Davidson, Kenneth S. M., and Locke, F. W. S., Jr.: Some Systematic Model Experiments on the Porpoising Characteristics of Flying-Boat Hulls. NACA ARR 3F12, 1943.

12. Locke, F. W. S., Jr.: A Graphical Method for Interpolation of Hydrodynamic Characteristics of Specific Flying Boats from Collapsed Results of General Tests of Flying-Boat-Hull Models. NACA TN 1259, 1948.

13. Clark, K. W., and Coombes, L. P.: Tank Tests of a Family of Four Hulls of Varying Length to Beam Ratio. Rep. No. BA 1350, British R.A.E. (Farnborough), Nov. 1936.

14. Shoemaker, James M., and Parkinson, John B.: Tank Tests of Flying-Boat Hulls. NACA TN 491, 1934.

15. Bell, Joe W., Garrison, Charlie C., and Zeck, Howard: Effect of Length-Beam Ratio on Resistance and Spray of Three Models of Flying-Boat Hulls. NACA ARR 3J23, 1943.

16. Gruson, M. F.: Similitude in Hydrodynamic Tests Involving Planing. NACA TM 795, 1936.

17. Diehl, Walter S.: Engineering Aerodynamics. The Ronald Press Co. (New York), 1928.

18. Korvin-Kroukovsky, Boris V., Savitsky, Daniel, and Lehman, William F.: Wetted Area and Center of Pressure of Planing Surfaces. Rep. No. 360, Exp. Towing Tank, Stevens Inst. Technology, Aug. 1949. Paper No. 244, Sherman M. Fairchild Pub. Fund, Inst. Aero. Sci., Aug. 1949.

19. Anon.: Uniform Procedure for the Calculation of Frictional Resistance and the Expansion of Model Test Data to Full Size. Bull. 1-2, The Soc. Naval Architects and Marine Eng., Aug. 1948.

20. Sottorf, W.: New Method of Extrapolation of the Resistance of a Model Planing Boat to Full Size. NACA TM 1007, 1942.

21. Rouse, Hunter: Elementary Mechanics of Fluids. John Wiley & Sons, Inc., 1946.

22. Carter, Arthur W., and Weinstein, Irving: Effect of Forebody Warp on the Hydrodynamic Qualities of a Hypothetical Flying Boat Having a Hull Length-Beam Ratio of 15. NACA TN 1828, 1949.

23. Abbott, Ira H., Von Doenhoff, Albert E., and Stivers, Louis S., Jr.: Summary of Airfoil Data. NACA Rep. 824, 1945. (Formerly ACR L5C05.)

24. Wood, K. D.: Technical Aerodynamics. Second ed., McGraw-Hill Book Co., Inc., 1947.

25. Hartman, Edwin P., and Biermann, David: The Aerodynamic Characteristics of Full-Scale Propellers Having 2, 3, and 4 Blades of Clark Y and R.A.F. 6 Airfoil Sections. NACA Rep. 640, 1938.

TABLE I

PRINCIPAL HULL DIMENSIONS OF SOME SMALL FLYING BOATS

SCALED TO A GROSS WEIGHT OF 3000 POUNDS

Name	Designation	Forebody length (in.)	Afterbody length (in.)	Beam at step (in.)	Step height (in.)	Step dead rise (deg)	Sternpost angle (deg)	Tail length (ft)	Tail span (ft)	Tail area (sq ft)	Tail aspect ratio
Amphibians	P-III-B	112.7	105.4	54.7	2.4	7.0	12.8	17.55	9.8	34.8	2.80
Bendix	51	140.3	144.4	45.6	4.1	25.0	8.1	15.88	8.9	36.4	2.18
Curtiss-Wright	CA-1	129.0	114.5	44.4	3.5	19.0	8.7	12.90	12.5	27.0	5.00
Douglas	Dolphin	144.1	113.5	41.5	4.0	20.0	11.4	18.18	12.7	40.0	4.03
Fleetwings	Seabird	146.9	117.0	46.3	---	19.5	----	16.10	10.1	30.0	3.41
Fokker	F-XI	154.8	95.8	55.6	3.0	24.0	8.3	19.40	12.7	49.0	3.30
Goodyear	GA-2	137.4	159.7	44.3	2.2	20.0	9.5	14.85	11.1	31.4	3.93
Grumman	G-21A	126.6	107.9	43.3	2.4	25.0	8.5	12.99	11.4	38.0	3.42
Grumman	G-44A	139.0	95.6	44.5	2.9	20.0	8.7	14.12	11.9	34.6	4.10
Keystone	Commuter	151.2	84.0	44.4	---	20.0	----	-----	11.7	48.0	2.85
Republic	Seabee RC-3	130.8	106.8	50.2	3.2	20.0	8.6	14.10	11.5	37.1	3.56
Sikorsky	S-39	130.9	109.1	49.1	---	22.5	----	15.83	14.5	40.0	5.26
Spencer-Larsen	SL-12C	186.0	99.6	49.9	---	15.0	----	-----	13.9	33.8	5.72
Average		140.7	111.8	47.2	3.2	19.8	9.4	15.63	11.8	36.9	3.77
Maximum		186.0	159.7	55.6	4.1	25.0	12.8	19.14	14.5	49.0	5.80
Minimum		112.7	84.0	41.5	2.2	7.0	8.1	12.90	8.9	27.0	2.18

TABLE II

PARTICULARS OF PARENT MODEL NO. 1024-01

Item	Full scale	Model
Scale	1	1/8
DIMENSIONS		
Beam, maximum, in.	48.00	6.00
Beam at main step, in.	47.72	5.96
Forebody length, in.	156.00	19.50
Afterbody length, in.	162.00	20.25
Afterbody angle, deg	6.6	6.6
Step height, in.	4.00	0.50
Sternpost angle, deg	8.0	8.0
Length-beam ratio	7.63	7.63
Center-of-gravity location		
Forward of step, in.	12.00	1.50
Above forebody keel, in.	52.00	6.50
Gross weight, Δ_o, lb	3000	5.86
Gross load coefficient, C_{Δ_o} (fresh water)	0.753	0.753
Pitching moment of inertia, lb sq in.	1.245×10^7	380
Wing span, ft	40.4	5.05
Wing incidence with forebody keel, deg	5.0	5.0
Horizontal tail area, sq ft	36.9	0.577
Tail length (c.g. to 35-percent M.A.C. of tail), ft	15.63	1.954
AERODYNAMIC CHARACTERISTICS		
C_L at $\tau = 6^o$ (take-off trim)	1.2	1.2
$dC_L/d\tau$ (wing), per deg	0.073	0.073
$dC_L/d\tau$ (tail), per deg	0.050	0.050
dM/dq, lb ft sec/rad	$30.7V_s$	$7.53 \times 10^{-3} V_m$
$dM/d\theta$, lb ft/deg	$0.0343V_s^2$	$6.71 \times 10^{-5} V_m^2$

Item	Ratio of full-scale dimension to model dimension
Speed	$\lambda^{1/2} = 2.81$
Length	$\lambda = 8.00$
Area	$\lambda^2 = 6.40 \times 10^1$
Volume	$\lambda^3 = 5.12 \times 10^2$
Moment	$\lambda^4 = 4.096 \times 10^3$
Moment of Inertia	$\lambda^5 = 3.277 \times 10^4$

TABLE III

DRAG COEFFICIENTS AND ENGINE AND PROPELLER CHARACTERISTICS

FOR EACH OF THE THREE WING AREAS USED FOR COMPUTING

FULL-SCALE FLIGHT PERFORMANCE

Wing area (sq ft) (1)	Take-off speed (mph)	Wing C_{D_o}	Tail C_{D_o}	Tip floats C_{D_o}	Nacelle C_{D_o} based on wing area	Hull C_{D_o} based on wing area	Hull frontal area (sq ft)	Hull C_{D_o} based on hull frontal area	Total C_{D_o} based on wing area	Aspect ratio, n (2)
272	60.0	0.012	0.0048	0.0012	0.00206	0.00971	22.0	0.12	0.02977	6.00
207	68.7	.012	.0048	.0012	.00326	.01275	22.0	.12	.03401	7.89
163	77.4	.012	.0048	.0012	.00568	.01620	22.0	.12	.03988	10.00

Wing area (sq ft)	Maximum speed (mph)	Engine				Propeller (3)		
		Manufacturer	Number	Power (bhp)	Speed (rpm)	Diameter (ft)	Blade angle at 0.75R (deg)	Power at maximum speed (thp)
272	135	Continental	E-185-5	185	2300	7.5	18	149
207	149	Franklin	6AB-215-B9F	215	2500	7.5	18	171
163	164	Franklin	0-425A	245	2060	8.0	22	207

[1]Wing section has an NACA 2415 root and an NACA 4412 tip (see reference 23).

[2]Total C_D = Total $C_{D_o} + \frac{C_L^2}{\pi n}$ where C_L is lift coefficient and n is effective aspect ratio (reference 17). Symbol n is taken here as equal to aspect ratio, span^2/wing area.

[3]See references 24 and 25.

TABLE IV

PARTICULARS OF MODEL NO. 1057-04 AND MODEL NO. 1290-01

Item	Model no. 1057-04 E.T.T. design 1/8 scale	Model no. 1290-01 NACA 40BE design 1/8 scale
DIMENSIONS		
Beam at main step, in.	5.96	6.00
Beam, max., in.	6.00	6.00
Beam, max. over spray strips, in.	6.0	6.22
Forebody length, in.	19.50	19.38
Afterbody length, in.	27.00	26.77
Afterbody angle, deg	8.0	8.5
Sternpost angle, deg	9.0	9.0
Step height, in.	0.50	0.23
Length-beam ratio	7.75	7.69
Center-of-gravity location		
Forward of step, in.	1.50	1.85
Above forebody keel, in.	6.50	7.18
Gross weight, Δ_o, lb	5.86	
Gross load coefficient, C_{Δ_o} (fresh water)	0.753	
Pitching moment of inertia, lb in.^{2}	380	
Wing span, ft	5.05	
Wing incidence with forebody keel, deg	5.0	
Horizontal tail area, sq ft	0.577	
Tail length (c.g. to 35 percent M.A.C. of tail), ft	1.954	
Aerodynamic characteristics		
C_L at $\tau = 6^o$ (take-off trim)	1.2	
$dC_L/d\tau$ (wing), per deg	.073	
$dC_L/d\tau$ (tail), per deg	.050	
dM/dq, lb ft sec/rad	$7.53 \times 10^{-3} V_m$	
$dM/d\theta$, lb ft/deg	$6.71 \times 10^{-5} V_m^2$	

Item	Ratio of full-scale dimension to model dimension
Speed	$\lambda^{1/2} = 2.81$
Length	$\lambda = 8.00$
Area	$\lambda^2 = 6.40 \times 10^1$
Volume	$\lambda^3 = 5.12 \times 10^2$
Moment	$\lambda^4 = 4.096 \times 10^3$
Moment of Inertia	$\lambda^5 = 3.277 \times 10^4$

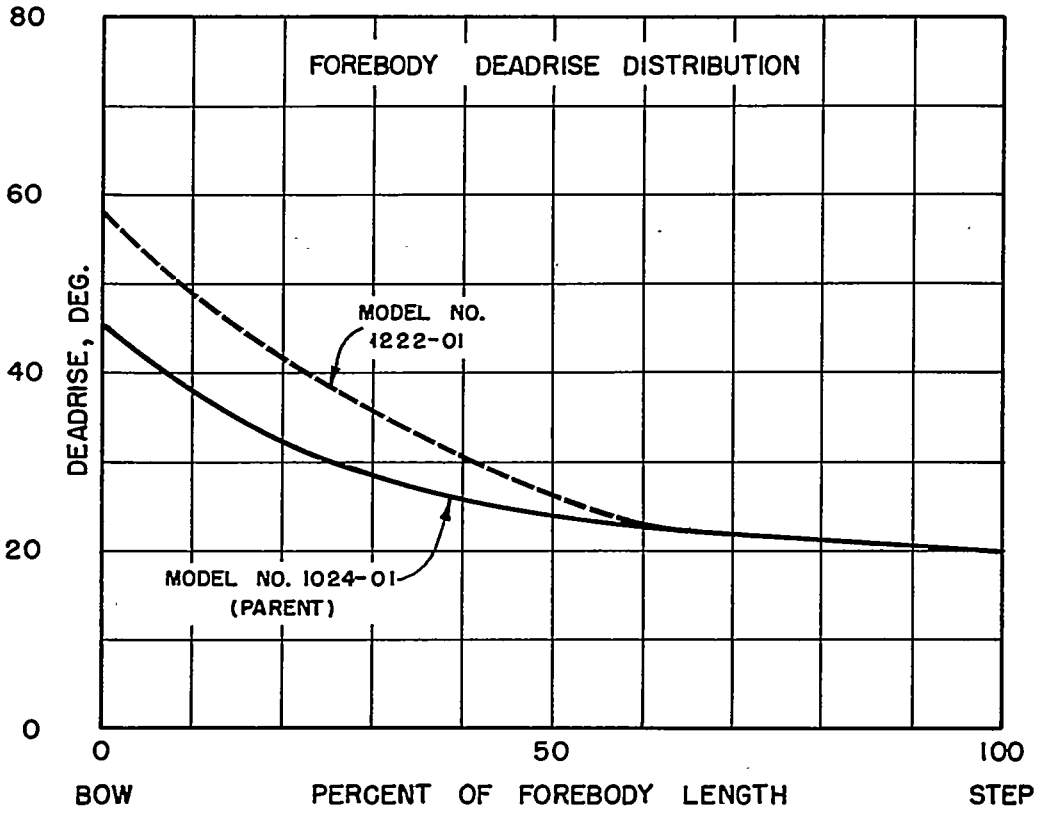

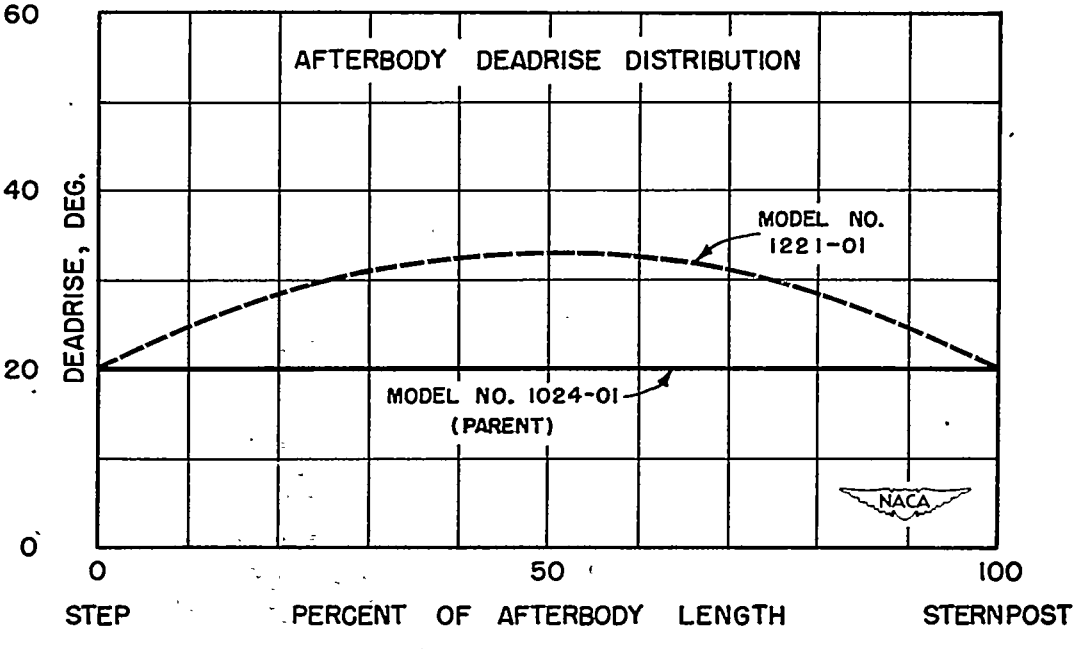

Figure 1.- Variation of dead rise with forebody and afterbody length.

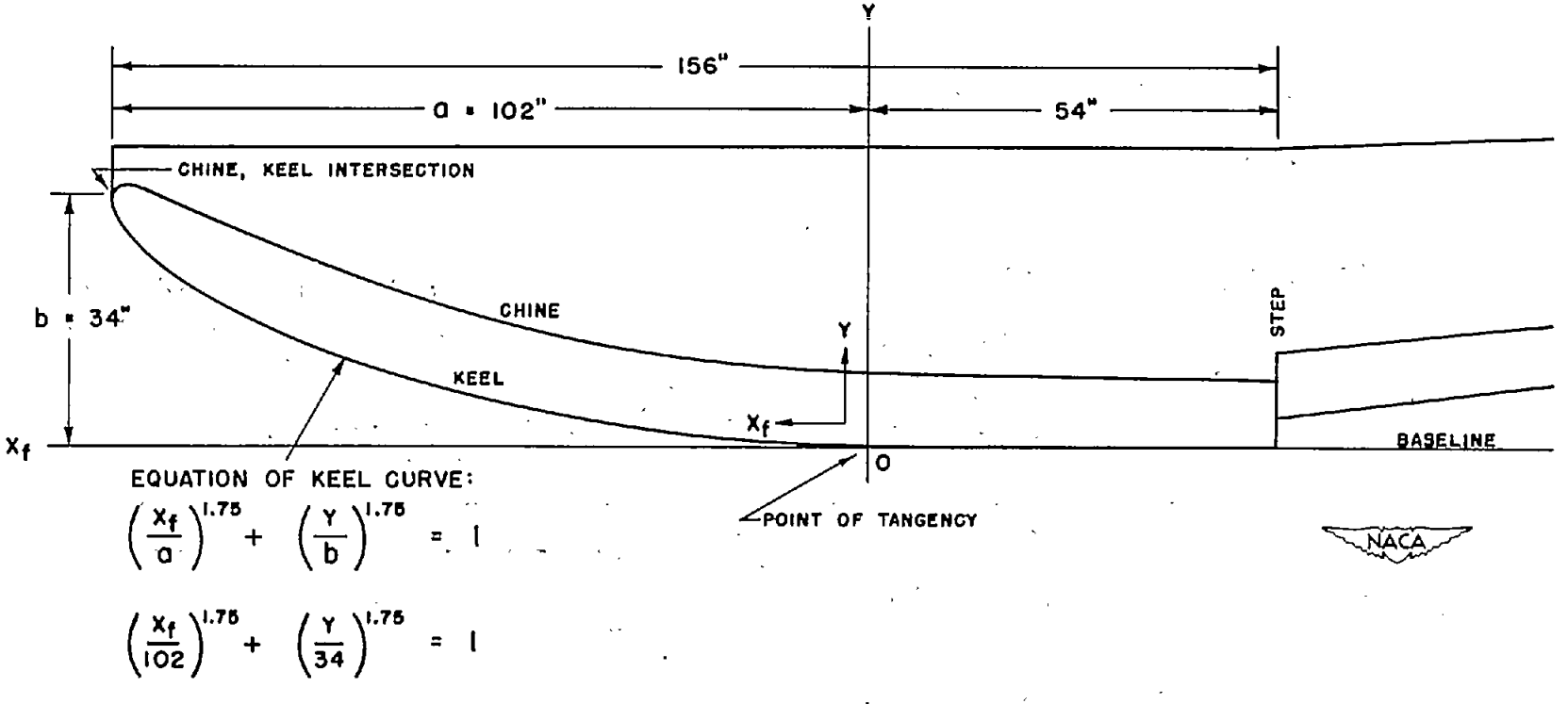

Figure 2.- Full-scale forebody keel curve equation.

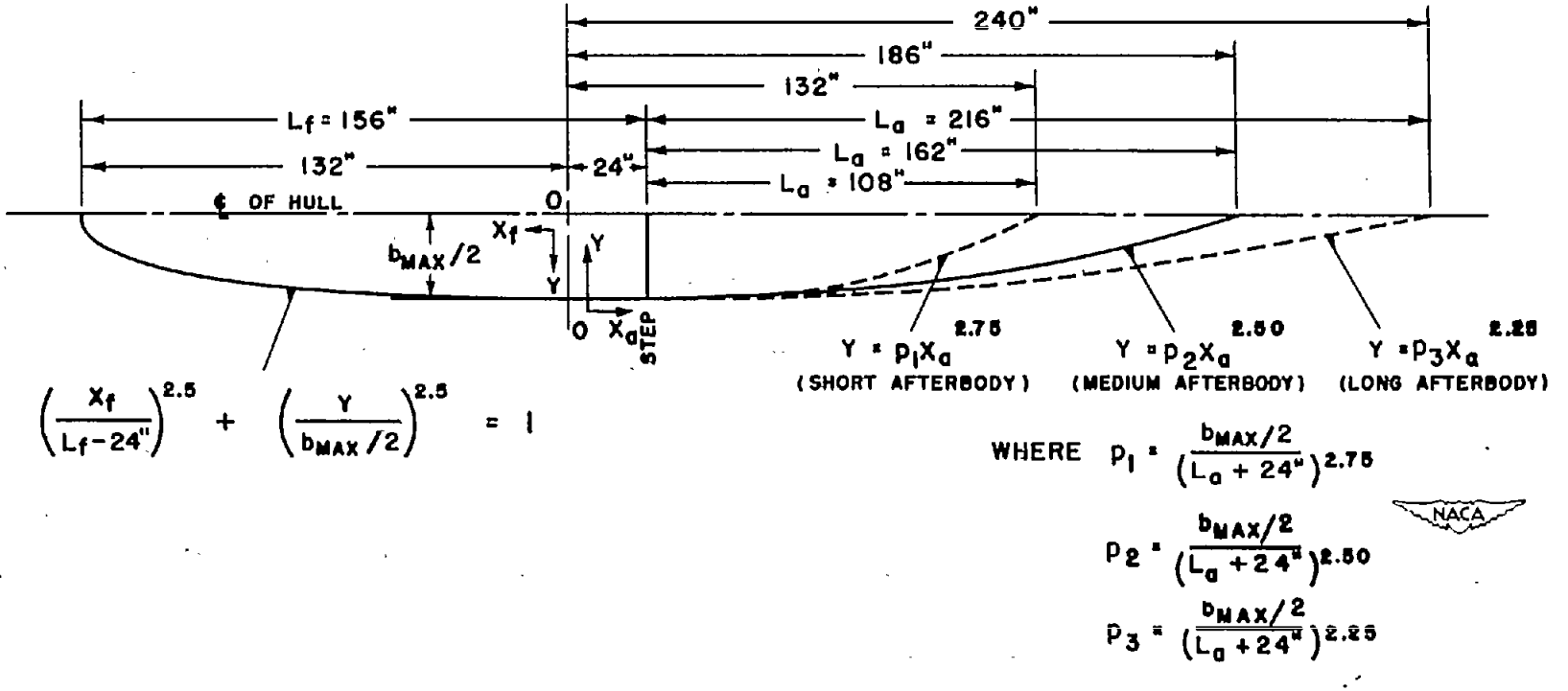

Figure 3.- Dimensions and full-scale plan-form curve equations.

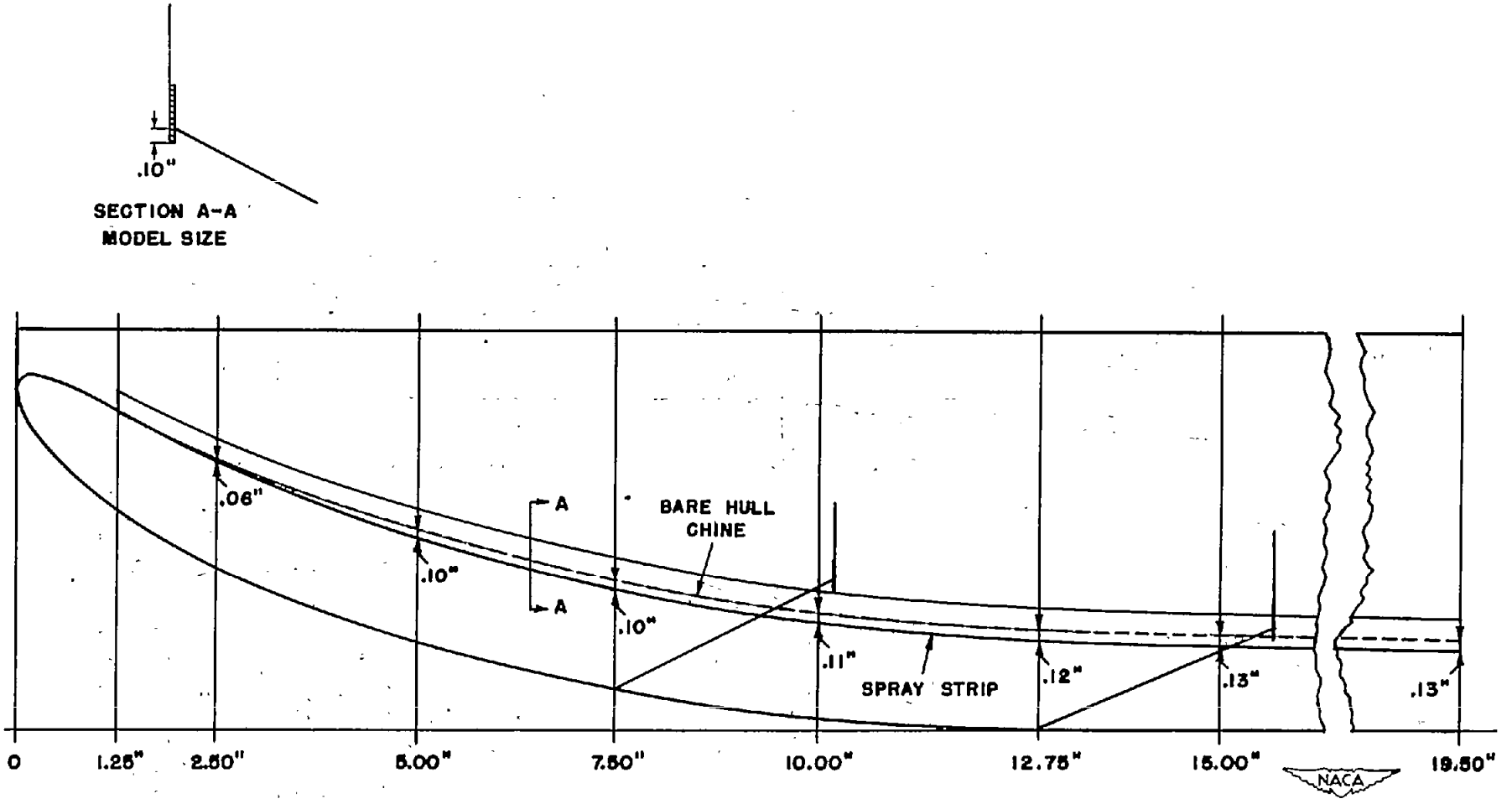

NOTES:

DIMENSIONS ARE IN INCHES FOR MODEL.

DRAWING ONE-HALF MODEL SIZE.

Figure 4.- E.T.T. series. Spray strip used on forebodies; spray strip 1/32 inch thick set flush with side of hull.

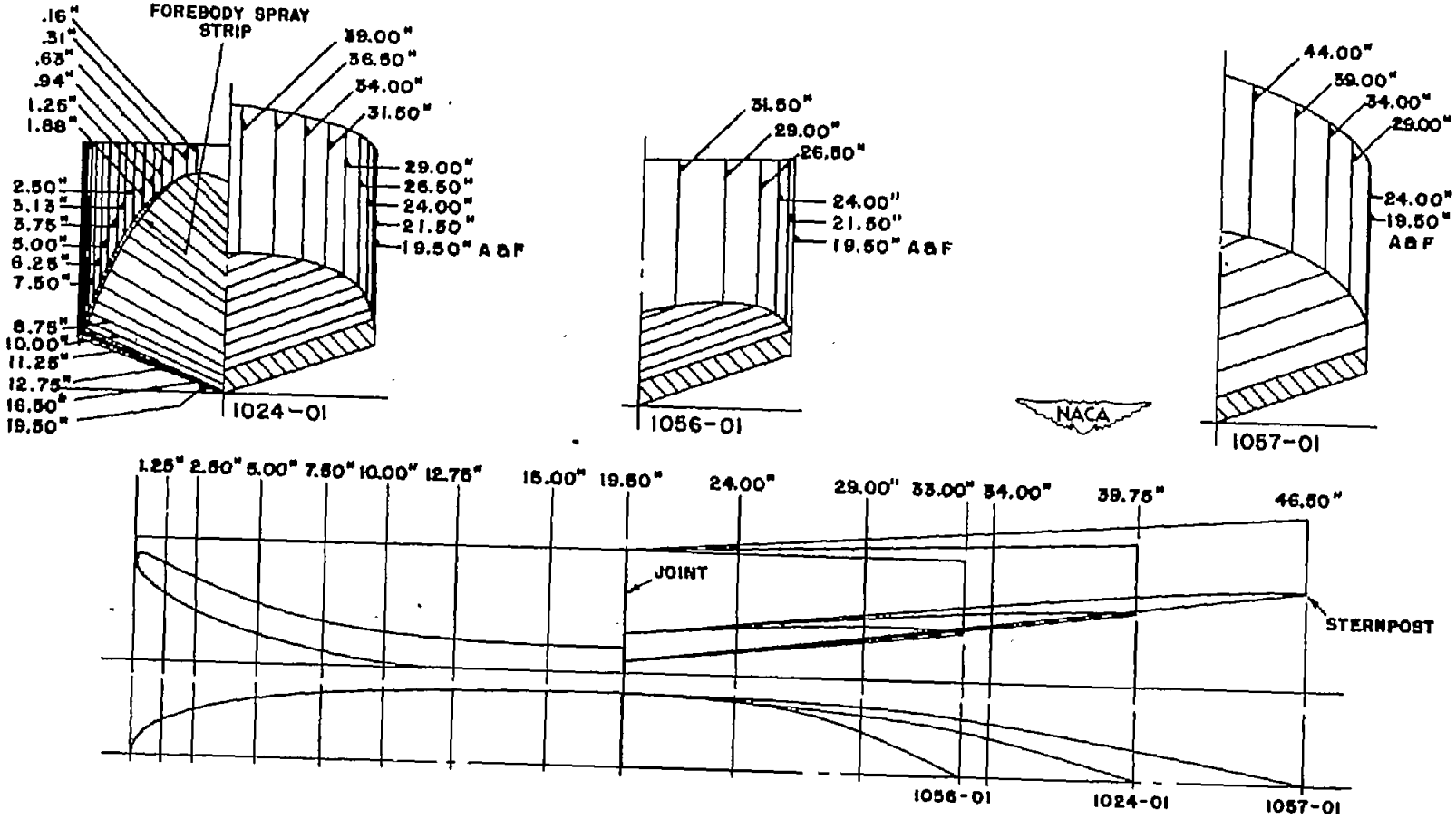

Figure 5.- E.T.T. series model hull lines with maximum beam of 6.00 inches.

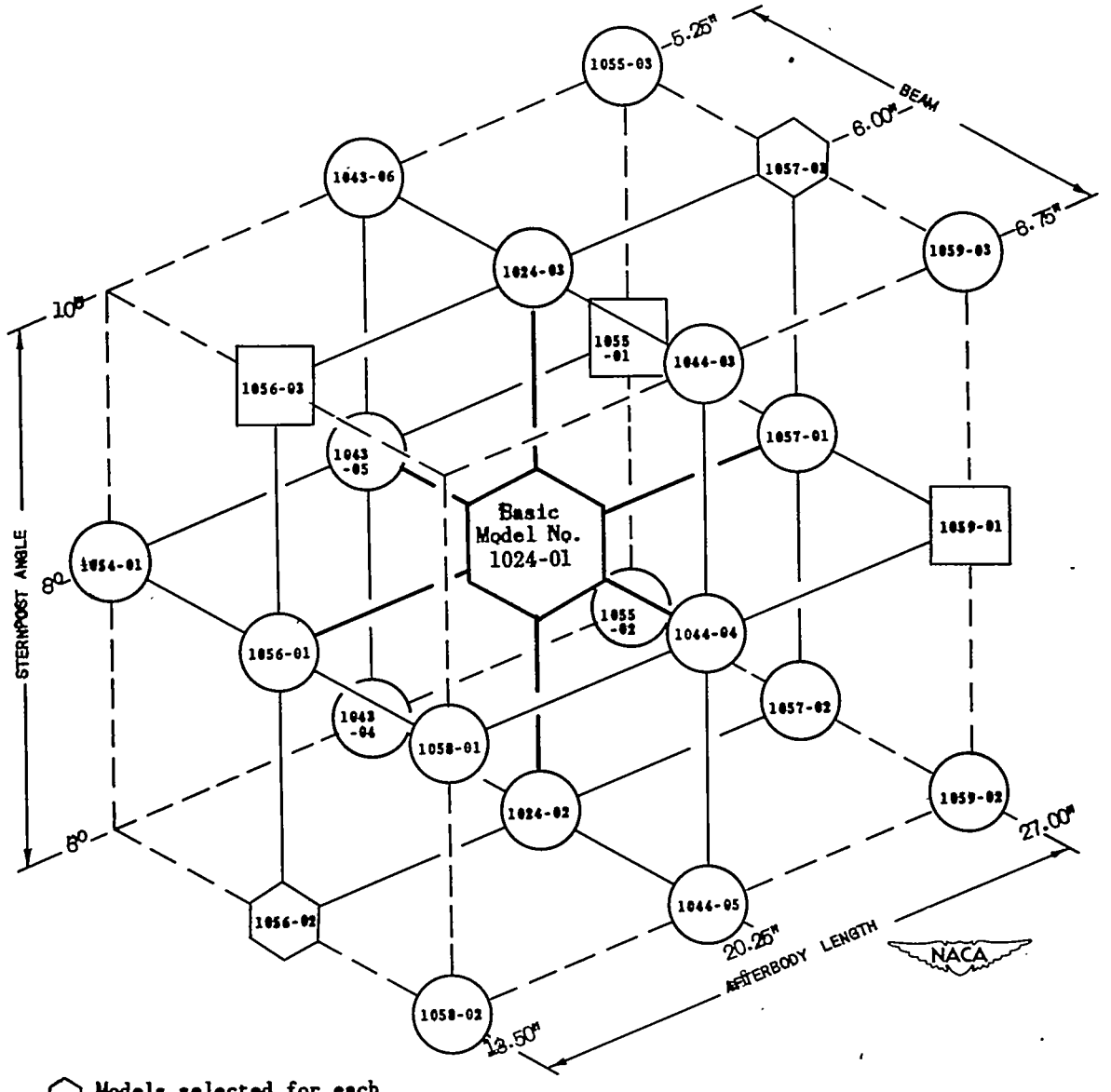

⬡ Models selected for each afterbody length for phase 3.

○ Other models tested.

□ Not tested.

Figure 6.- E.T.T. series.

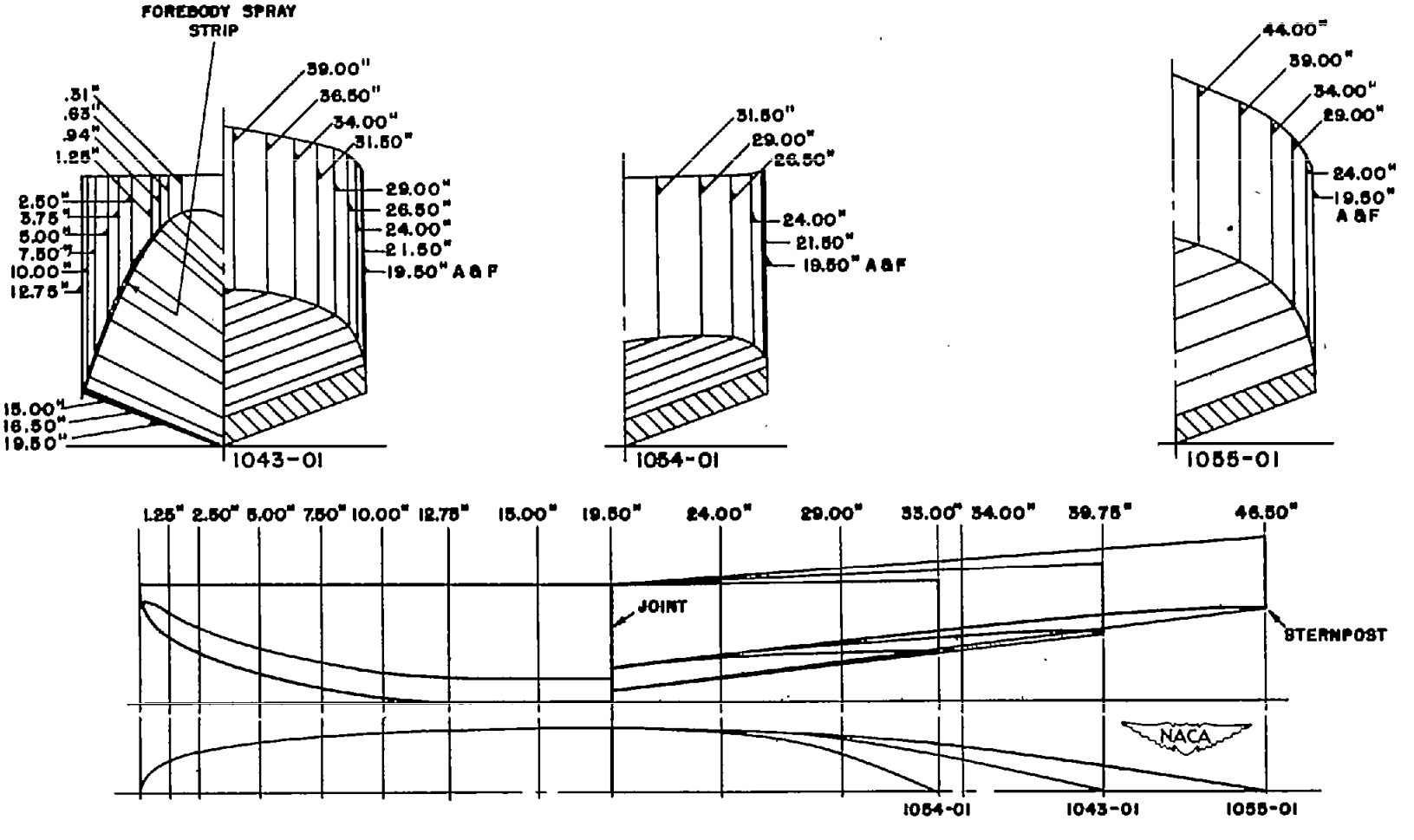

Figure 7.- E.T.T. series model hull lines with maximum beam of 5.25 inches.

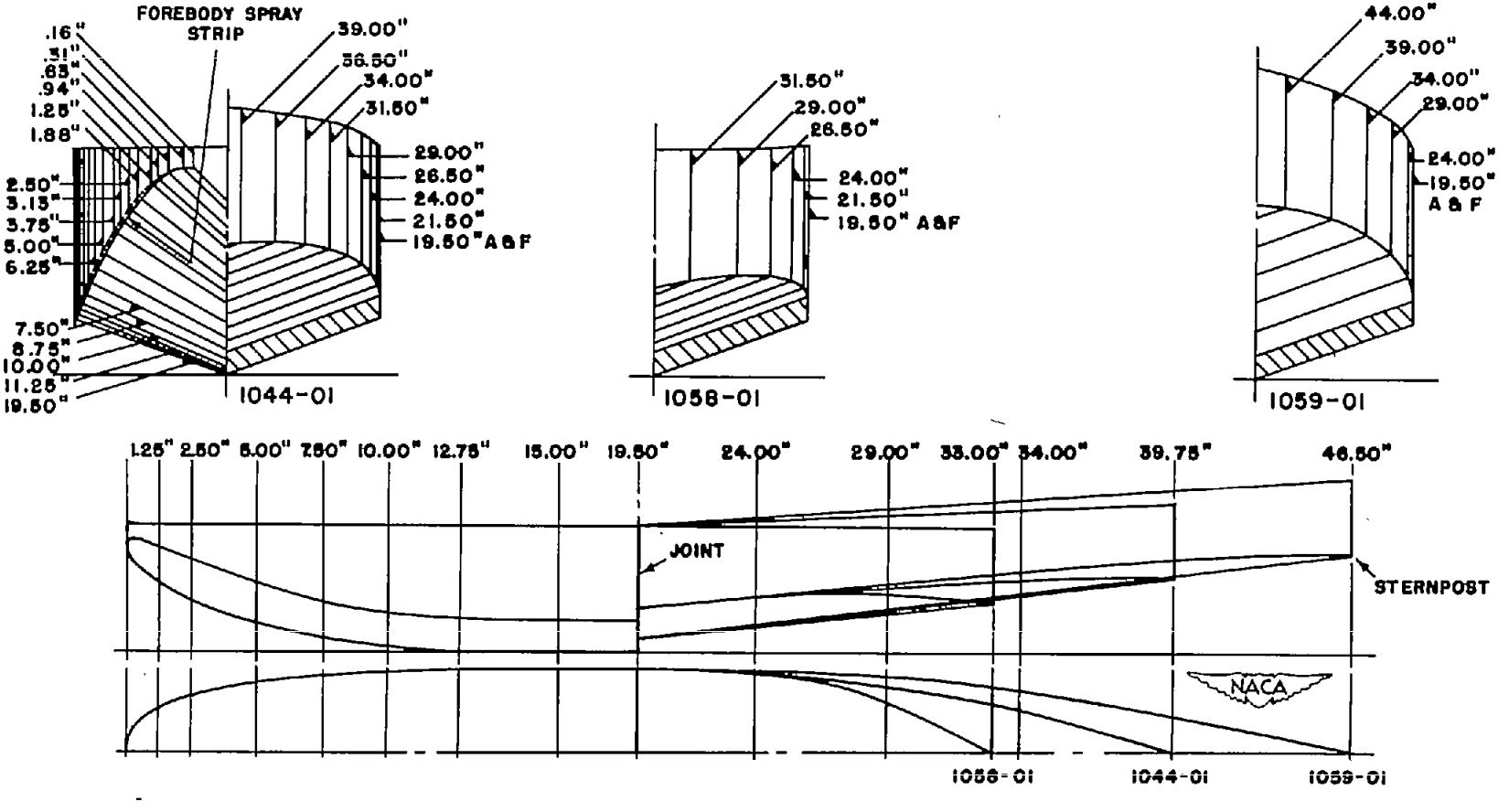

Figure 8.- E.T.T. series model hull lines with maximum beam of 6.75 inches.

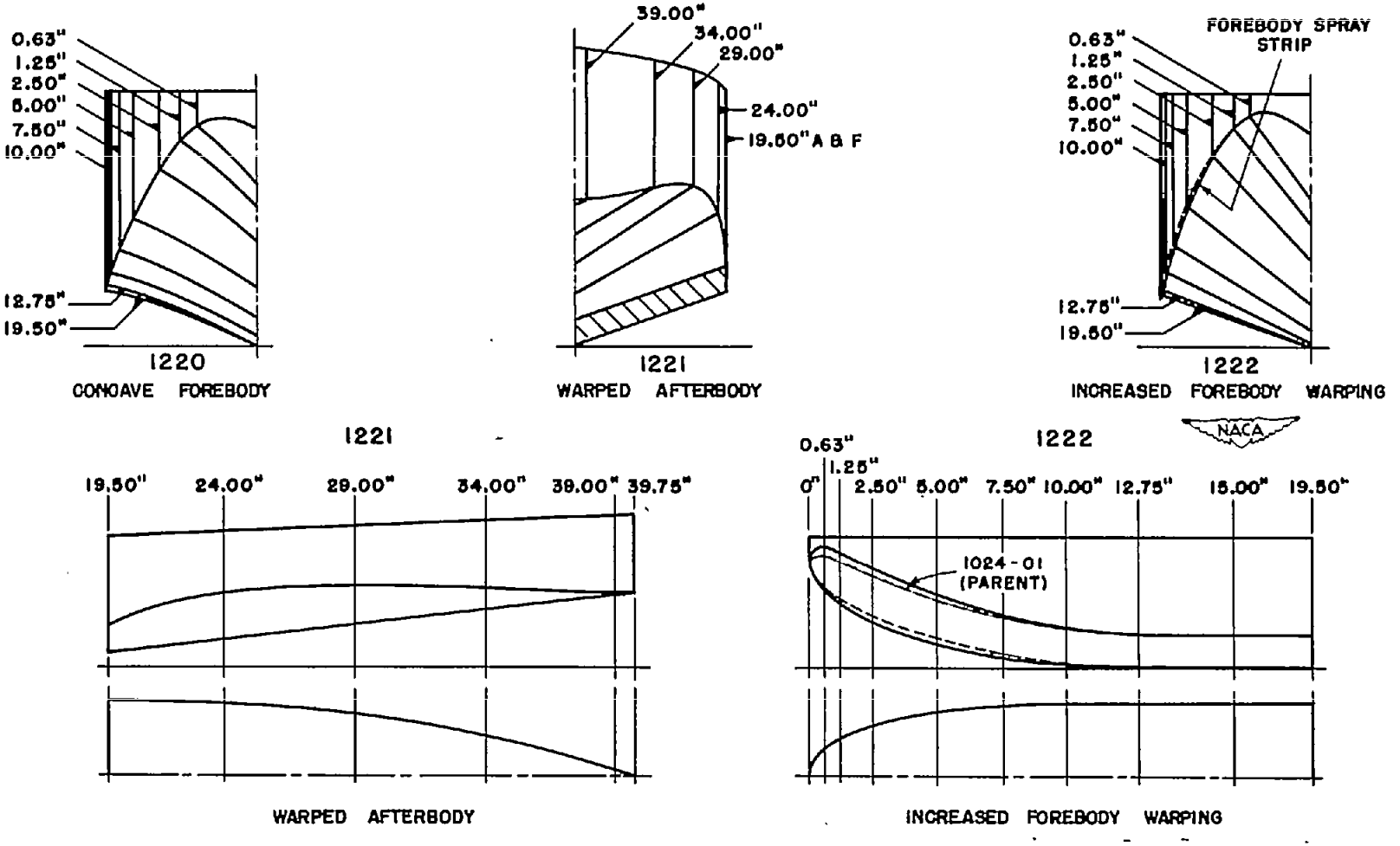

Figure 9.- E.T.T. series hull alterations. Maximum beam, 6.00 inches.

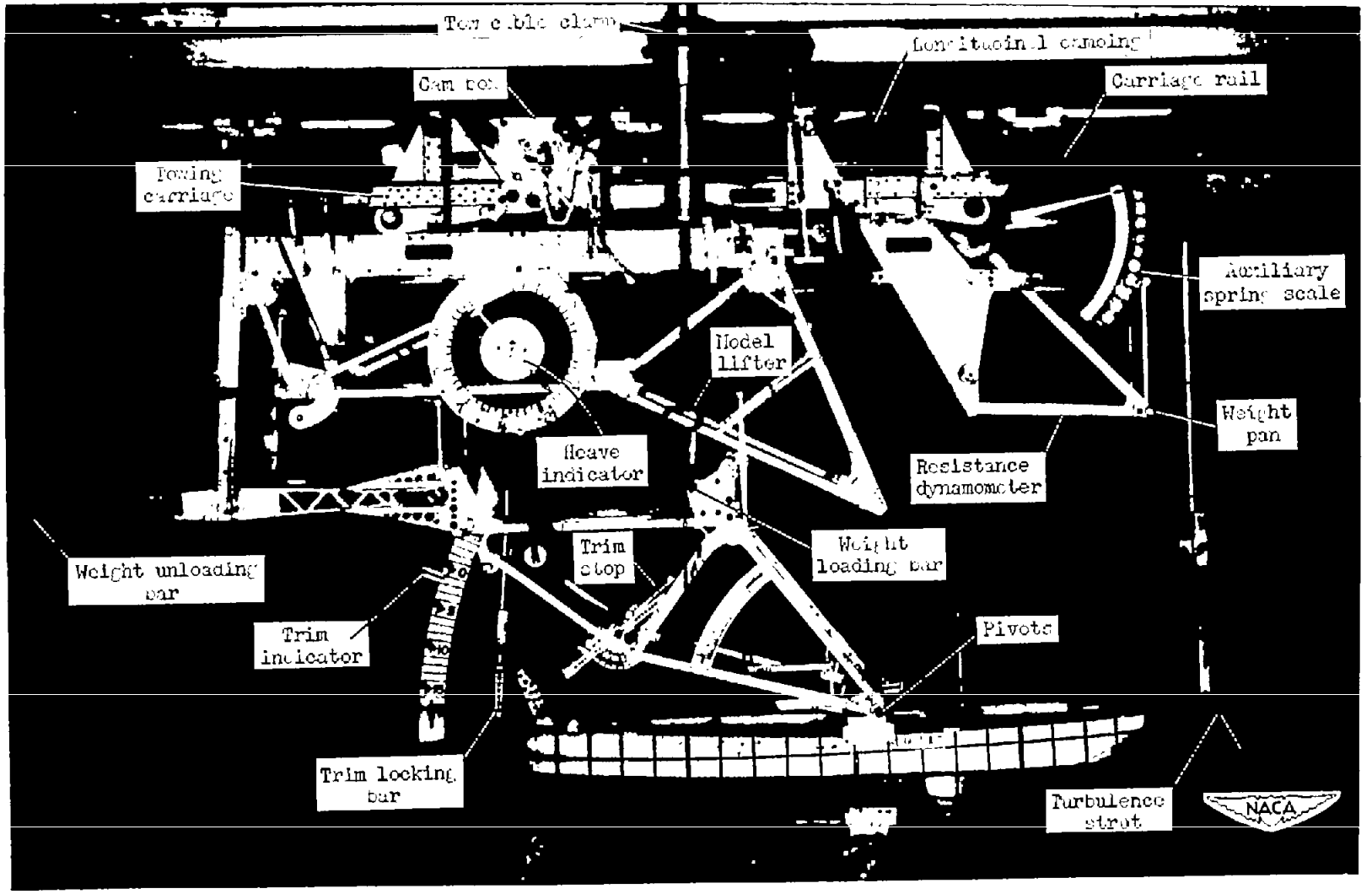

Figure 10.- Apparatus used in tests for characteristics of spray, resistance, longitudinal stability, and static properties.

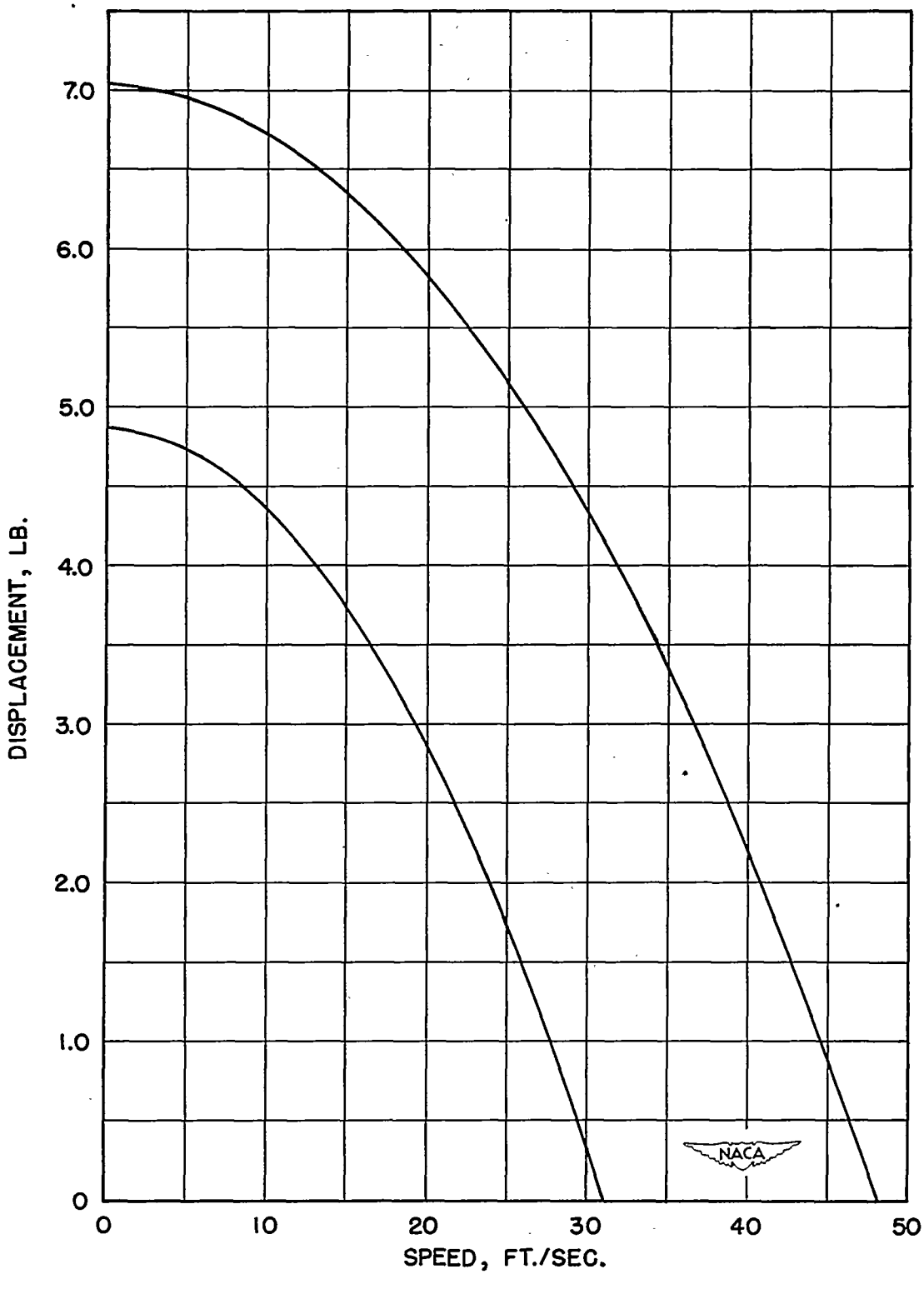

Figure 11.- E.T.T. series load and speed range for model tests.

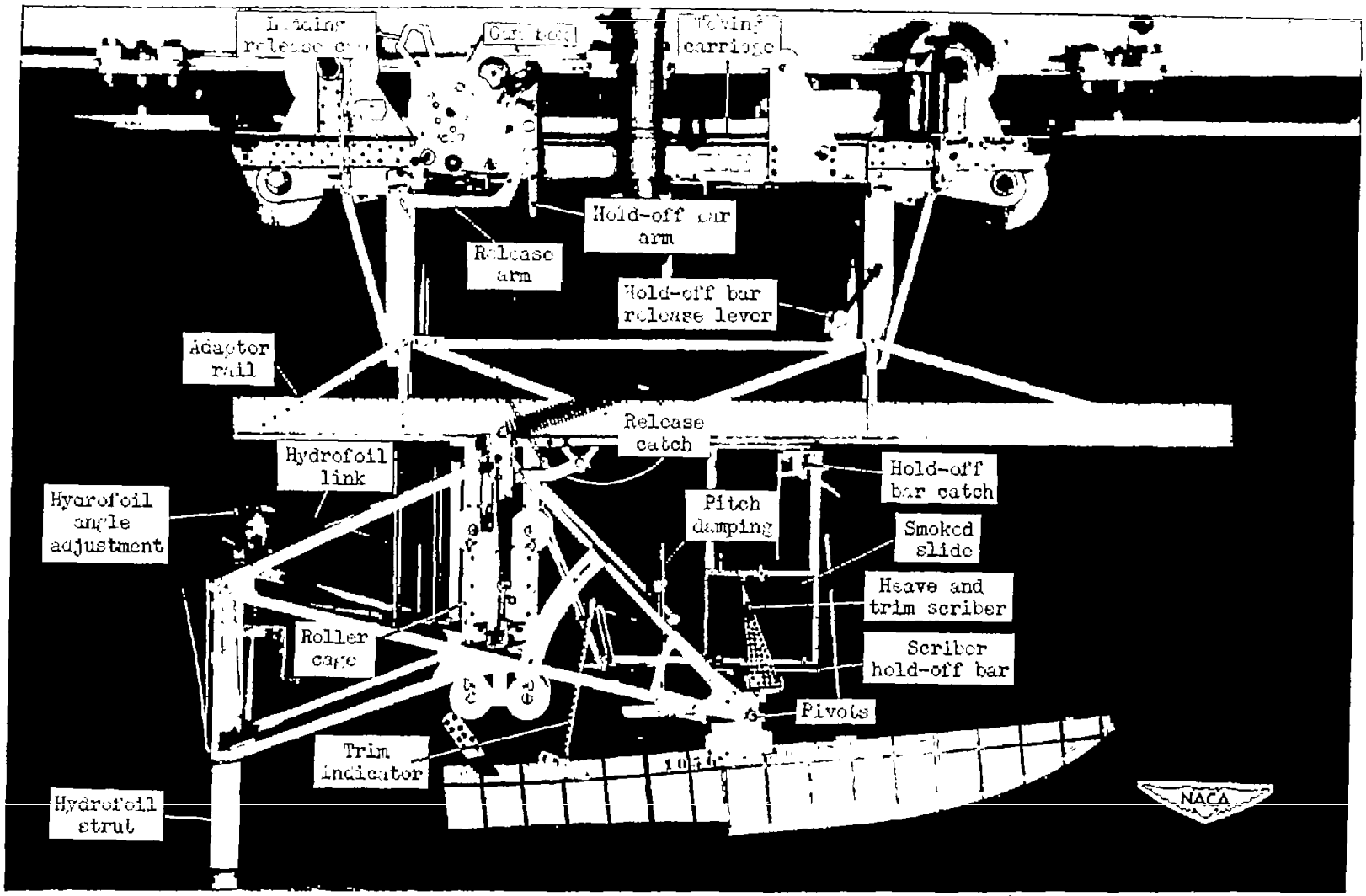

Figure 12.- Apparatus used in test for skipping characteristics.

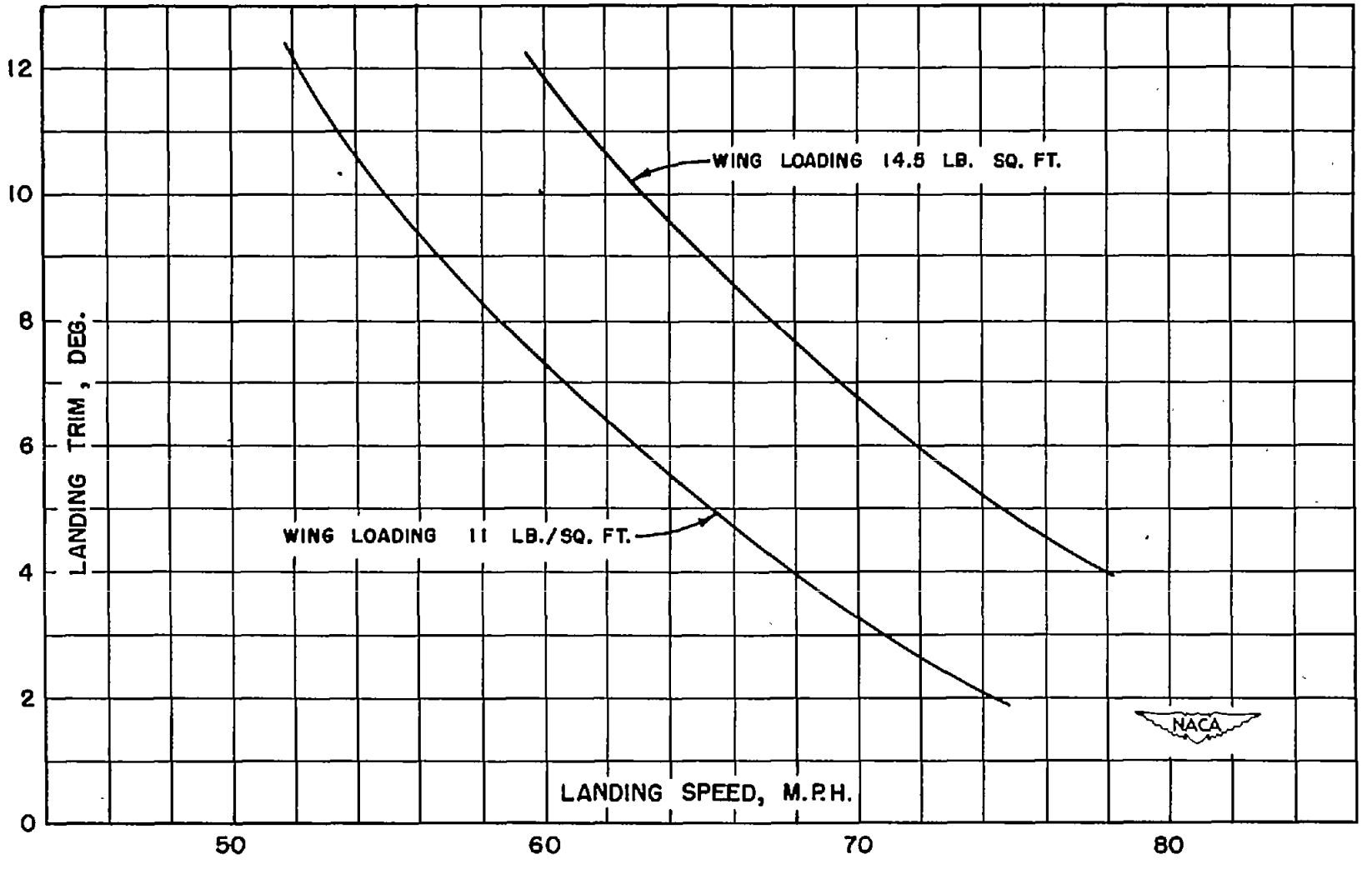

Figure 13.- Landing trim and speed for gross load of 3000 pounds (zero glide-path angle).

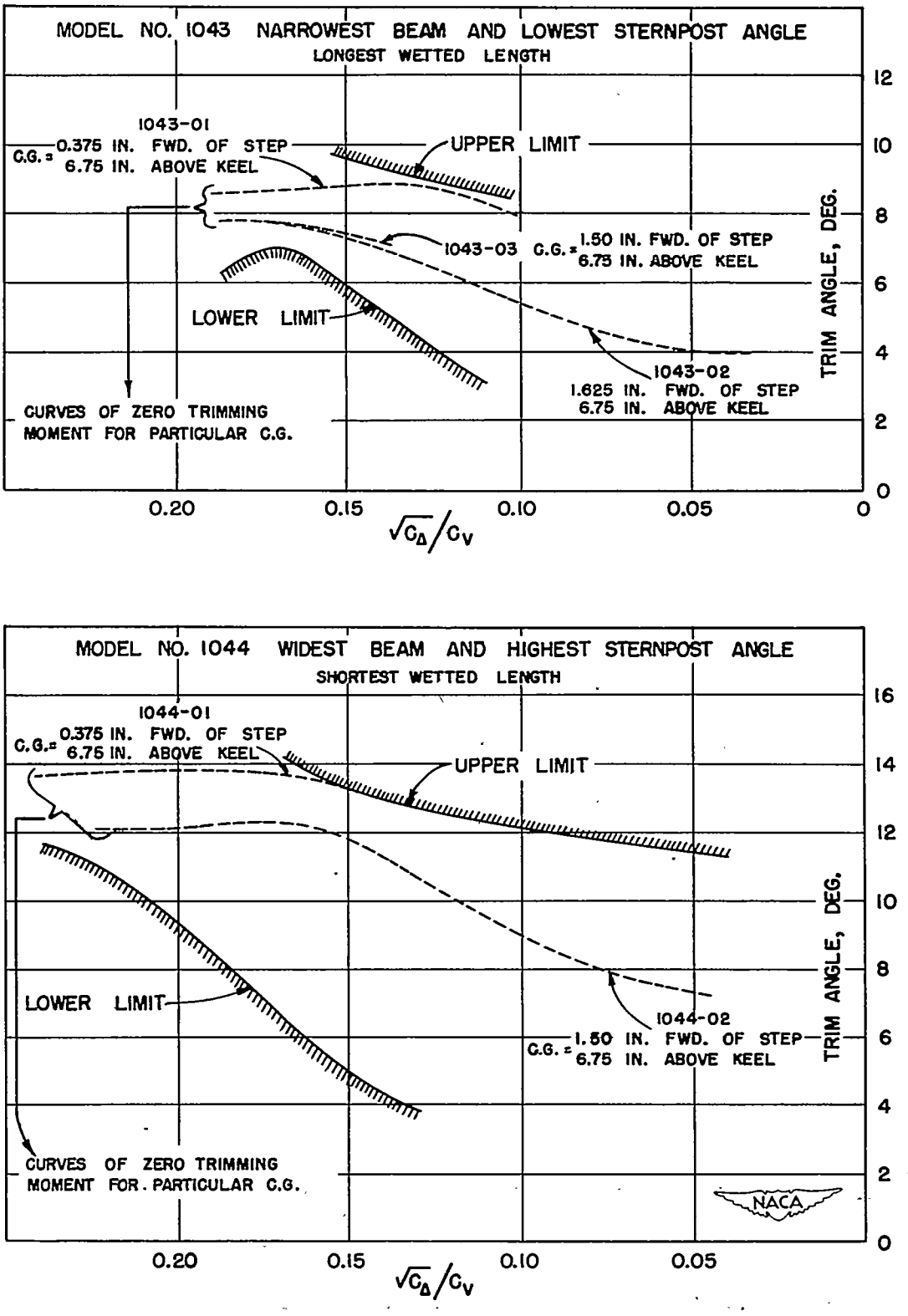

Figure 14.- Curves for determining longitudinal center-of-gravity location.

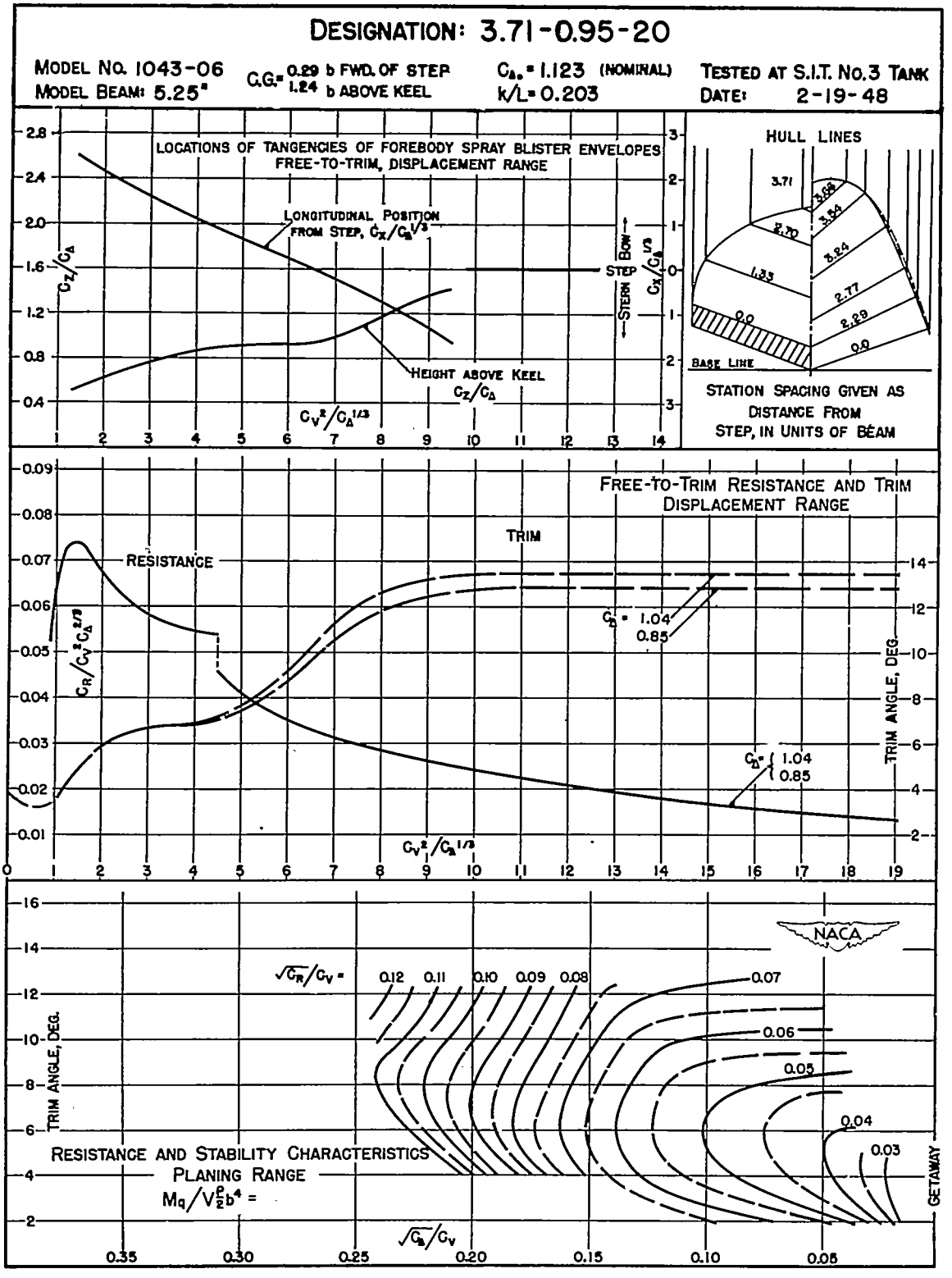
DESIGNATION: 3.71-0.95-20
MODEL NO. 1043-06
MODEL BEAM: 5.25"
C.G.= 0.29 b FWD. OF STEP
1.24 b ABOVE KEEL
C_Δ = 1.123 (NOMINAL)
k/L = 0.203
TESTED AT S.I.T. No.3 TANK
DATE: 2-19-48
LOCATIONS OF TANGENCIES OF FOREBODY SPRAY BLISTER ENVELOPES FREE-TO-TRIM, DISPLACEMENT RANGE
LONGITUDINAL POSITION FROM STEP, $C_x/C_\Delta^{1/3}$
HEIGHT ABOVE KEEL C_z/C_Δ
C_z/C_Δ
$C_x/C_\Delta^{1/3}$
BOW
STEP
STERN
$C_V^2/C_\Delta^{1/3}$
HULL LINES
3.71
3.08
3.34
2.70
2.24
1.33
2.77
2.29
0.0
0.0
BASE LINE
STATION SPACING GIVEN AS DISTANCE FROM STEP, IN UNITS OF BEAM
FREE-TO-TRIM RESISTANCE AND TRIM DISPLACEMENT RANGE
RESISTANCE
TRIM
C_Δ = 1.04
0.85
$C_R/C_V^2C_\Delta^{2/3}$
TRIM ANGLE, DEG.
$C_V^2/C_\Delta^{1/3}$
RESISTANCE AND STABILITY CHARACTERISTICS
PLANING RANGE
$Mq/V\rho b^4$ =
$\sqrt{C_R}/C_V$ =
0.12 0.11 0.10 0.09 0.08 0.07 0.06 0.05 0.04 0.03
GETAWAY
$\sqrt{C_\Delta}/C_V$
NACA

Figure 15.

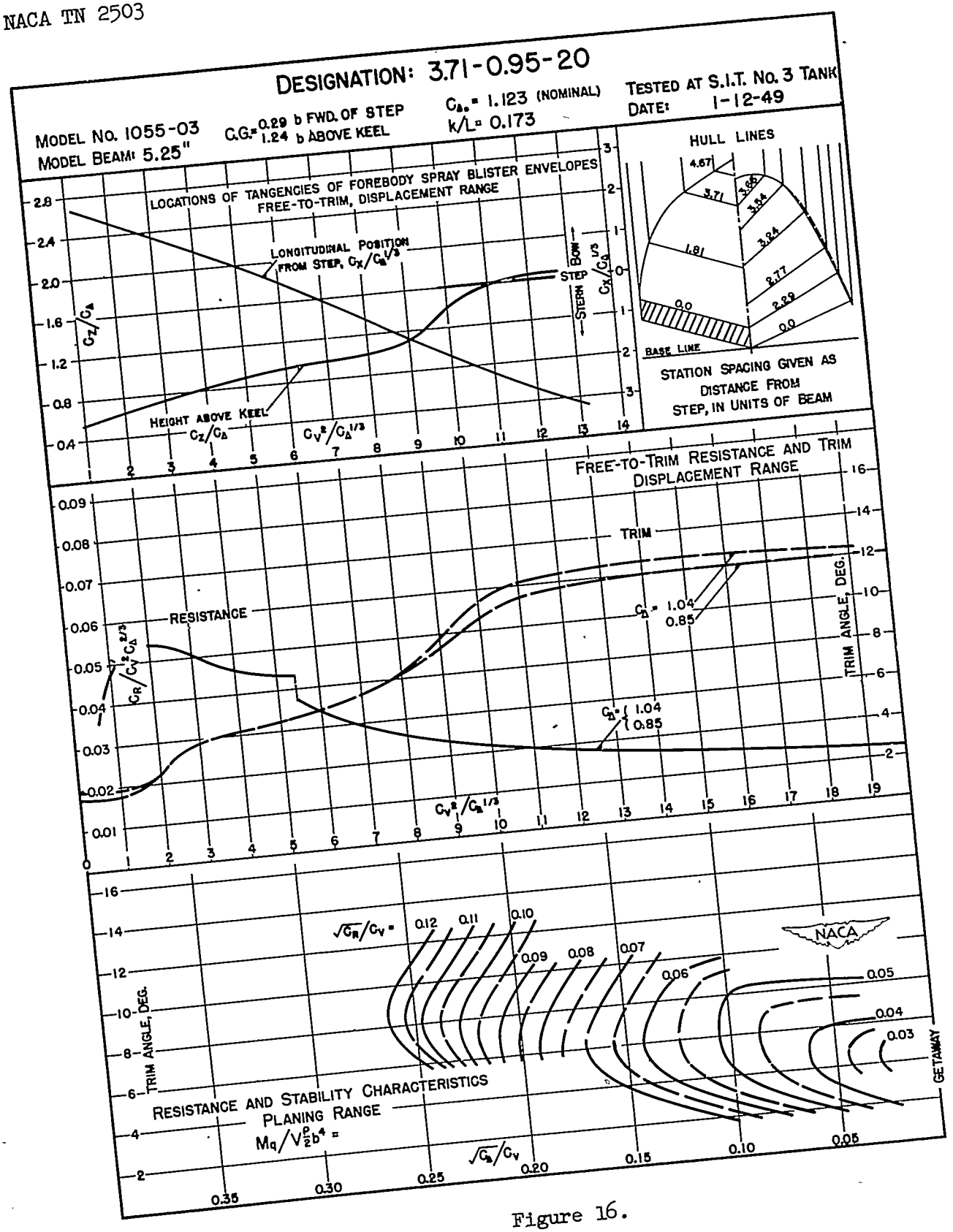
DESIGNATION: 3.71-0.95-20
MODEL NO. 1055-03
MODEL BEAM: 5.25"
C.G.= 0.29 b FWD. OF STEP
1.24 b ABOVE KEEL
C_{Δ_0} = 1.123 (NOMINAL)
k/L= 0.173
TESTED AT S.I.T. No. 3 TANK
DATE: 1-12-49
LOCATIONS OF TANGENCIES OF FOREBODY SPRAY BLISTER ENVELOPES FREE-TO-TRIM, DISPLACEMENT RANGE
LONGITUDINAL POSITION FROM STEP, $C_X/C_\Delta^{1/3}$
HEIGHT ABOVE KEEL
C_Z/C_Δ
$C_V^2/C_\Delta^{1/3}$
STEP
BOW
STERN
$C_X/C_\Delta^{1/3}$
HULL LINES
4.67
3.71
3.65
3.54
3.24
3.77
2.89
1.81
0.0
BASE LINE
STATION SPACING GIVEN AS DISTANCE FROM STEP, IN UNITS OF BEAM
FREE-TO-TRIM RESISTANCE AND TRIM DISPLACEMENT RANGE
RESISTANCE
TRIM
C_Δ = 1.04
0.85
$C_R/C_V^2C_\Delta^{2/3}$
TRIM ANGLE, DEG.
RESISTANCE AND STABILITY CHARACTERISTICS PLANING RANGE
$Mq/V\frac{\rho}{2}b^4$ =
$\sqrt{C_R}/C_V$ = 0.12 0.11 0.10 0.09 0.08 0.07 0.06 0.05 0.04 0.03
NACA
GETAWAY
$\sqrt{C_\Delta}/C_V$

Figure 16.

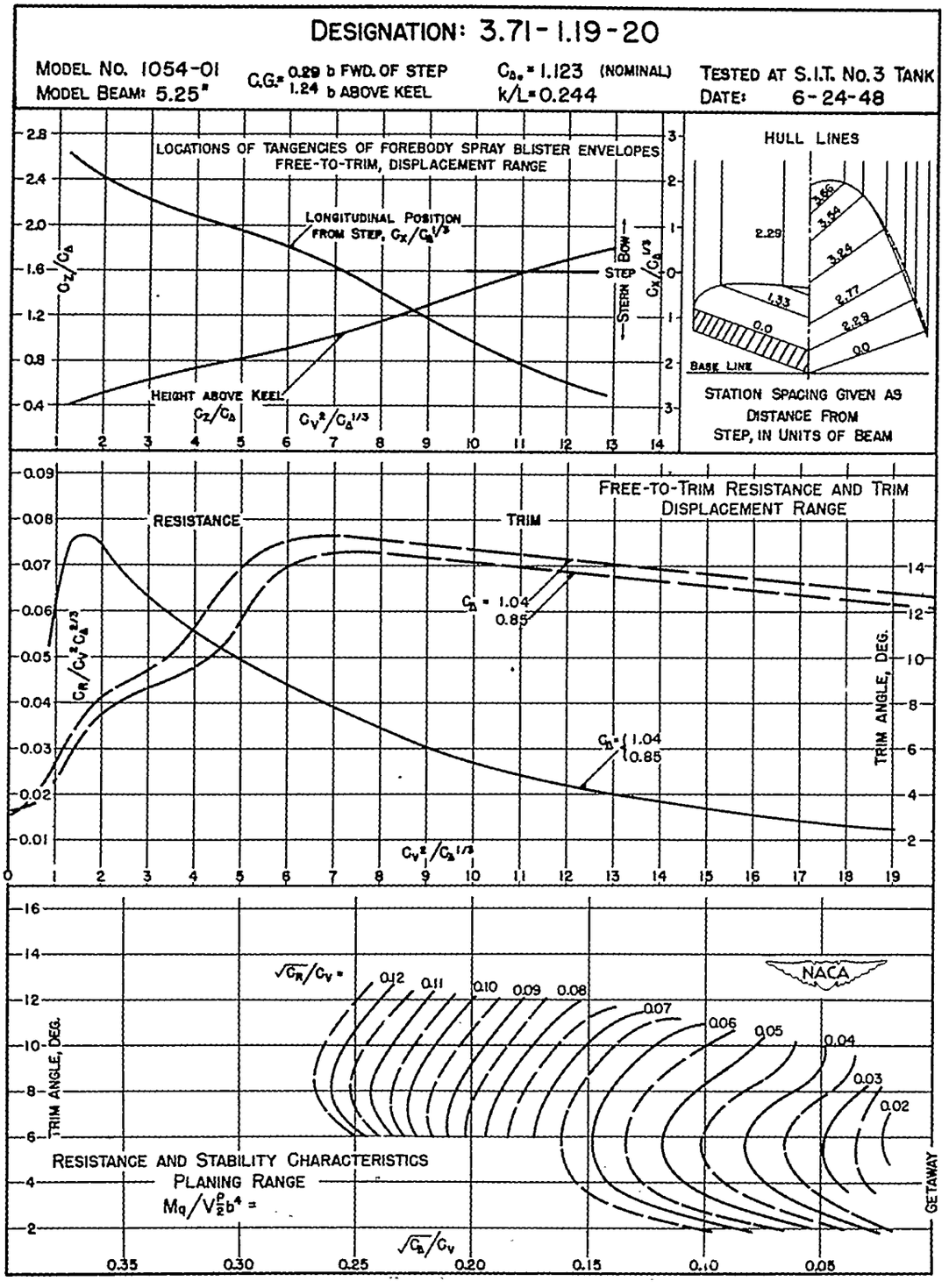
DESIGNATION: 3.71-1.19-20
MODEL NO. 1054-01
MODEL BEAM: 5.25"
C.G.: 0.29 b FWD. OF STEP
1.24 b ABOVE KEEL
C_{Δ_o} = 1.123 (NOMINAL)
k/L = 0.244
TESTED AT S.I.T. No.3 TANK
DATE: 6-24-48
LOCATIONS OF TANGENCIES OF FOREBODY SPRAY BLISTER ENVELOPES FREE-TO-TRIM, DISPLACEMENT RANGE
LONGITUDINAL POSITION FROM STEP, $C_X/C_\Delta^{1/3}$
HEIGHT ABOVE KEEL, C_Z/C_Δ
$C_V^2/C_\Delta^{1/3}$
STEP
BOW
STERN
HULL LINES
2.29
1.33
0.0
3.66
3.44
3.24
2.77
2.29
0.0
BASE LINE
STATION SPACING GIVEN AS DISTANCE FROM STEP, IN UNITS OF BEAM
FREE-TO-TRIM RESISTANCE AND TRIM DISPLACEMENT RANGE
RESISTANCE
TRIM
C_Δ = 1.04
0.85
$C_R/C_V^2C_\Delta^{2/3}$
TRIM ANGLE, DEG.
RESISTANCE AND STABILITY CHARACTERISTICS
PLANING RANGE
$Mq/V\frac{\rho}{2}b^4$ =
$\sqrt{C_R}/C_V$ =
0.12
0.11
0.10
0.09
0.08
0.07
0.06
0.05
0.04
0.03
0.02
NACA
$\sqrt{C_\Delta}/C_V$
GETAWAY

Figure 17.

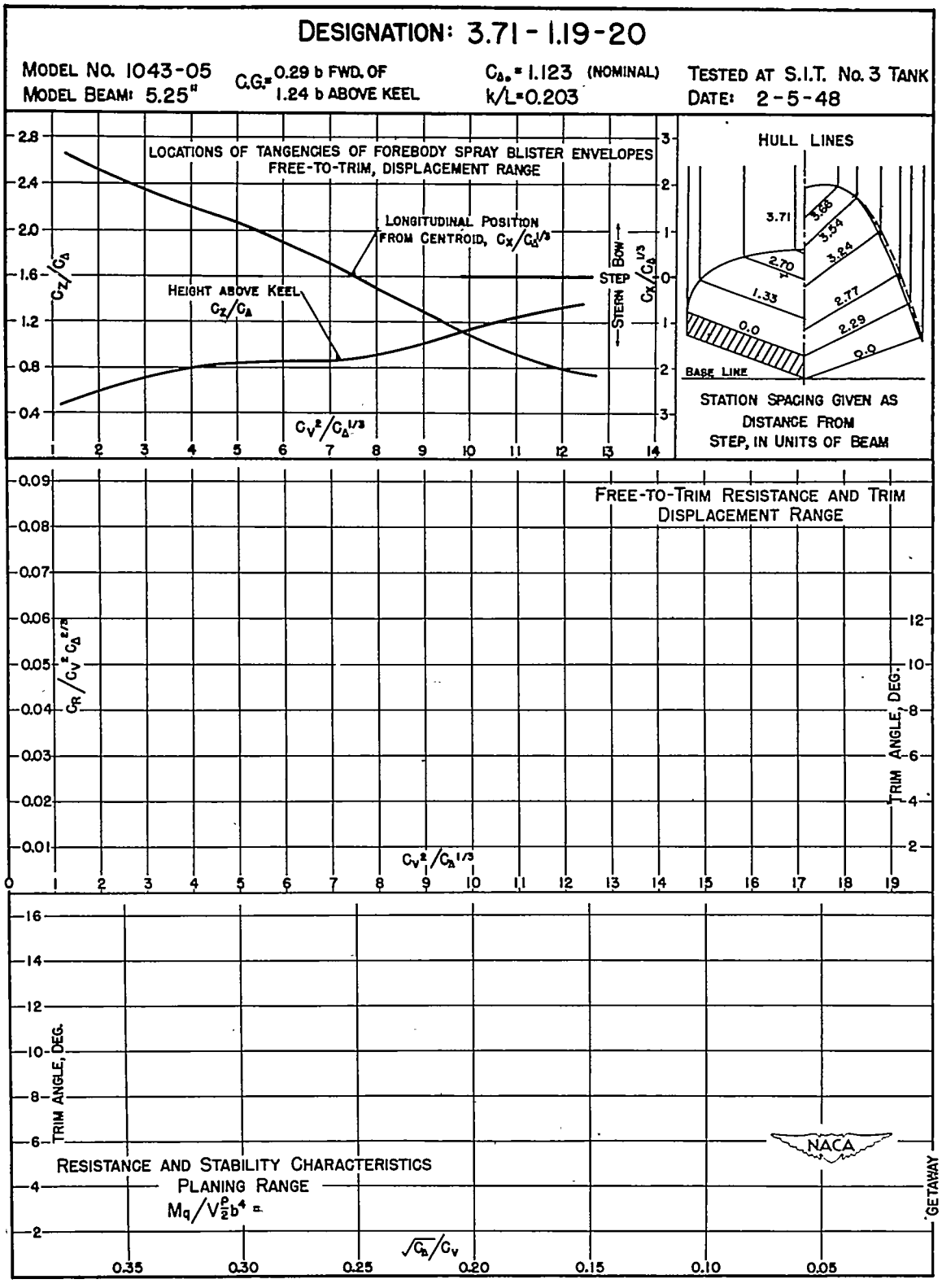
DESIGNATION: 3.71 - 1.19 - 20
MODEL NO. 1043-05
MODEL BEAM: 5.25"
C.G. = 0.29 b FWD. OF 1.24 b ABOVE KEEL
C_{Δ_0} = 1.123 (NOMINAL)
k/L = 0.203
TESTED AT S.I.T. No. 3 TANK
DATE: 2-5-48
LOCATIONS OF TANGENCIES OF FOREBODY SPRAY BLISTER ENVELOPES FREE-TO-TRIM, DISPLACEMENT RANGE
LONGITUDINAL POSITION FROM CENTROID, $C_x/C_\Delta^{1/3}$
HEIGHT ABOVE KEEL C_z/C_Δ
C_z/C_Δ
$C_x/C_\Delta^{1/3}$
BOW
STEP
STERN
$C_V^2/C_\Delta^{1/3}$
HULL LINES
3.71
3.68
3.54
3.84
2.70
1.33
2.77
2.29
0.0
0.0
BASE LINE
STATION SPACING GIVEN AS DISTANCE FROM STEP, IN UNITS OF BEAM
FREE-TO-TRIM RESISTANCE AND TRIM DISPLACEMENT RANGE
$C_R/C_V^2 C_\Delta^{2/3}$
TRIM ANGLE, DEG.
$C_V^2/C_\Delta^{1/3}$
RESISTANCE AND STABILITY CHARACTERISTICS
PLANING RANGE
$Mq/V\frac{\rho}{2}b^4$ =
$\sqrt{C_b}/C_V$
NACA
GETAWAY

Figure 18.

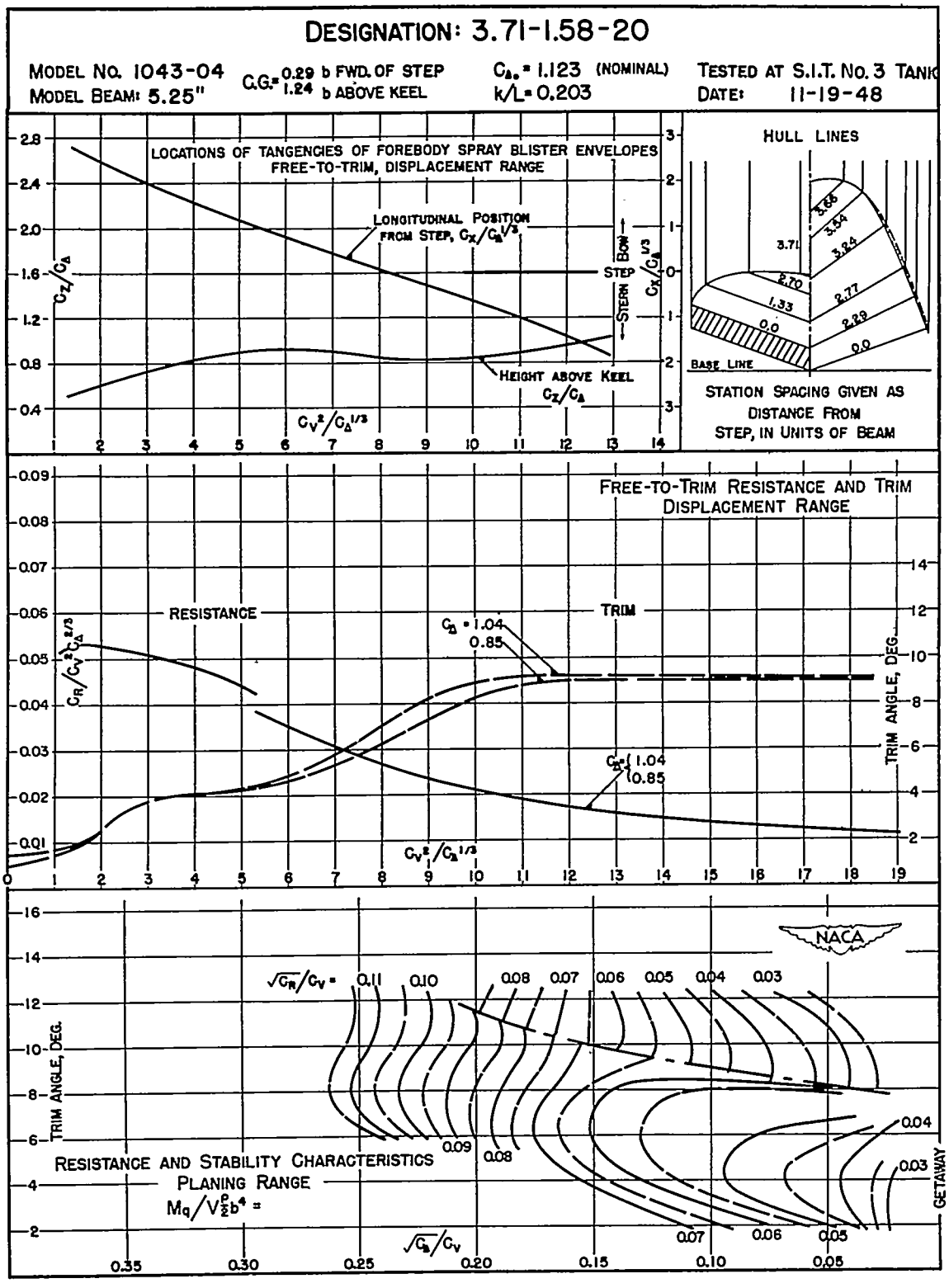
DESIGNATION: 3.71-1.58-20
MODEL NO. 1043-04
MODEL BEAM: 5.25"
C.G. 0.29 b FWD. OF STEP
1.24 b ABOVE KEEL
C_{Δ_o} = 1.123 (NOMINAL)
k/L = 0.203
TESTED AT S.I.T. No. 3 TANK
DATE: 11-19-48
LOCATIONS OF TANGENCIES OF FOREBODY SPRAY BLISTER ENVELOPES FREE-TO-TRIM, DISPLACEMENT RANGE
LONGITUDINAL POSITION FROM STEP, $C_x/C_\Delta^{1/3}$
HEIGHT ABOVE KEEL C_z/C_Δ
STEP
BOW
STERN
C_z/C_Δ
$C_x/C_\Delta^{1/3}$
$C_V^2/C_\Delta^{1/3}$
HULL LINES
3.85
3.54
3.24
3.71
2.70
2.77
1.33
2.29
0.0
0.0
BASE LINE
STATION SPACING GIVEN AS DISTANCE FROM STEP, IN UNITS OF BEAM
FREE-TO-TRIM RESISTANCE AND TRIM DISPLACEMENT RANGE
RESISTANCE
TRIM
C_Δ = 1.04
0.85
$C_R/C_V^2C_\Delta^{2/3}$
TRIM ANGLE, DEG.
$C_V^2/C_\Delta^{1/3}$
NACA
$\sqrt{C_R}/C_V$ = 0.11 0.10 0.09 0.08 0.07 0.06 0.05 0.04 0.03
TRIM ANGLE, DEG.
RESISTANCE AND STABILITY CHARACTERISTICS
PLANING RANGE
$M_q/V\sqrt{\rho}b^4$ =
$\sqrt{C_\Delta}/C_V$
GETAWAY

Figure 19.

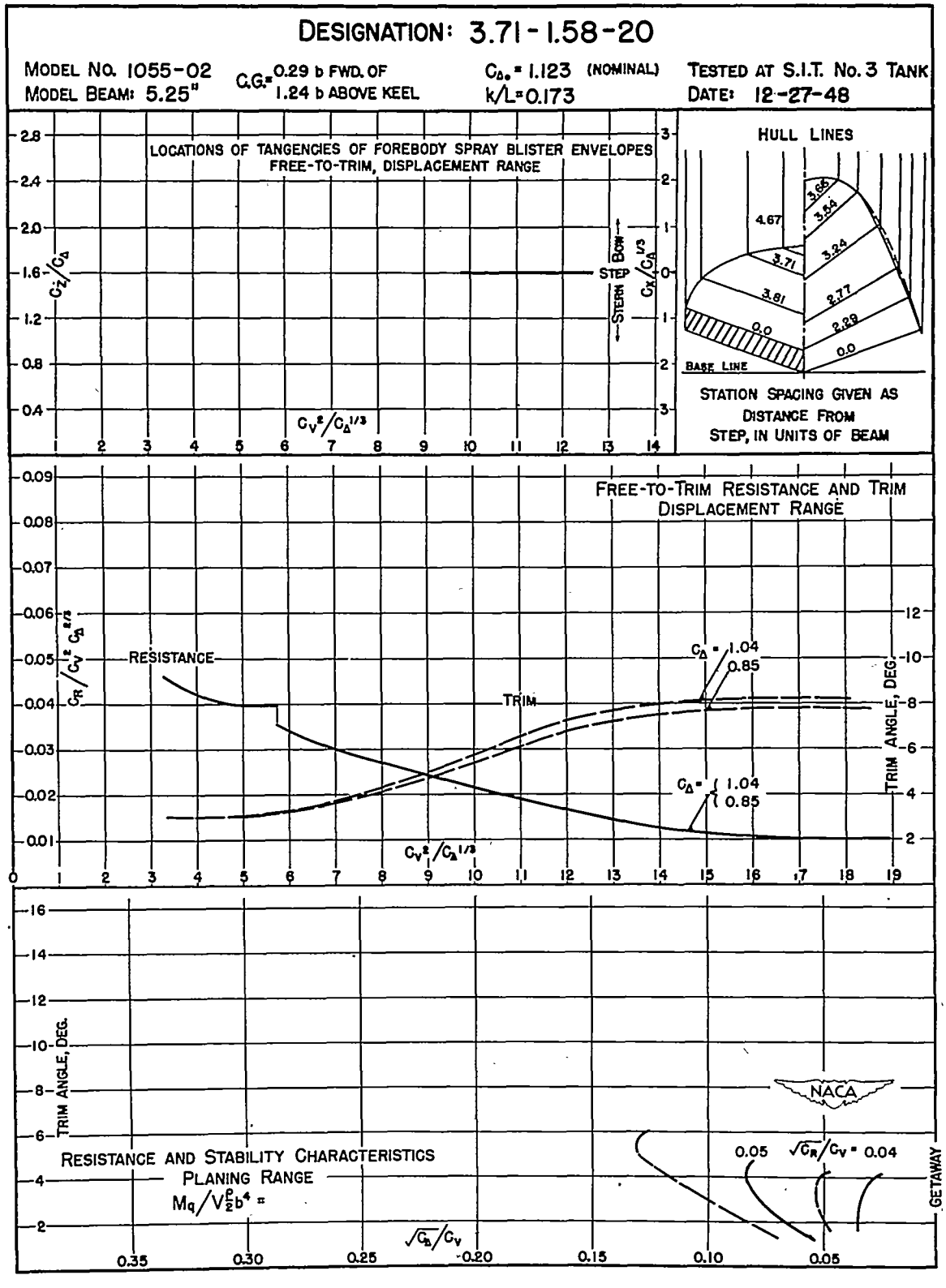
DESIGNATION: 3.71 - 1.58 - 20
MODEL NO. 1055-02
MODEL BEAM: 5.25"
C.G. 0.29 b FWD. OF 1.24 b ABOVE KEEL
C_{Δ_o} = 1.123 (NOMINAL)
k/L = 0.173
TESTED AT S.I.T. No. 3 TANK
DATE: 12-27-48
LOCATIONS OF TANGENCIES OF FOREBODY SPRAY BLISTER ENVELOPES FREE-TO-TRIM, DISPLACEMENT RANGE
C_z/C_Δ
$C_V^2/C_\Delta^{1/3}$
STEP
BOW
STERN
$C_x/C_\Delta^{1/3}$
HULL LINES
4.67
3.65
3.54
3.71
3.24
3.81
2.77
2.29
0.0
0.0
BASE LINE
STATION SPACING GIVEN AS DISTANCE FROM STEP, IN UNITS OF BEAM
FREE-TO-TRIM RESISTANCE AND TRIM DISPLACEMENT RANGE
$C_R/C_V^2 C_\Delta^{1/3}$
RESISTANCE
TRIM
C_Δ = 1.04
0.85
TRIM ANGLE, DEG.
RESISTANCE AND STABILITY CHARACTERISTICS
PLANING RANGE
$Mq/V\frac{\rho}{2}b^4$ =
$\sqrt{C_R}/C_V$
0.05 $\sqrt{C_R}/C_V$ = 0.04
NACA
GETAWAY

Figure 20.

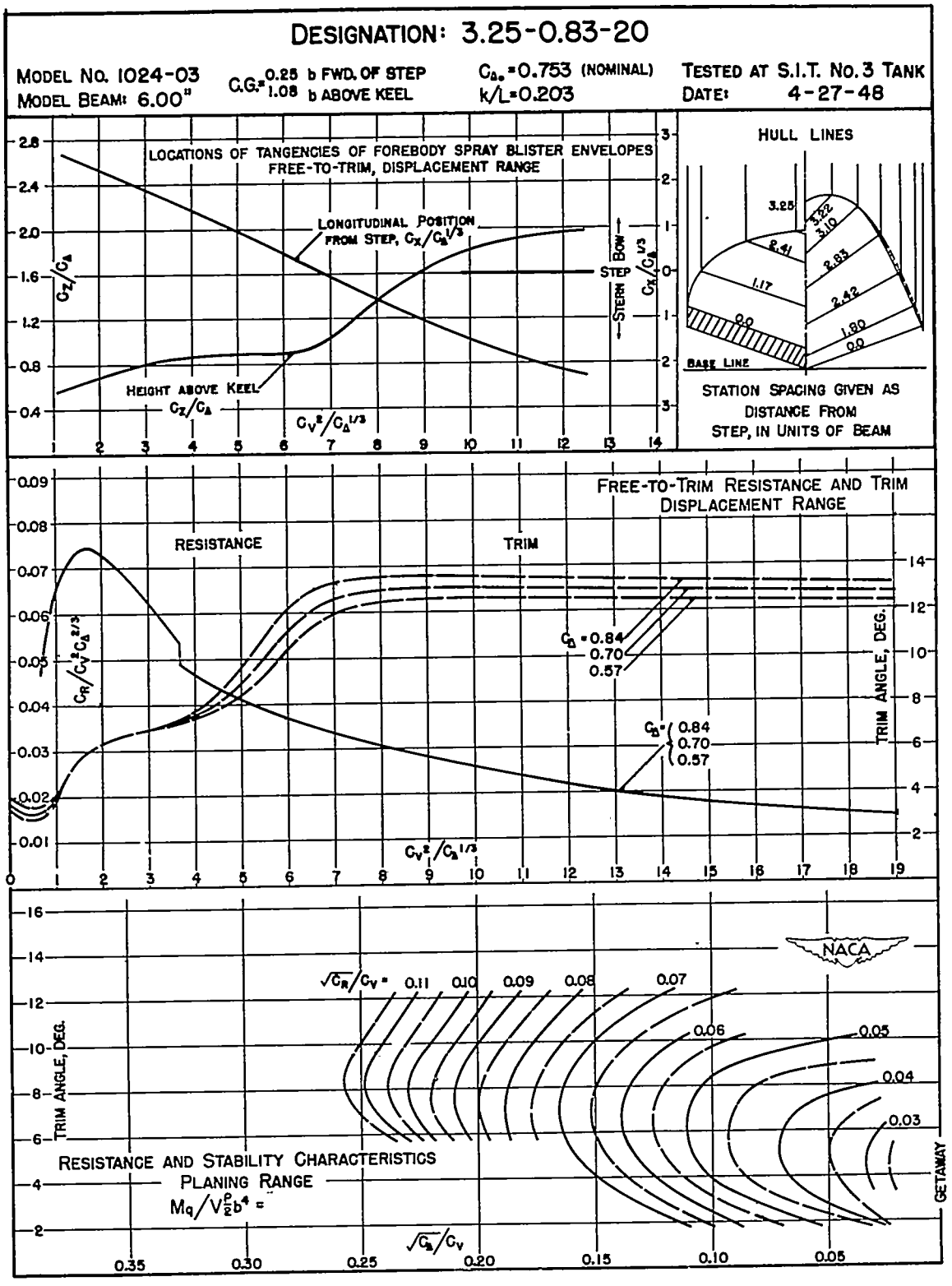
DESIGNATION: 3.25-0.83-20
MODEL NO. 1024-03
MODEL BEAM: 6.00"
C.G. 0.25 b FWD. OF STEP
1.08 b ABOVE KEEL
C_{Δ_o} = 0.753 (NOMINAL)
k/L = 0.203
TESTED AT S.I.T. NO. 3 TANK
DATE: 4-27-48
LOCATIONS OF TANGENCIES OF FOREBODY SPRAY BLISTER ENVELOPES FREE-TO-TRIM, DISPLACEMENT RANGE
LONGITUDINAL POSITION FROM STEP, $C_X/C_\Delta^{1/3}$
HEIGHT ABOVE KEEL C_Z/C_Δ
C_Z/C_Δ
$C_X/C_\Delta^{1/3}$
BOW
STEP
STERN
$C_V^2/C_\Delta^{1/3}$
HULL LINES
3.25
3.22
3.10
2.41
2.83
1.17
2.42
1.80
0.0
0.0
BASE LINE
STATION SPACING GIVEN AS DISTANCE FROM STEP, IN UNITS OF BEAM
FREE-TO-TRIM RESISTANCE AND TRIM DISPLACEMENT RANGE
RESISTANCE
TRIM
$C_R/C_V^2C_\Delta^{2/3}$
C_Δ = 0.84
0.70
0.57
TRIM ANGLE, DEG.
$C_V^2/C_\Delta^{1/3}$
NACA
$\sqrt{C_R}/C_V$ = 0.11 0.10 0.09 0.08 0.07 0.06 0.05 0.04 0.03
TRIM ANGLE, DEG.
RESISTANCE AND STABILITY CHARACTERISTICS
PLANING RANGE
$Mq/V\frac{\rho}{2}b^4$ =
$\sqrt{C_\Delta}/C_V$
GETAWAY

Figure 21.

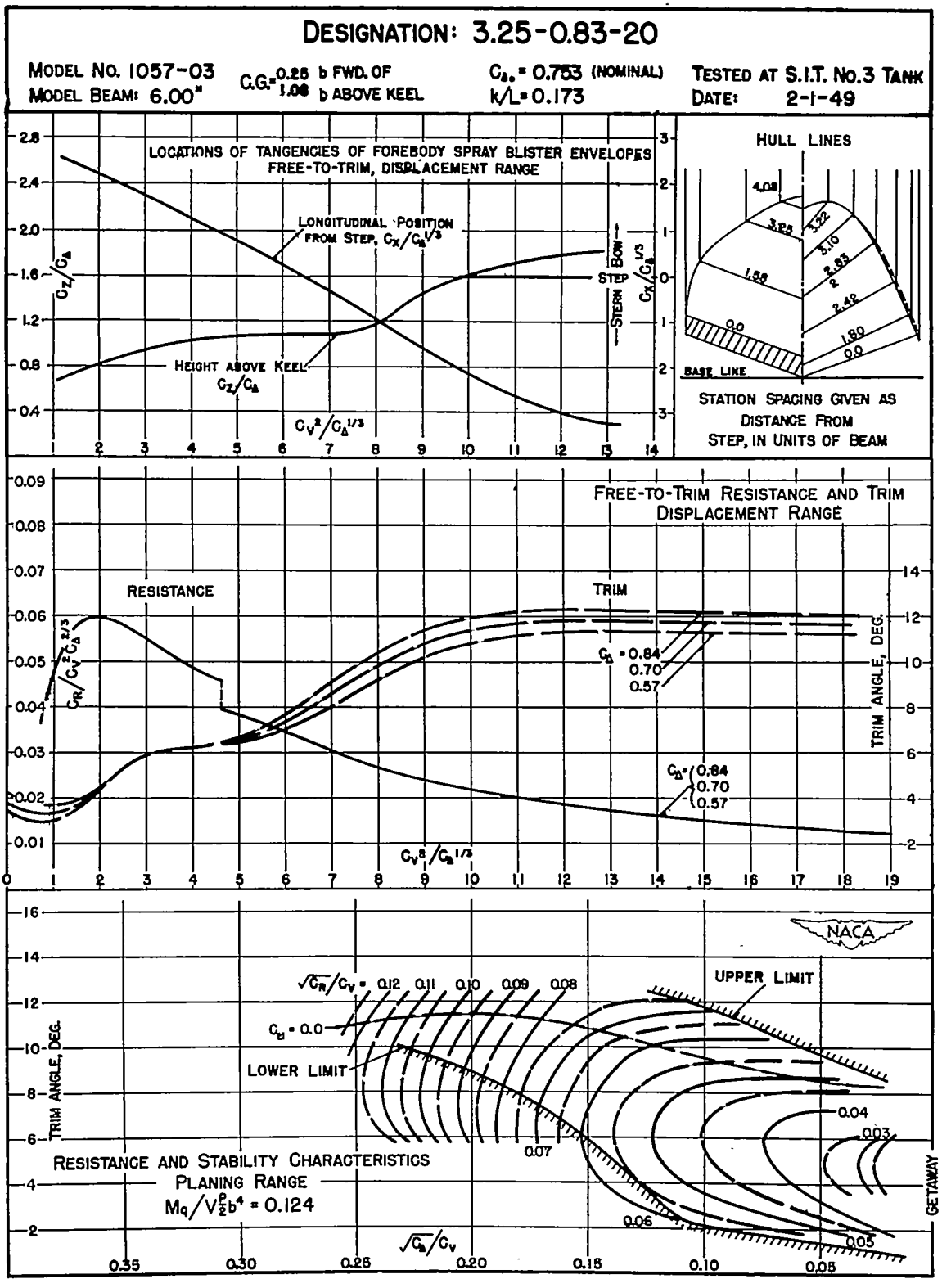
DESIGNATION: 3.25-0.83-20
MODEL NO. 1057-03
MODEL BEAM: 6.00"
C.G. = 0.25 b FWD. OF
1.08 b ABOVE KEEL
C_{Δ_0} = 0.753 (NOMINAL)
k/L = 0.173
TESTED AT S.I.T. NO.3 TANK
DATE: 2-1-49
LOCATIONS OF TANGENCIES OF FOREBODY SPRAY BLISTER ENVELOPES FREE-TO-TRIM, DISPLACEMENT RANGE
LONGITUDINAL POSITION FROM STEP, $C_x/C_\Delta^{1/3}$
HEIGHT ABOVE KEEL C_z/C_Δ
C_z/C_Δ
$C_x/C_\Delta^{1/3}$
BOW
STEP
STERN
$C_V^2/C_\Delta^{1/3}$
HULL LINES
4.08
3.25
3.22
3.10
2.83
2.42
1.88
1.89
0.0
BASE LINE
STATION SPACING GIVEN AS DISTANCE FROM STEP, IN UNITS OF BEAM
FREE-TO-TRIM RESISTANCE AND TRIM DISPLACEMENT RANGE
RESISTANCE
TRIM
$C_R/C_V^2C_\Delta^{2/3}$
C_D = 0.84
0.70
0.57
TRIM ANGLE, DEG.
$C_V^2/C_\Delta^{1/3}$
NACA
$\sqrt{C_R}/C_V$ = 0.12 0.11 0.10 0.09 0.08
UPPER LIMIT
C_D = 0.0
LOWER LIMIT
0.07
0.04
0.03
0.06
0.05
GETAWAY
TRIM ANGLE, DEG.
RESISTANCE AND STABILITY CHARACTERISTICS
PLANING RANGE
$M_q/V\frac{\rho}{2}b^4$ = 0.124
$\sqrt{C_\Delta}/C_V$

Figure 22.

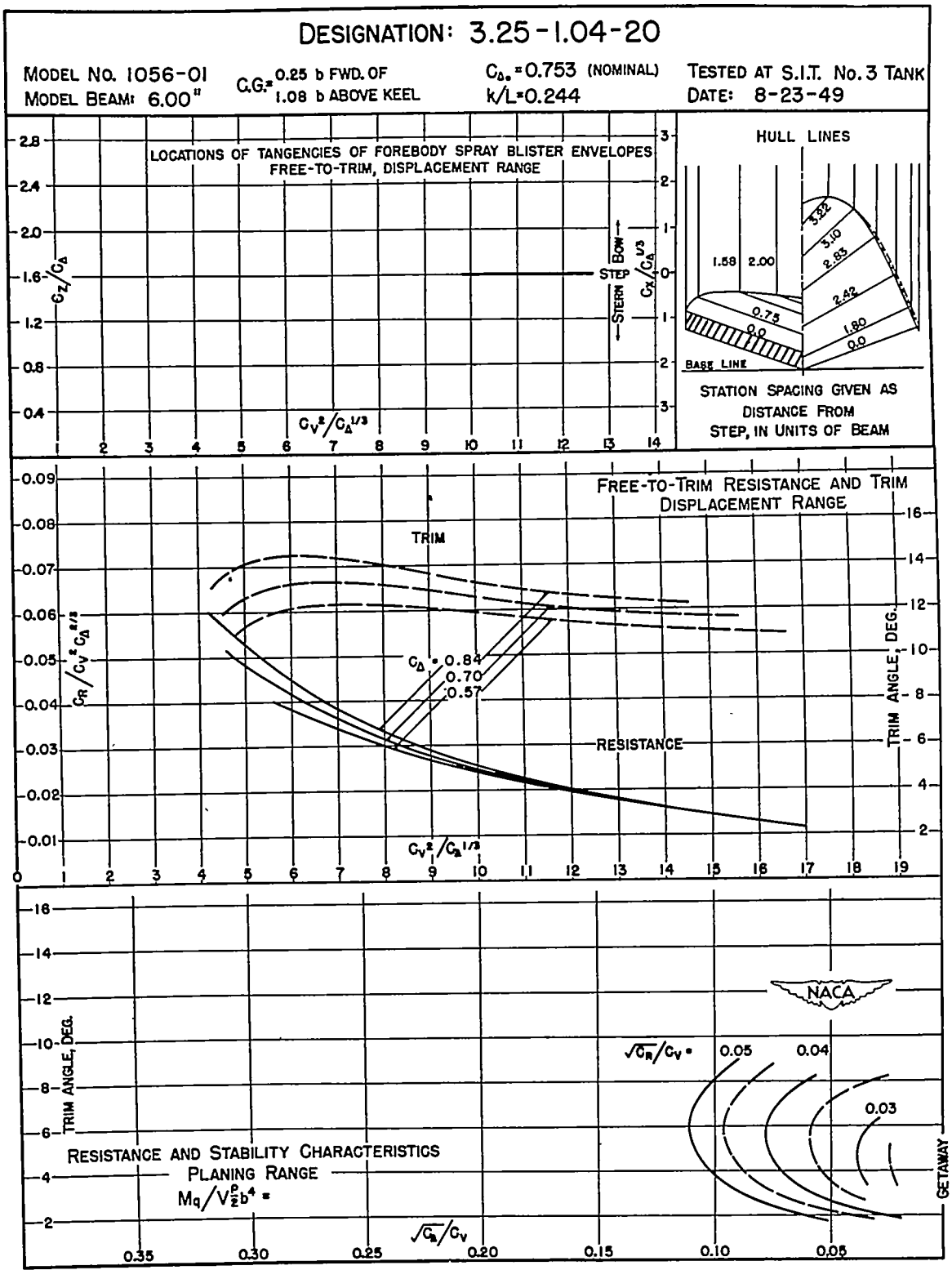
DESIGNATION: 3.25-1.04-20
MODEL NO. 1056-01
MODEL BEAM: 6.00"
C.G. 0.25 b FWD. OF 1.08 b ABOVE KEEL
C_{Δ_o} = 0.753 (NOMINAL)
k/L = 0.244
TESTED AT S.I.T. No. 3 TANK
DATE: 8-23-49
LOCATIONS OF TANGENCIES OF FOREBODY SPRAY BLISTER ENVELOPES FREE-TO-TRIM, DISPLACEMENT RANGE
C_Z/C_Δ
$C_V^2/C_\Delta^{1/3}$
STEP
BOW
STERN
$C_X/C_\Delta^{1/3}$
HULL LINES
3.32
3.10
2.85
2.42
1.80
0.0
1.58
2.00
0.75
0.0
BASE LINE
STATION SPACING GIVEN AS DISTANCE FROM STEP, IN UNITS OF BEAM
FREE-TO-TRIM RESISTANCE AND TRIM DISPLACEMENT RANGE
TRIM
C_Δ = 0.84
0.70
0.57
RESISTANCE
$C_R/C_V^2 C_\Delta^{2/3}$
TRIM ANGLE, DEG.
RESISTANCE AND STABILITY CHARACTERISTICS
PLANING RANGE
$Mq/V_E^2 b^4$ =
$\sqrt{C_\Delta}/C_V$
$\sqrt{C_R}/C_V$ = 0.05
0.04
0.03
NACA
GETAWAY

Figure 23.

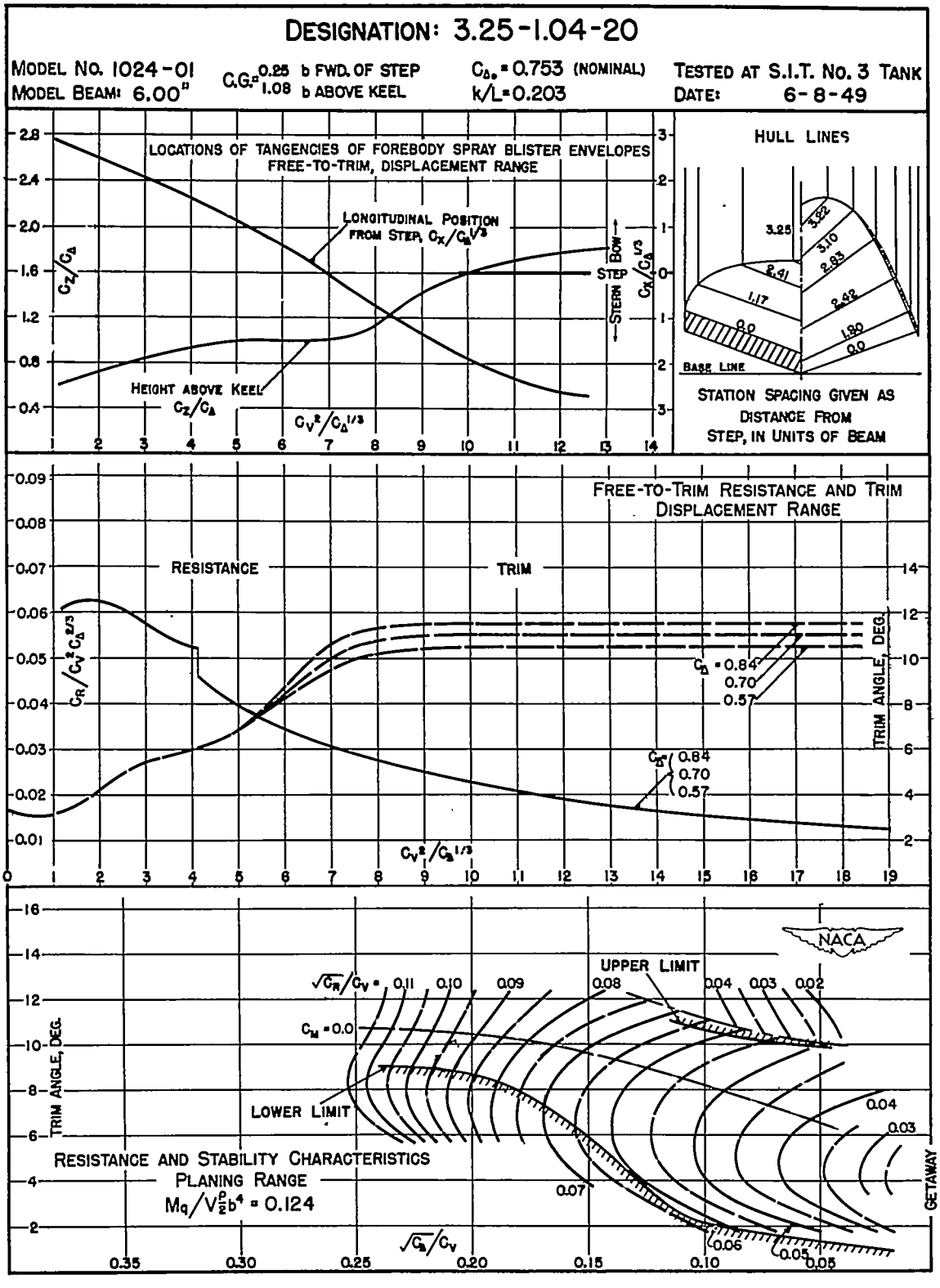
DESIGNATION: 3.25-1.04-20
MODEL NO. 1024-01
MODEL BEAM: 6.00"
C.G. 0.25 b FWD. OF STEP
1.08 b ABOVE KEEL
C_{Δ_0} = 0.753 (NOMINAL)
k/L=0.203
TESTED AT S.I.T. NO. 3 TANK
DATE: 6-8-49
LOCATIONS OF TANGENCIES OF FOREBODY SPRAY BLISTER ENVELOPES FREE-TO-TRIM, DISPLACEMENT RANGE
LONGITUDINAL POSITION FROM STEP, $C_X/C_\Delta^{1/3}$
HEIGHT ABOVE KEEL C_Z/C_Δ
C_Z/C_Δ
$C_X/C_\Delta^{1/3}$
BOW
STERN
STEP
$C_V^2/C_\Delta^{1/3}$
HULL LINES
3.25
3.22
3.10
2.83
2.41
2.42
1.17
1.90
0.0
0.0
BASE LINE
STATION SPACING GIVEN AS DISTANCE FROM STEP, IN UNITS OF BEAM
FREE-TO-TRIM RESISTANCE AND TRIM DISPLACEMENT RANGE
RESISTANCE
TRIM
$C_R/C_V^2C_\Delta^{2/3}$
C_Δ = 0.84
0.70
0.57
TRIM ANGLE, DEG.
$C_V^2/C_\Delta^{1/3}$
NACA
UPPER LIMIT
$\sqrt{C_R}/C_V$ = 0.11 0.10 0.09 0.08 0.04 0.03 0.02
C_M = 0.0
LOWER LIMIT
0.04
0.03
0.07
0.06
0.05
0.05
GETAWAY
RESISTANCE AND STABILITY CHARACTERISTICS
PLANING RANGE
$Mq/V\frac{\rho}{2}b^4$ = 0.124
$\sqrt{C_\Delta}/C_V$

Figure 24.

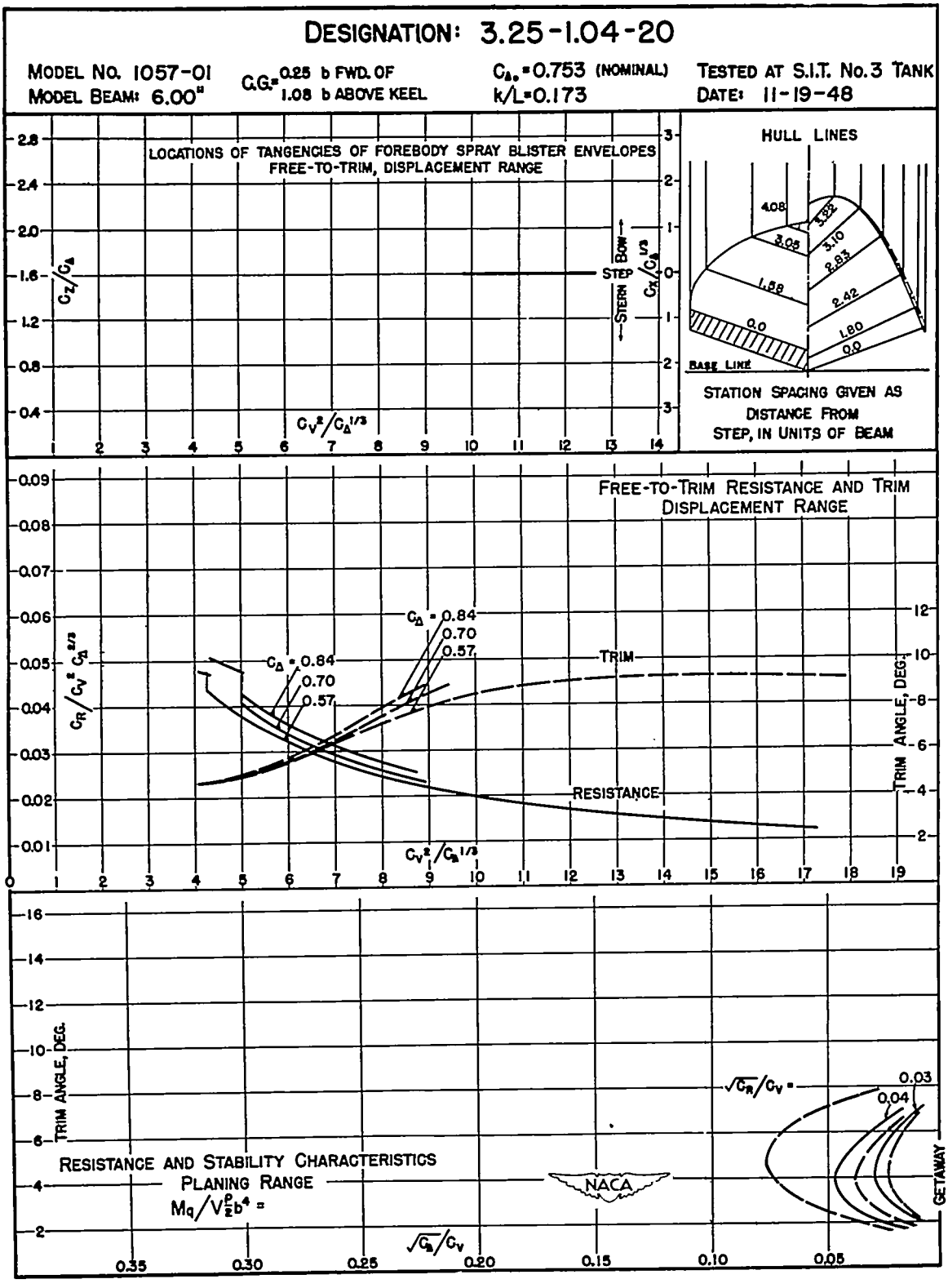
DESIGNATION: 3.25-1.04-20
MODEL NO. 1057-01
MODEL BEAM: 6.00"
C.G. 0.25 b FWD. OF 1.08 b ABOVE KEEL
C_{Δ_0} = 0.753 (NOMINAL)
k/L=0.173
TESTED AT S.I.T. No.3 TANK
DATE: 11-19-48
LOCATIONS OF TANGENCIES OF FOREBODY SPRAY BLISTER ENVELOPES FREE-TO-TRIM, DISPLACEMENT RANGE
C_Z/C_Δ
$C_V^2/C_\Delta^{1/3}$
STEP
BOW
STERN
$C_X/C_\Delta^{1/3}$
HULL LINES
4.08
3.33
3.05
3.10
2.83
1.58
2.42
0.0
1.80
0.0
BASE LINE
STATION SPACING GIVEN AS DISTANCE FROM STEP, IN UNITS OF BEAM
FREE-TO-TRIM RESISTANCE AND TRIM DISPLACEMENT RANGE
$C_R/C_V^2 C_\Delta^{2/3}$
C_Δ = 0.84
0.70
0.57
TRIM
RESISTANCE
TRIM ANGLE, DEG.
$C_V^2/C_\Delta^{1/3}$
RESISTANCE AND STABILITY CHARACTERISTICS
PLANING RANGE
$Mq/V\frac{\rho}{2}b^4$ =
$\sqrt{C_\Delta}/C_V$
$\sqrt{C_R}/C_V$ =
0.03
0.04
GETAWAY
NACA

Figure 25.

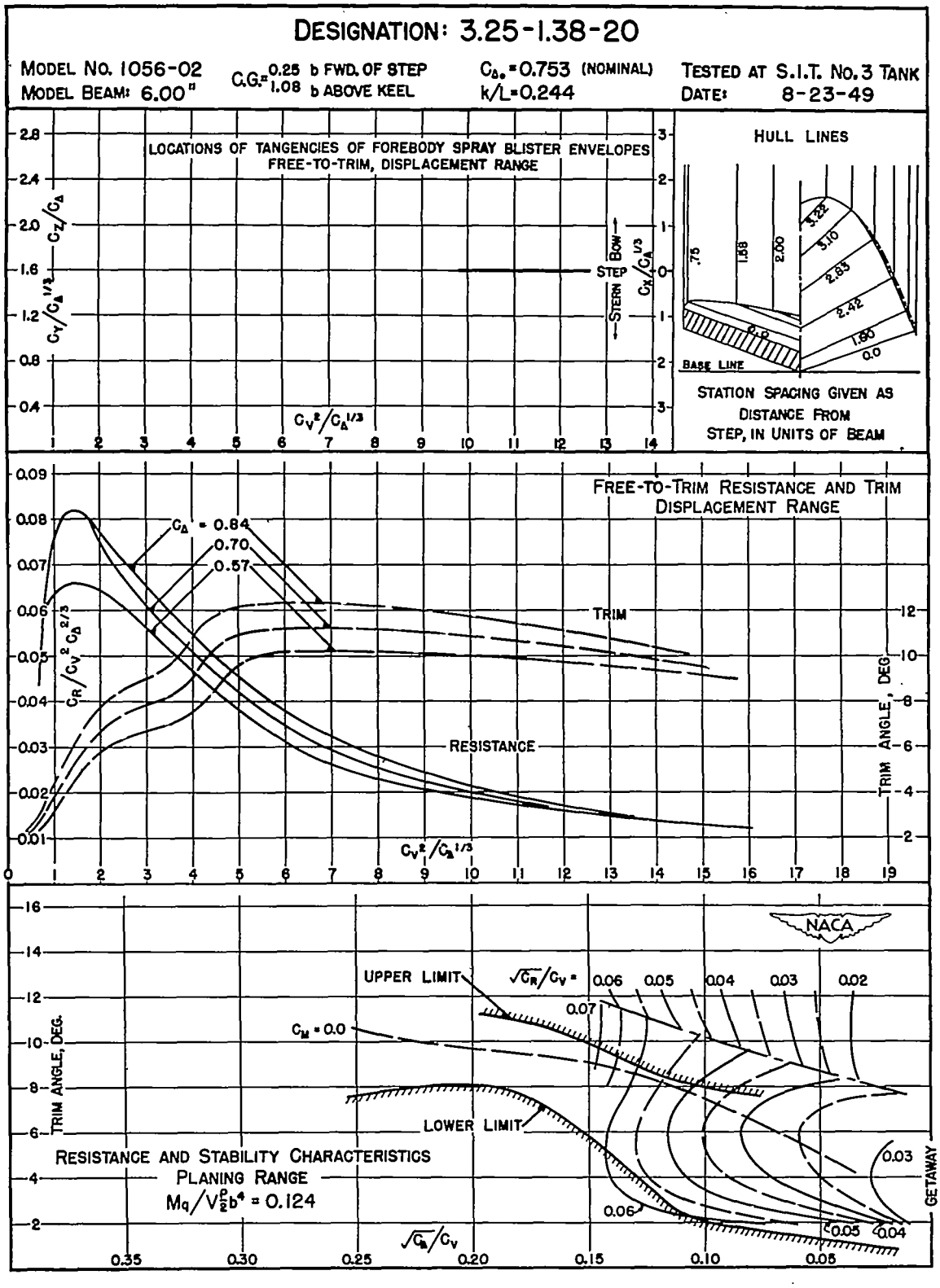
DESIGNATION: 3.25-1.38-20
MODEL NO. 1056-02
MODEL BEAM: 6.00"
C.G. 0.25 b FWD. OF STEP
1.08 b ABOVE KEEL
C_{Δ_o} = 0.753 (NOMINAL)
k/L = 0.244
TESTED AT S.I.T. No. 3 TANK
DATE: 8-23-49
LOCATIONS OF TANGENCIES OF FOREBODY SPRAY BLISTER ENVELOPES FREE-TO-TRIM, DISPLACEMENT RANGE
$C_V/C_\Delta^{1/3}$
C_Z/C_Δ
$C_H/C_\Delta^{1/3}$
BOW
STEP
STERN
$C_V^2/C_\Delta^{1/3}$
HULL LINES
.75
1.68
2.00
3.22
3.10
2.83
2.42
1.90
0.0
BASE LINE
STATION SPACING GIVEN AS DISTANCE FROM STEP, IN UNITS OF BEAM
FREE-TO-TRIM RESISTANCE AND TRIM DISPLACEMENT RANGE
C_Δ = 0.84
0.70
0.57
TRIM
RESISTANCE
$C_R/C_V^2 C_\Delta^{2/3}$
TRIM ANGLE, DEG
$C_V^2/C_\Delta^{1/3}$
NACA
UPPER LIMIT
$\sqrt{C_R}/C_V$ =
0.06
0.05
0.04
0.03
0.02
0.07
C_M = 0.0
LOWER LIMIT
TRIM ANGLE, DEG.
RESISTANCE AND STABILITY CHARACTERISTICS
PLANING RANGE
$Mq/V\rho b^4$ = 0.124
$\sqrt{C_\Delta}/C_V$
GETAWAY
0.03
0.06
0.05
0.04

Figure 26

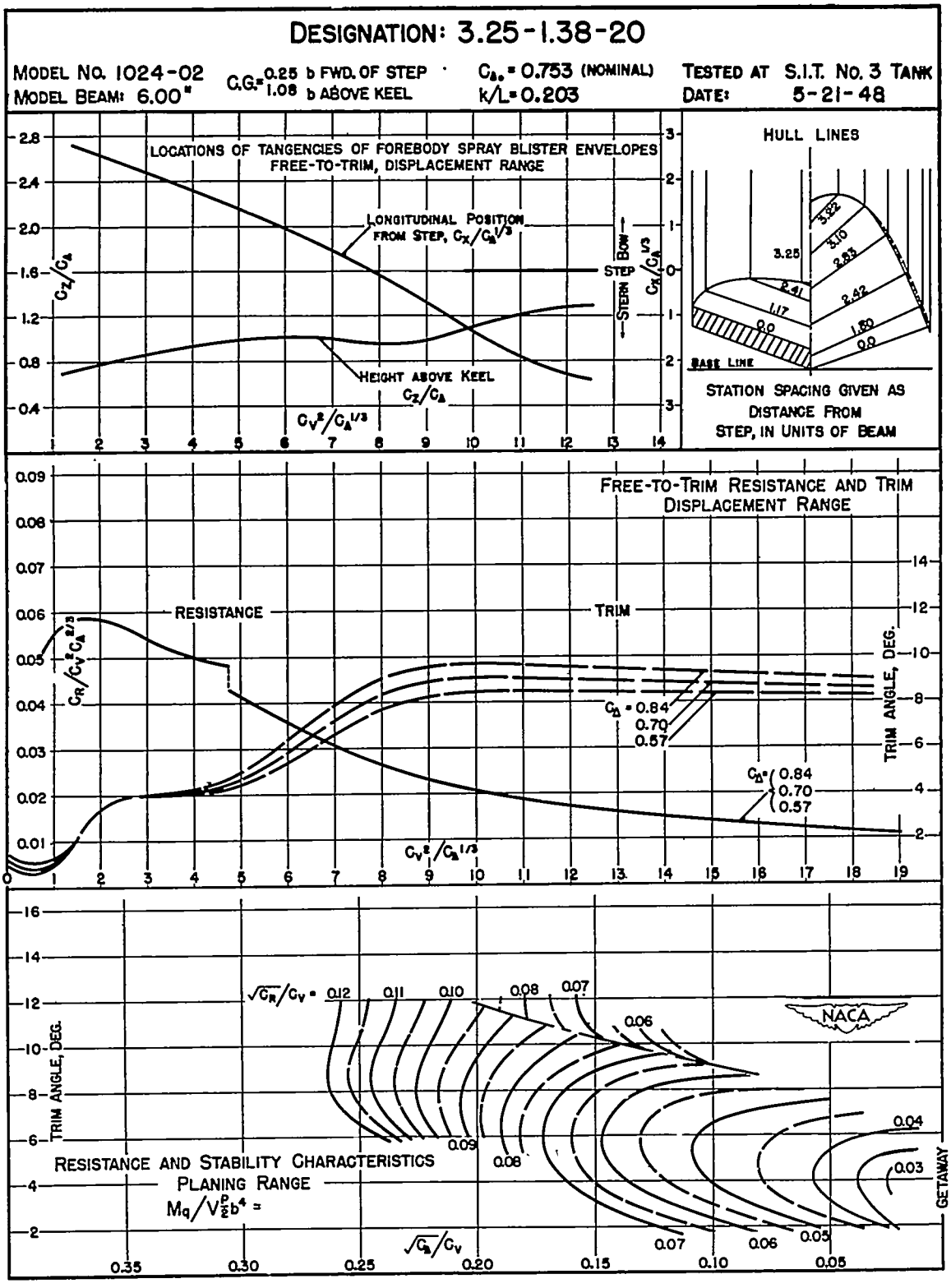
DESIGNATION: 3.25-1.38-20
MODEL NO. 1024-02
MODEL BEAM: 6.00"
C.G.= 0.25 b FWD. OF STEP, 1.08 b ABOVE KEEL
C_{Δ_0} = 0.753 (NOMINAL)
k/L = 0.203
TESTED AT S.I.T. No. 3 TANK
DATE: 5-21-48
LOCATIONS OF TANGENCIES OF FOREBODY SPRAY BLISTER ENVELOPES FREE-TO-TRIM, DISPLACEMENT RANGE
LONGITUDINAL POSITION FROM STEP, $C_X/C_\Delta^{1/3}$
HEIGHT ABOVE KEEL C_Z/C_Δ
C_Z/C_Δ
$C_X/C_\Delta^{1/3}$
BOW
STEP
STERN
$C_V^2/C_\Delta^{1/3}$
HULL LINES
3.25
3.22
3.10
2.83
2.41
2.42
1.17
0.0
1.80
0.0
BASE LINE
STATION SPACING GIVEN AS DISTANCE FROM STEP, IN UNITS OF BEAM
FREE-TO-TRIM RESISTANCE AND TRIM DISPLACEMENT RANGE
RESISTANCE
TRIM
$C_R/C_V^2C_\Delta^{2/3}$
TRIM ANGLE, DEG.
C_Δ = 0.84
0.70
0.57
$C_V^2/C_\Delta^{1/3}$
RESISTANCE AND STABILITY CHARACTERISTICS
PLANING RANGE
$Mq/V\frac{P}{L}b^4$ =
$\sqrt{C_R}/C_V$ = 0.12 0.11 0.10 0.08 0.07 0.06 0.09 0.08 0.07 0.06 0.05
NACA
0.04
0.03
GETAWAY
$\sqrt{C_\Delta}/C_V$

Figure 27.

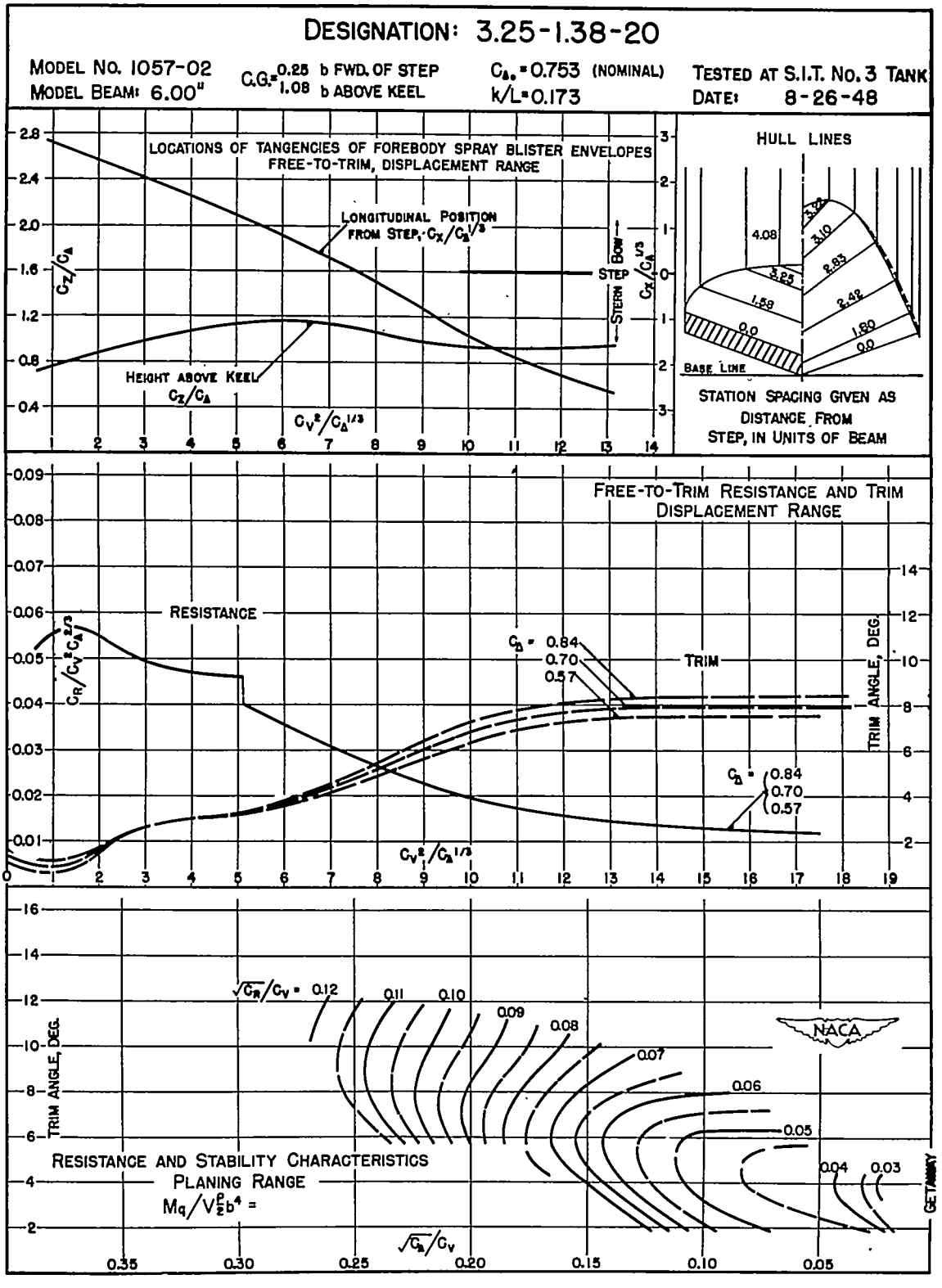
DESIGNATION: 3.25-1.38-20
MODEL NO. 1057-02
MODEL BEAM: 6.00"
C.G. 0.25 b FWD. OF STEP
1.08 b ABOVE KEEL
C_{Δ_0} = 0.753 (NOMINAL)
k/L = 0.173
TESTED AT S.I.T. No. 3 TANK
DATE: 8-26-48
LOCATIONS OF TANGENCIES OF FOREBODY SPRAY BLISTER ENVELOPES FREE-TO-TRIM, DISPLACEMENT RANGE
LONGITUDINAL POSITION FROM STEP, $C_X/C_\Delta^{1/3}$
HEIGHT ABOVE KEEL C_Z/C_Δ
C_Z/C_Δ
$C_X/C_\Delta^{1/3}$
BOW
STEP
STERN
$C_V^2/C_\Delta^{1/3}$
HULL LINES
4.08
3.25
1.58
0.0
3.20
3.10
2.83
2.42
1.60
0.0
BASE LINE
STATION SPACING GIVEN AS DISTANCE FROM STEP, IN UNITS OF BEAM
FREE-TO-TRIM RESISTANCE AND TRIM DISPLACEMENT RANGE
RESISTANCE
$C_R/C_V^2C_\Delta^{2/3}$
C_Δ = 0.84
0.70
0.57
TRIM
TRIM ANGLE, DEG.
$C_V^2/C_\Delta^{1/3}$
$\sqrt{C_R}/C_V$ = 0.12
0.11
0.10
0.09
0.08
0.07
0.06
0.05
0.04
0.03
NACA
RESISTANCE AND STABILITY CHARACTERISTICS
PLANING RANGE
$Mq/V\frac{\rho}{2}b^4$ =
$\sqrt{C_\Delta}/C_V$
GETAWAY

Figure 28.

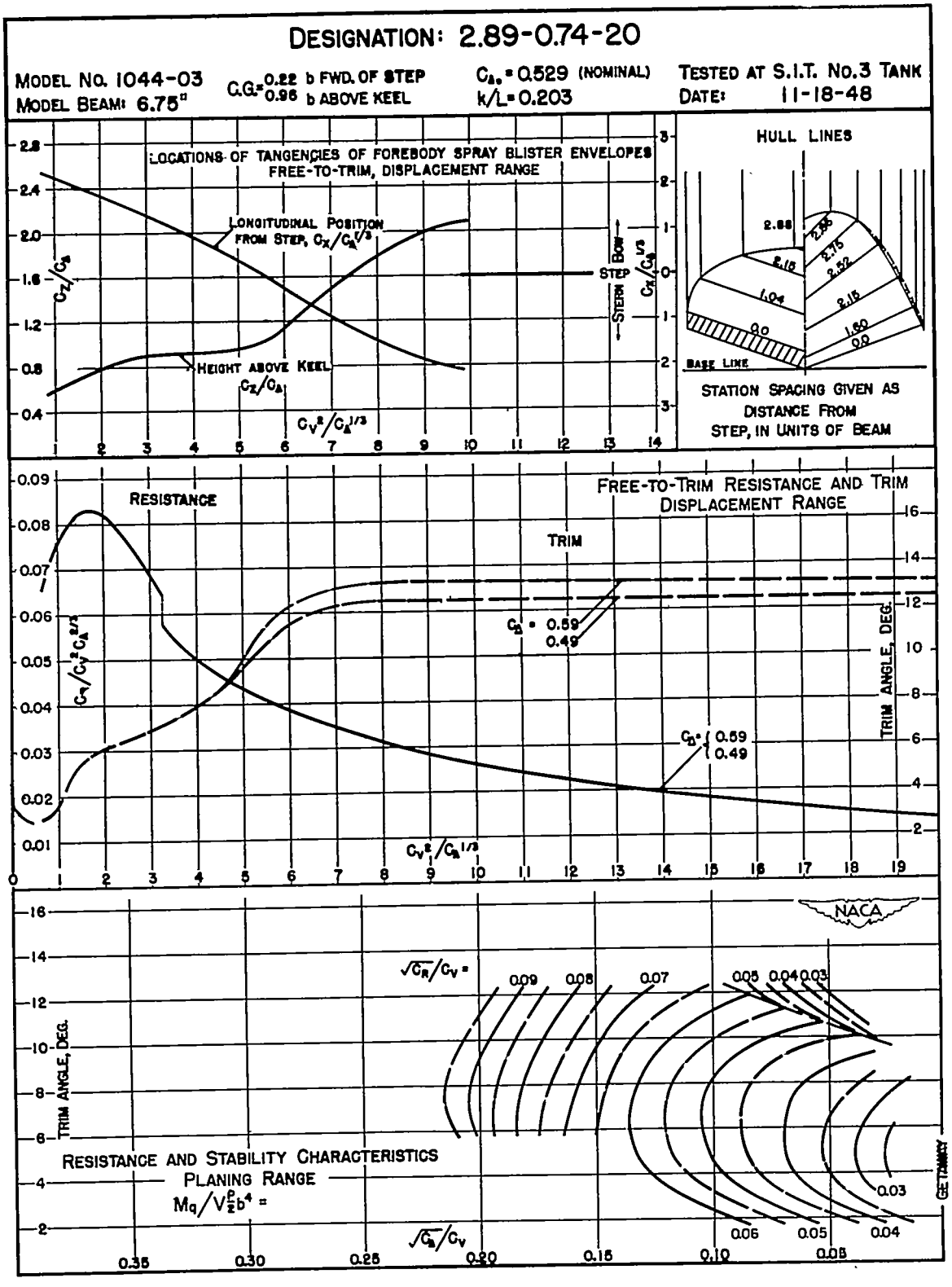
DESIGNATION: 2.89-0.74-20
MODEL NO. 1044-03
MODEL BEAM: 6.75"
C.G. 0.22 b FWD. OF STEP
0.96 b ABOVE KEEL
C_{Δ_0} = 0.529 (NOMINAL)
k/L = 0.203
TESTED AT S.I.T. NO.3 TANK
DATE: 11-18-48
LOCATIONS OF TANGENCIES OF FOREBODY SPRAY BLISTER ENVELOPES FREE-TO-TRIM, DISPLACEMENT RANGE
LONGITUDINAL POSITION FROM STEP, $C_x/C_\Delta^{1/3}$
HEIGHT ABOVE KEEL C_z/C_Δ
C_z/C_Δ
C_x/C_Δ
BOW
STEP
STERN
$C_V^2/C_\Delta^{1/3}$
HULL LINES
2.88
2.88
2.75
2.52
2.15
1.94
2.15
1.60
0.0
0.0
BASE LINE
STATION SPACING GIVEN AS DISTANCE FROM STEP, IN UNITS OF BEAM
RESISTANCE
FREE-TO-TRIM RESISTANCE AND TRIM DISPLACEMENT RANGE
TRIM
C_Δ = 0.59
0.49
C_Δ = 0.59
0.49
$C_R/C_V^2C_\Delta^{2/3}$
TRIM ANGLE, DEG.
$C_V^2/C_\Delta^{1/3}$
NACA
$\sqrt{C_R}/C_V$ =
0.09
0.08
0.07
0.05
0.04
0.03
0.06
0.05
0.04
TRIM ANGLE, DEG.
RESISTANCE AND STABILITY CHARACTERISTICS
PLANING RANGE
$Mq/V\frac{\rho}{2}b^4$ =
$\sqrt{C_\Delta}/C_V$
0.35
0.30
0.25
0.20
0.15
0.10
0.05
GETTINGER

Figure 29.

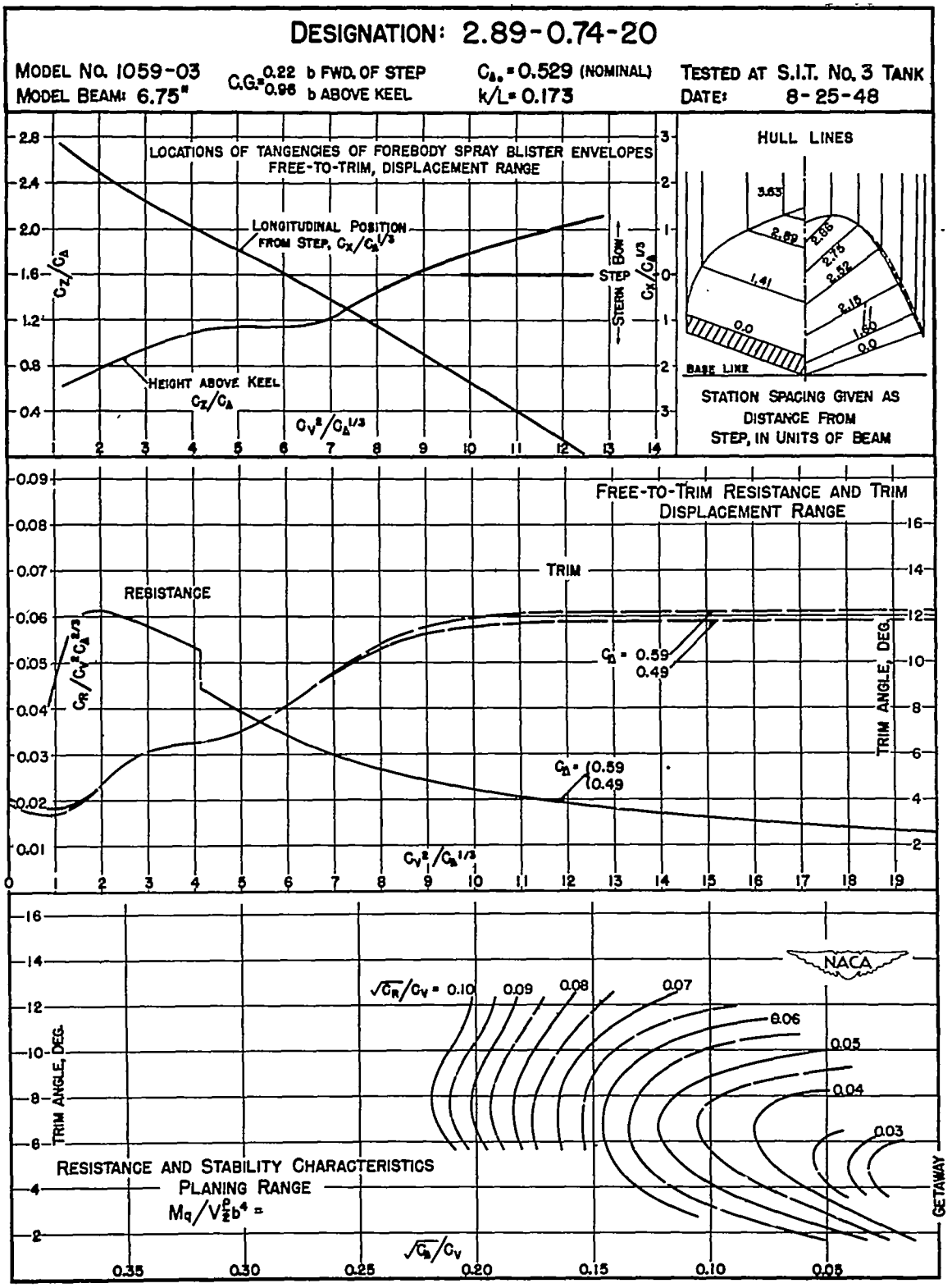
DESIGNATION: 2.89-0.74-20
MODEL NO. 1059-03
MODEL BEAM: 6.75"
C.G. 0.22 b FWD. OF STEP
0.96 b ABOVE KEEL
C_{Δ_0} = 0.529 (NOMINAL)
k/L = 0.173
TESTED AT S.I.T. No. 3 TANK
DATE: 8-25-48
LOCATIONS OF TANGENCIES OF FOREBODY SPRAY BLISTER ENVELOPES FREE-TO-TRIM, DISPLACEMENT RANGE
LONGITUDINAL POSITION FROM STEP, $C_X/C_\Delta^{1/3}$
HEIGHT ABOVE KEEL C_Z/C_Δ
$C_V^2/C_\Delta^{1/3}$
BOW
STEP
STERN
HULL LINES
3.63
2.89
2.86
2.76
2.52
1.41
2.15
1.65
0.0
0.0
BASE LINE
STATION SPACING GIVEN AS DISTANCE FROM STEP, IN UNITS OF BEAM
FREE-TO-TRIM RESISTANCE AND TRIM DISPLACEMENT RANGE
RESISTANCE
TRIM
C_Δ = 0.59
0.49
C_Δ = 0.59
0.49
$C_R/C_V^2C_\Delta^{2/3}$
TRIM ANGLE, DEG.
RESISTANCE AND STABILITY CHARACTERISTICS
PLANING RANGE
$Mq/V\rho b^4$ =
$\sqrt{C_R}/C_V$ = 0.10
0.09
0.08
0.07
0.06
0.05
0.04
0.03
NACA
GETAWAY
$\sqrt{C_\Delta}/C_V$

Figure 30.

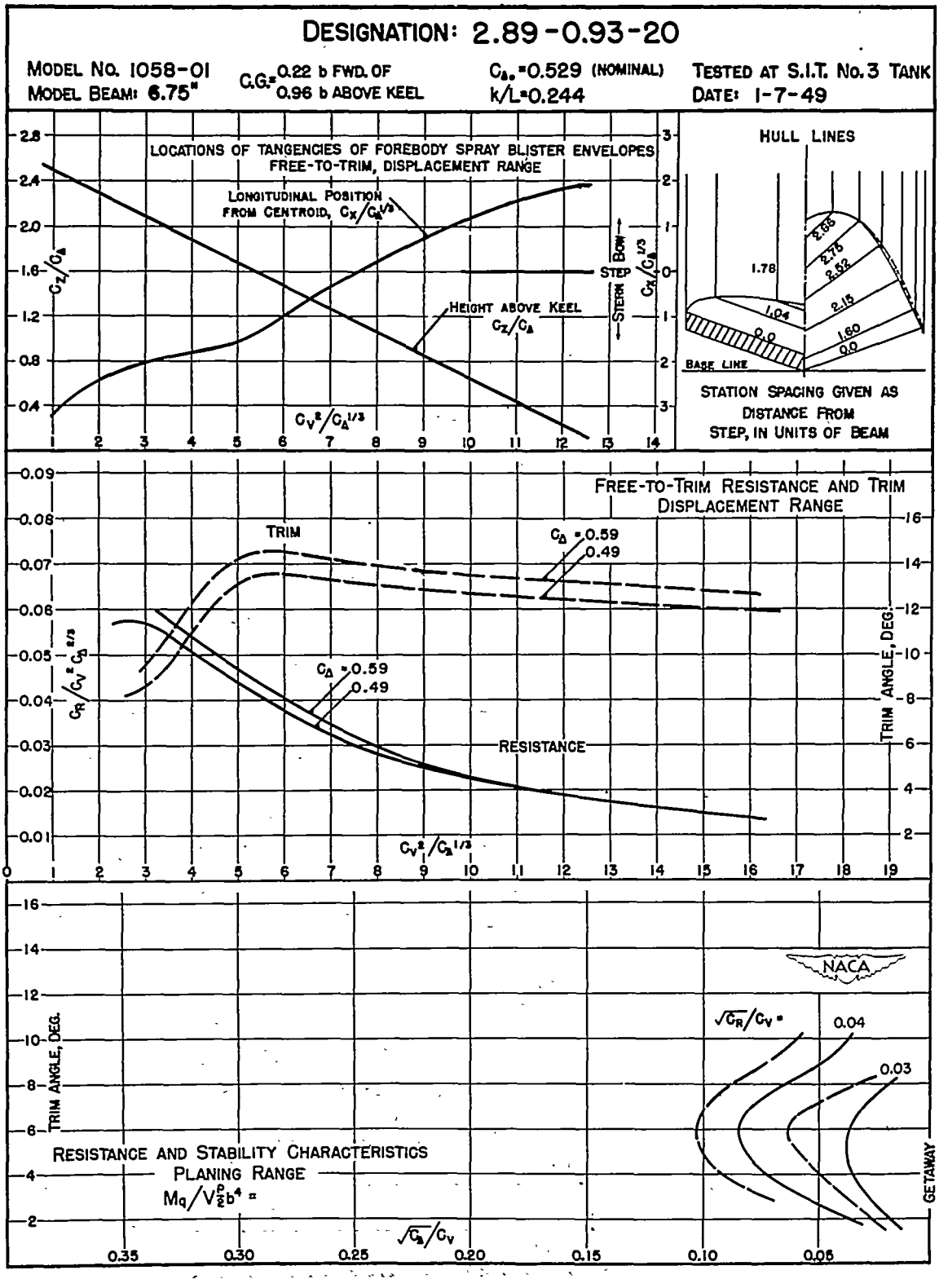
DESIGNATION: 2.89-0.93-20
MODEL NO. 1058-01
MODEL BEAM: 6.75"
C.G.=0.22 b FWD. OF 0.96 b ABOVE KEEL
C_{Δ_0}=0.529 (NOMINAL)
k/L=0.244
TESTED AT S.I.T. No. 3 TANK
DATE: 1-7-49
LOCATIONS OF TANGENCIES OF FOREBODY SPRAY BLISTER ENVELOPES FREE-TO-TRIM, DISPLACEMENT RANGE
LONGITUDINAL POSITION FROM CENTROID, $C_x/C_\Delta^{1/3}$
HEIGHT ABOVE KEEL C_z/C_Δ
C_z/C_Δ
$C_x/C_\Delta^{1/3}$
STEP
BOW
STERN
$C_V^2/C_\Delta^{1/3}$
HULL LINES
1.78
2.65
2.75
2.52
2.15
1.04
0.0
1.60
9.0
BASE LINE
STATION SPACING GIVEN AS DISTANCE FROM STEP, IN UNITS OF BEAM
FREE-TO-TRIM RESISTANCE AND TRIM DISPLACEMENT RANGE
TRIM
C_Δ =0.59
0.49
RESISTANCE
$C_R/C_V^2 C_\Delta^{2/3}$
TRIM ANGLE, DEG.
RESISTANCE AND STABILITY CHARACTERISTICS
PLANING RANGE
$M_q/V\rho b^4$ =
$\sqrt{C_\Delta}/C_V$
NACA
$\sqrt{C_R}/C_V$ =
0.04
0.03
GETAWAY

Figure 31.

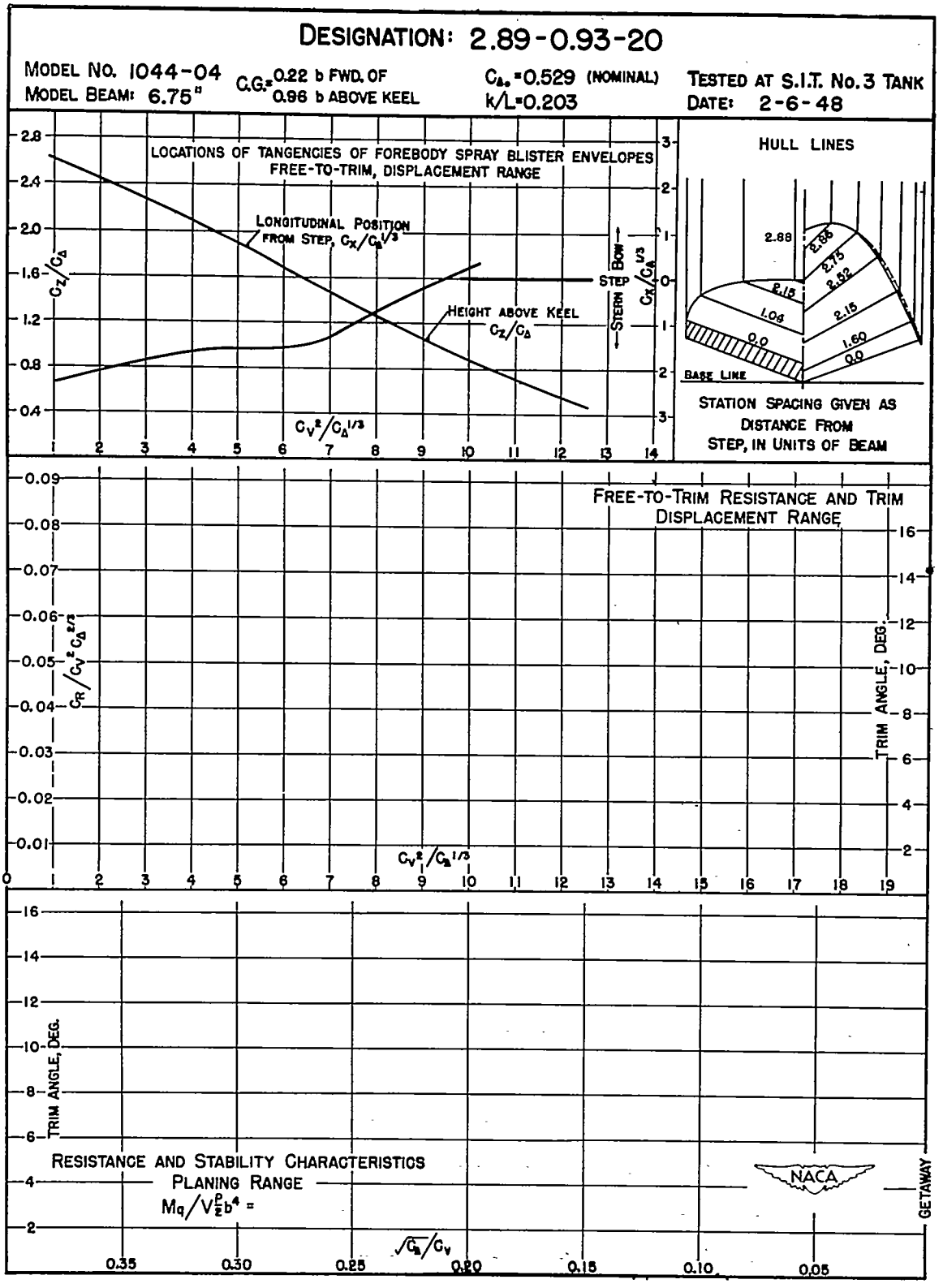
DESIGNATION: 2.89-0.93-20
MODEL NO. 1044-04
MODEL BEAM: 6.75"
C.G. 0.22 b FWD. OF 0.96 b ABOVE KEEL
C_{Δ_0}=0.529 (NOMINAL)
k/L=0.203
TESTED AT S.I.T. No. 3 TANK
DATE: 2-6-48
LOCATIONS OF TANGENCIES OF FOREBODY SPRAY BLISTER ENVELOPES FREE-TO-TRIM, DISPLACEMENT RANGE
LONGITUDINAL POSITION FROM STEP, $C_x/C_\Delta^{1/3}$
HEIGHT ABOVE KEEL C_z/C_Δ
C_z/C_Δ
$C_x/C_\Delta^{1/3}$
BOW
STEP
STERN
$C_V^2/C_\Delta^{1/3}$
HULL LINES
2.89
2.86
2.75
2.52
2.15
1.04
0.0
2.15
1.60
0.0
BASE LINE
STATION SPACING GIVEN AS DISTANCE FROM STEP, IN UNITS OF BEAM
FREE-TO-TRIM RESISTANCE AND TRIM DISPLACEMENT RANGE
$C_R/C_V^2C_\Delta^{2/3}$
TRIM ANGLE, DEG.
RESISTANCE AND STABILITY CHARACTERISTICS
PLANING RANGE
$Mq/V\frac{\rho}{2}b^4$ =
$\sqrt{C_\Delta}/C_V$
NACA
GETAWAY

Figure 32.

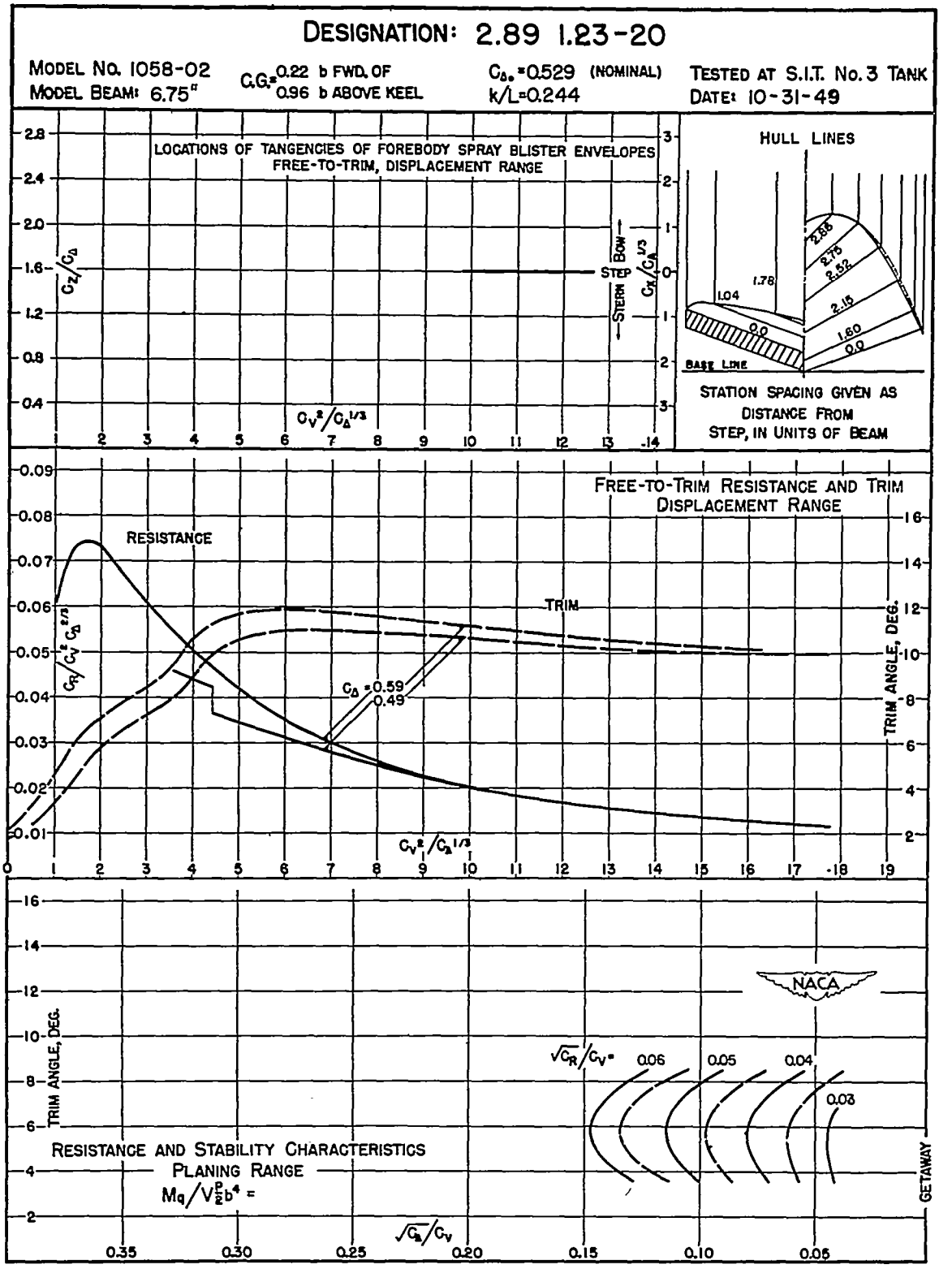
DESIGNATION: 2.89 1.23-20
MODEL NO. 1058-02
MODEL BEAM: 6.75"
C.G. 0.22 b FWD. OF
0.96 b ABOVE KEEL
C_{Δ_0}=0.529 (NOMINAL)
k/L=0.244
TESTED AT S.I.T. No. 3 TANK
DATE: 10-31-49
LOCATIONS OF TANGENCIES OF FOREBODY SPRAY BLISTER ENVELOPES FREE-TO-TRIM, DISPLACEMENT RANGE
C_Z/C_Δ
$C_V^2/C_\Delta^{1/3}$
STEP
BOW
STERN
$C_A/C_\Delta^{1/3}$
HULL LINES
2.85
2.75
2.52
2.15
1.60
0.0
1.78
1.04
0.0
BASE LINE
STATION SPACING GIVEN AS DISTANCE FROM STEP, IN UNITS OF BEAM
FREE-TO-TRIM RESISTANCE AND TRIM DISPLACEMENT RANGE
RESISTANCE
TRIM
C_Δ =0.59
0.49
$C_R/C_V^2 C_\Delta^{2/3}$
TRIM ANGLE, DEG.
RESISTANCE AND STABILITY CHARACTERISTICS
PLANING RANGE
$Mq/V\frac{D}{2}b^4$ =
$\sqrt{C_R}/C_V$ =
0.06
0.05
0.04
0.03
$\sqrt{C_\Delta}/C_V$
GETAWAY
NACA

Figure 33.

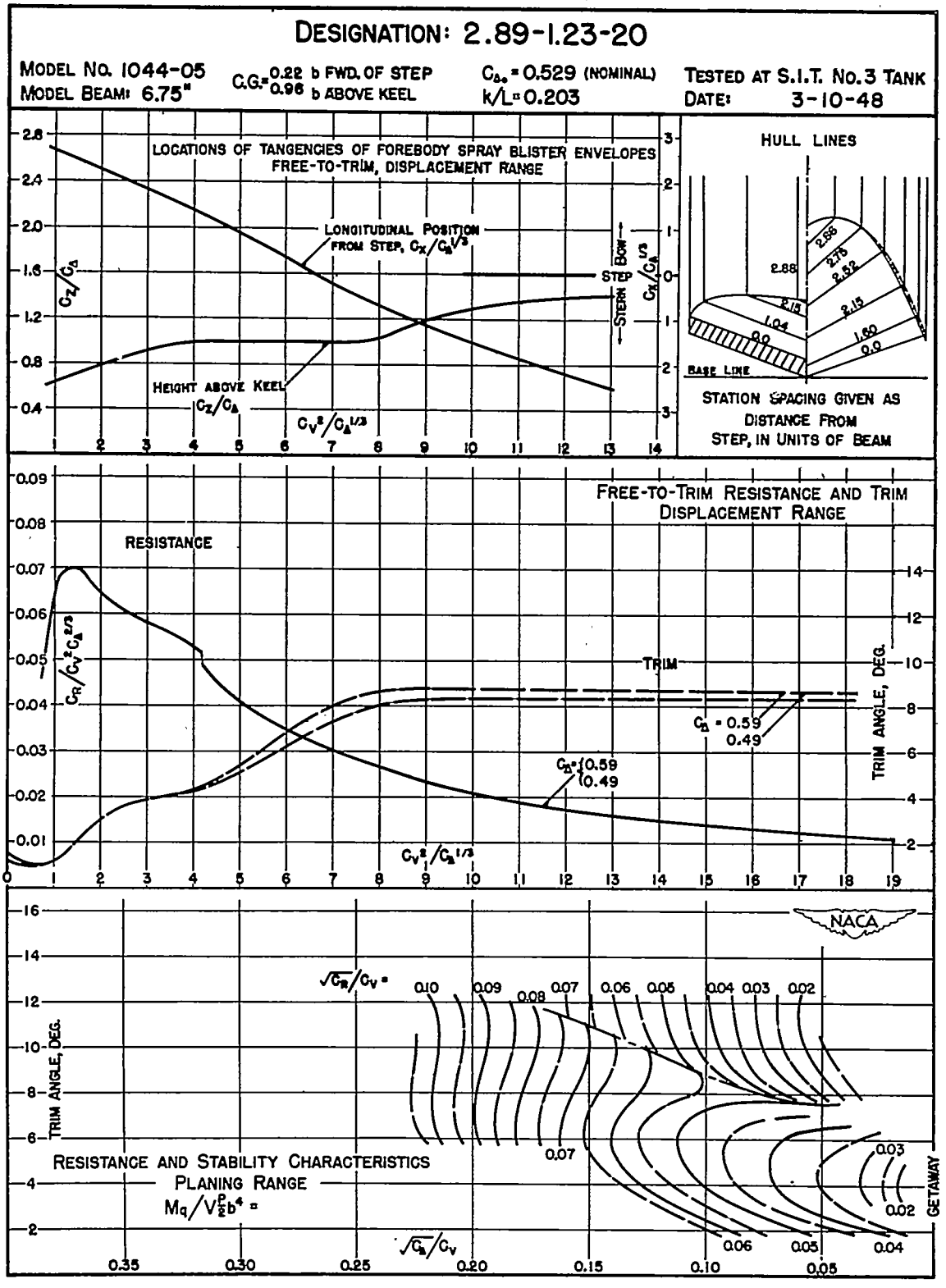
DESIGNATION: 2.89-1.23-20
MODEL NO. 1044-05
MODEL BEAM: 6.75"
C.G. 0.22 b FWD. OF STEP
0.96 b ABOVE KEEL
C_{Δ_0} = 0.529 (NOMINAL)
k/L = 0.203
TESTED AT S.I.T. NO. 3 TANK
DATE: 3-10-48
LOCATIONS OF TANGENCIES OF FOREBODY SPRAY BLISTER ENVELOPES FREE-TO-TRIM, DISPLACEMENT RANGE
LONGITUDINAL POSITION FROM STEP, $C_x/C_\Delta^{1/3}$
HEIGHT ABOVE KEEL C_z/C_Δ
C_z/C_Δ
$C_x/C_\Delta^{1/3}$
STEP
STERN
BOW
$C_V^2/C_\Delta^{1/3}$
HULL LINES
2.68
2.75
2.52
2.88
2.15
2.15
1.04
1.60
0.0
0.0
BASE LINE
STATION SPACING GIVEN AS DISTANCE FROM STEP, IN UNITS OF BEAM
FREE-TO-TRIM RESISTANCE AND TRIM DISPLACEMENT RANGE
RESISTANCE
$C_R/C_V^2C_\Delta^{2/3}$
TRIM
C_Δ = 0.59
0.49
TRIM ANGLE, DEG.
$C_V^2/C_\Delta^{1/3}$
NACA
$\sqrt{C_R}/C_V$ =
0.10
0.09
0.08
0.07
0.06
0.05
0.04
0.03
0.02
TRIM ANGLE, DEG.
RESISTANCE AND STABILITY CHARACTERISTICS
PLANING RANGE
$Mq/V\frac{\rho}{2}b^4$ =
GETAWAY
$\sqrt{C_R}/C_V$

Figure 34.

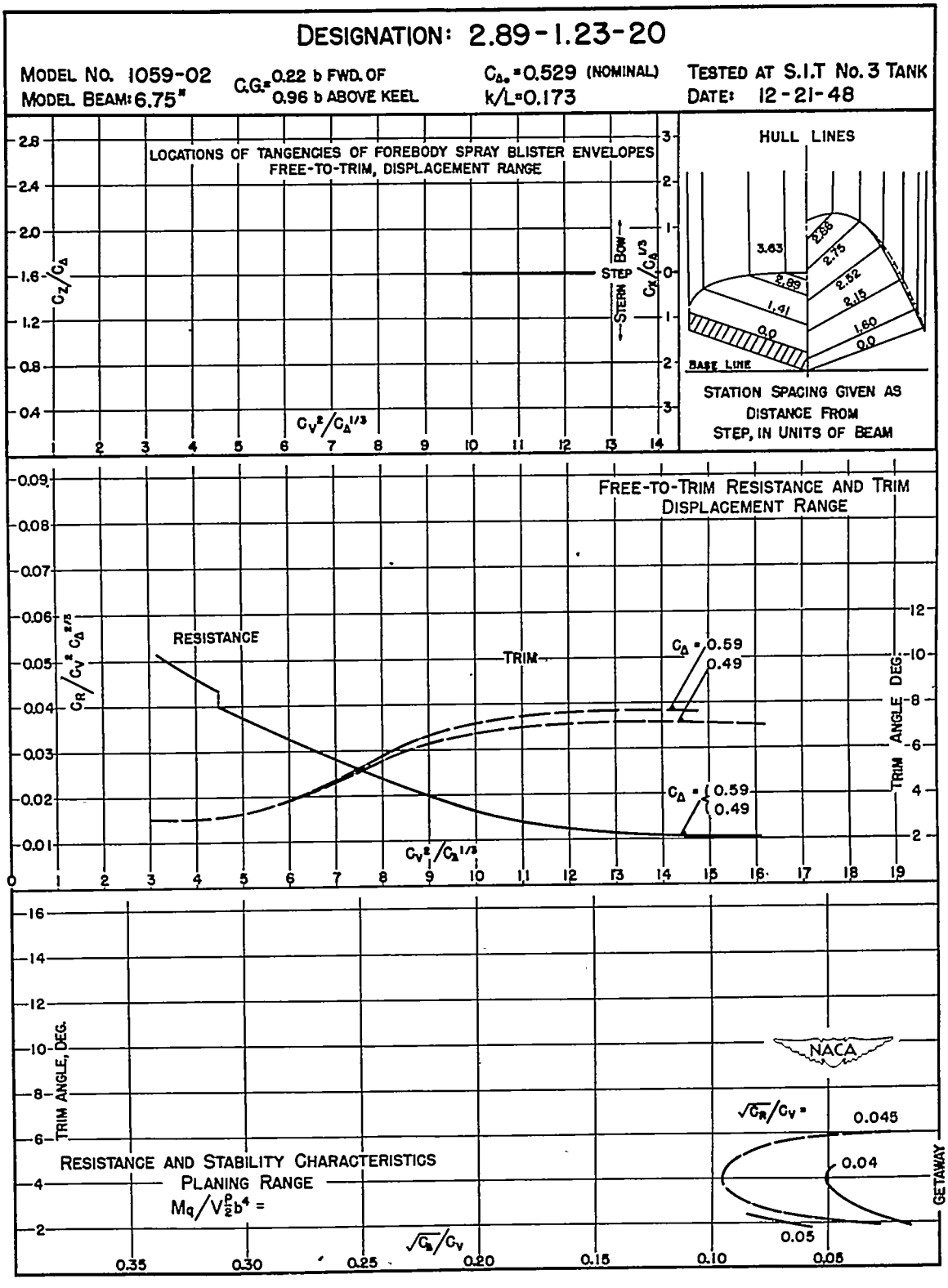
DESIGNATION: 2.89-1.23-20
MODEL NO. 1059-02
MODEL BEAM: 6.75"
C.G. = 0.22 b FWD. OF 0.96 b ABOVE KEEL
C_{Δ_o} = 0.529 (NOMINAL)
k/L = 0.173
TESTED AT S.I.T No. 3 TANK
DATE: 12-21-48
LOCATIONS OF TANGENCIES OF FOREBODY SPRAY BLISTER ENVELOPES FREE-TO-TRIM, DISPLACEMENT RANGE
C_Z/C_Δ
$C_V^2/C_\Delta^{1/3}$
STEP
BOW
STERN
$C_X/C_\Delta^{1/3}$
HULL LINES
3.63
2.88
2.75
2.89
2.52
1.41
2.15
0.0
1.60
0.0
BASE LINE
STATION SPACING GIVEN AS DISTANCE FROM STEP, IN UNITS OF BEAM
FREE-TO-TRIM RESISTANCE AND TRIM DISPLACEMENT RANGE
$C_R/C_V^2 C_\Delta^{2/3}$
RESISTANCE
TRIM
C_Δ = 0.59
0.49
C_Δ = 0.59
0.49
TRIM ANGLE, DEG.
$C_V^2/C_\Delta^{1/3}$
TRIM ANGLE, DEG.
RESISTANCE AND STABILITY CHARACTERISTICS
PLANING RANGE
$Mq/V\frac{\rho}{2}b^4$ =
$\sqrt{C_R}/C_V$
$\sqrt{C_R}/C_V$ = 0.045
0.04
0.05
GETAWAY
NACA

Figure 35.

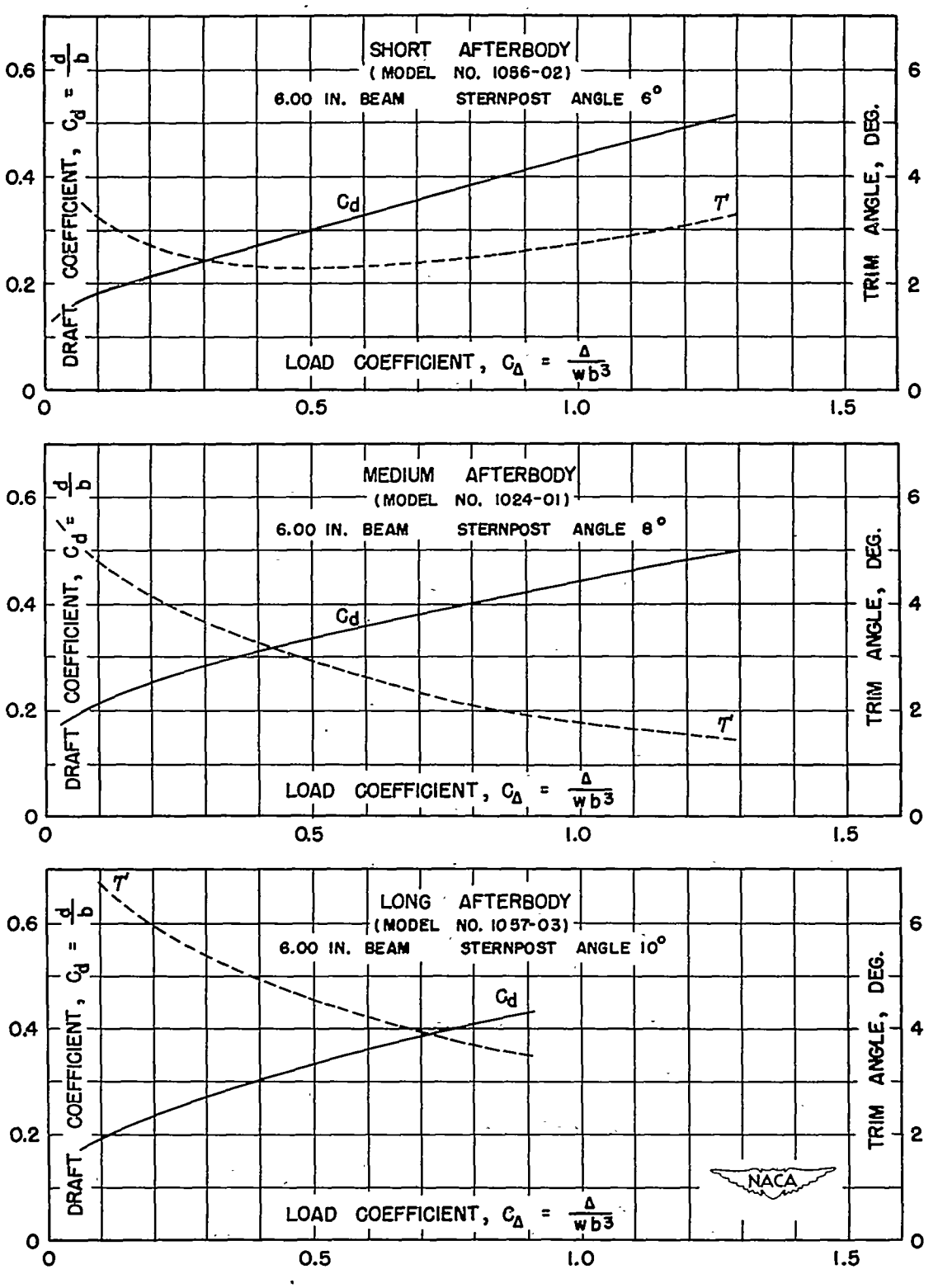

Figure 36.- Static properties at $C_M = 0$ with constant beam and varying sternpost angle and afterbody length.

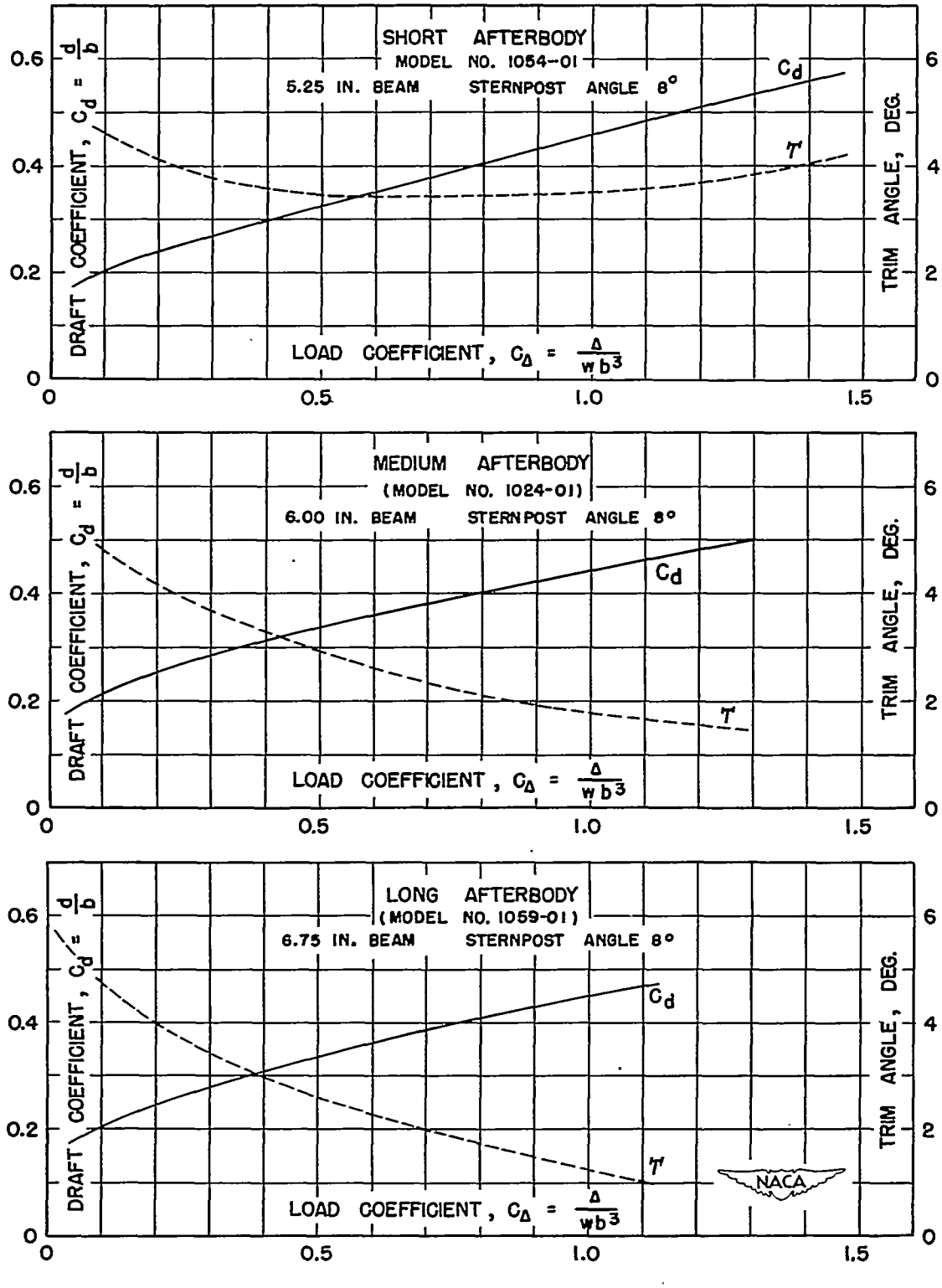

Figure 37.- Static properties at $C_M = 0$ with constant sternpost angle and varying beam and afterbody length.

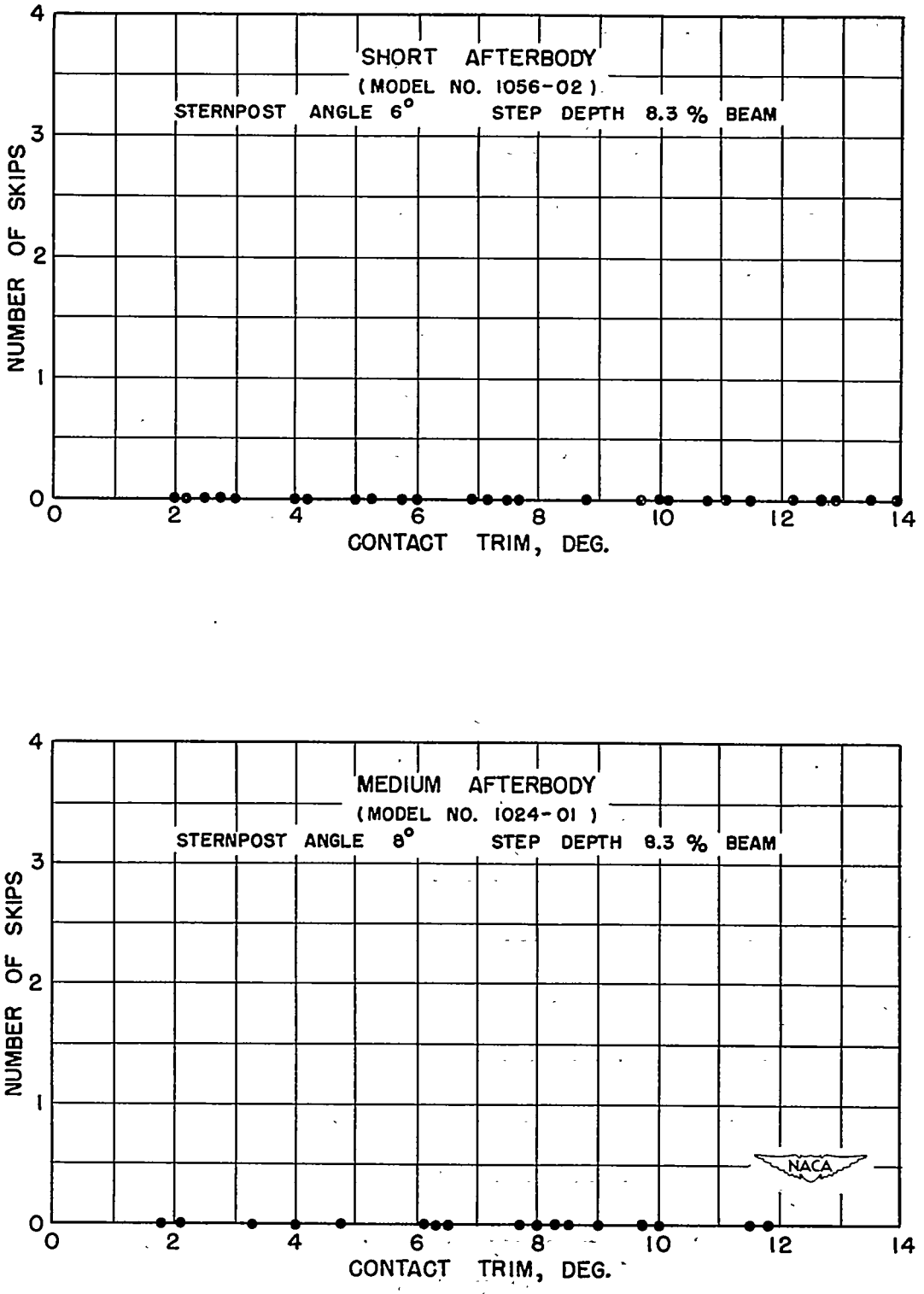

Figure 38.- Number of skips encountered on landing of short- and medium-afterbody hulls. Gross weight, 3000 pounds; wing loading, 11 pounds per square foot.

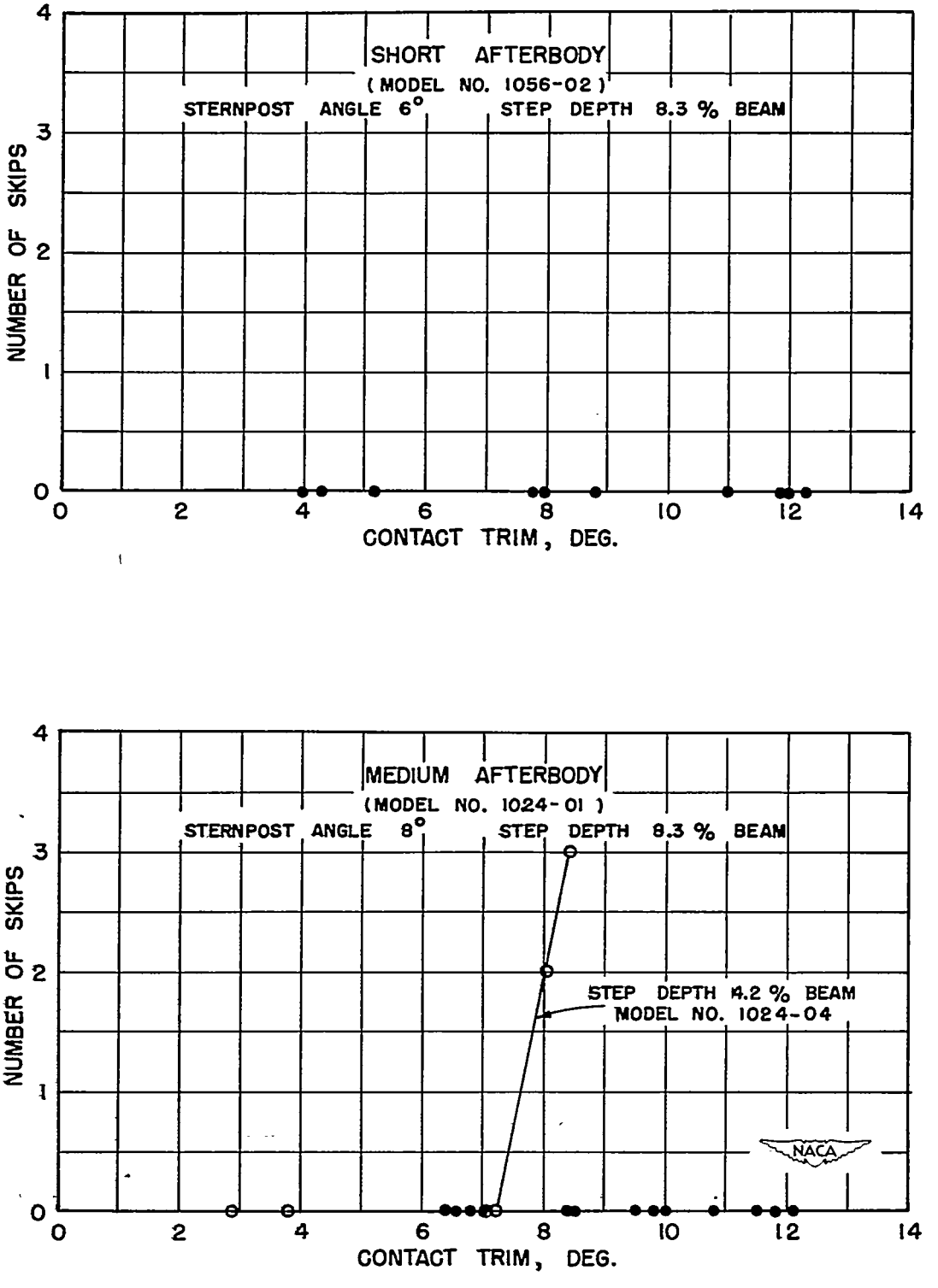

Figure 39.- Number of skips encountered on landing of short- and medium-afterbody hulls. Gross weight, 3000 pounds; wing loading, 14.5 pounds per square foot.

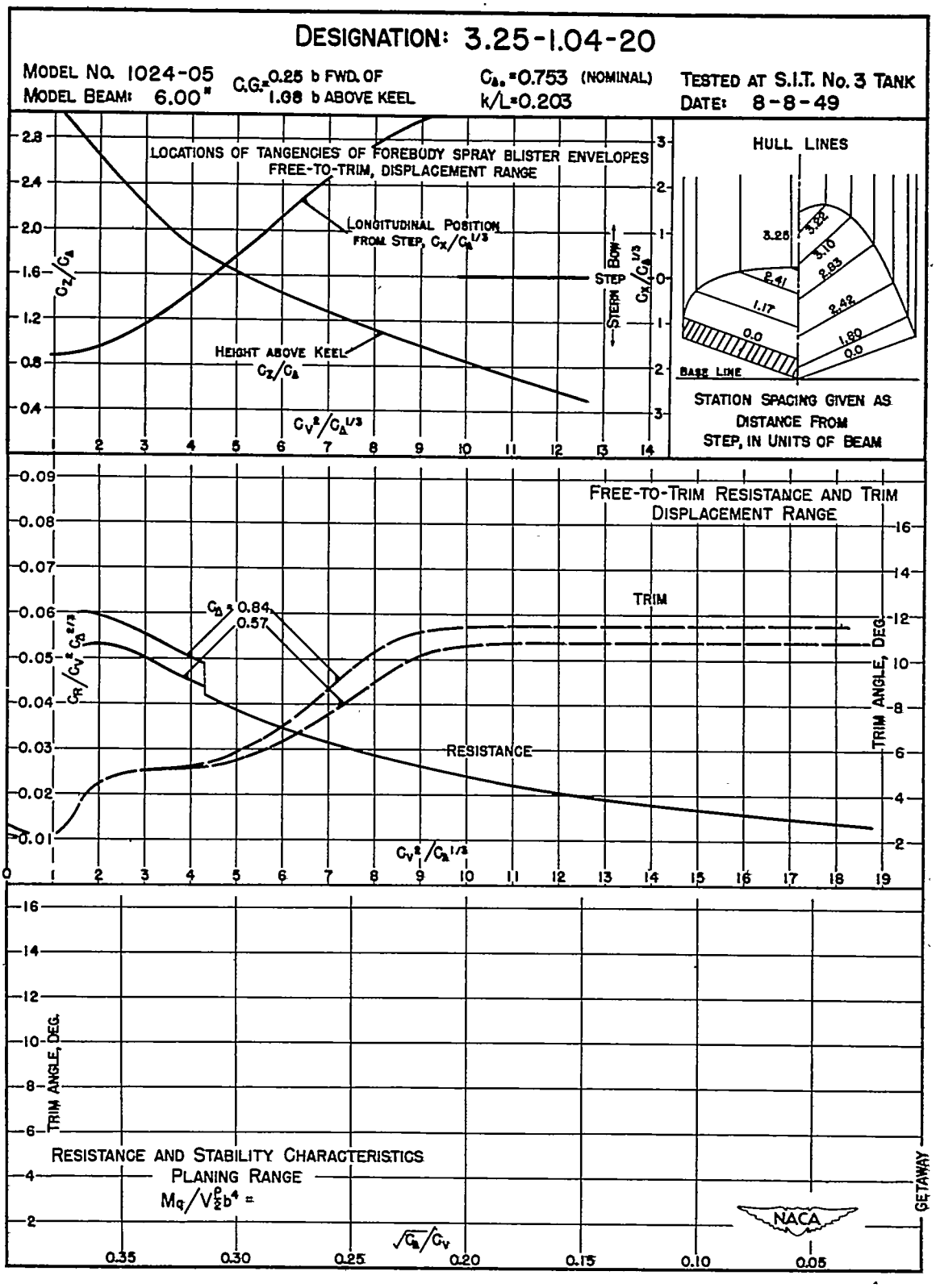
DESIGNATION: 3.25-1.04-20
MODEL NO. 1024-05
MODEL BEAM: 6.00"
C.G. = 0.25 b FWD. OF
1.08 b ABOVE KEEL
C_{Δ_0} = 0.753 (NOMINAL)
k/L = 0.203
TESTED AT S.I.T. No. 3 TANK
DATE: 8-8-49
LOCATIONS OF TANGENCIES OF FOREBODY SPRAY BLISTER ENVELOPES FREE-TO-TRIM, DISPLACEMENT RANGE
LONGITUDINAL POSITION FROM STEP, $C_x/C_\Delta^{1/3}$
HEIGHT ABOVE KEEL C_z/C_Δ
C_z/C_Δ
$C_x/C_\Delta^{1/3}$
BOW
STEP
STERN
$C_V^2/C_\Delta^{1/3}$
HULL LINES
3.25
3.22
3.10
2.83
2.41
2.42
1.17
1.89
0.0
0.0
BASE LINE
STATION SPACING GIVEN AS DISTANCE FROM STEP, IN UNITS OF BEAM
FREE-TO-TRIM RESISTANCE AND TRIM DISPLACEMENT RANGE
C_Δ = 0.84
0.57
TRIM
RESISTANCE
$C_R/C_V^2 C_\Delta^{2/3}$
TRIM ANGLE, DEG.
$C_V^2/C_\Delta^{1/3}$
TRIM ANGLE, DEG.
RESISTANCE AND STABILITY CHARACTERISTICS
PLANING RANGE
$M_q/V\frac{\rho}{2}b^4$ =
$\sqrt{C_\Delta}/C_V$
GETAWAY
NACA

Figure 40.

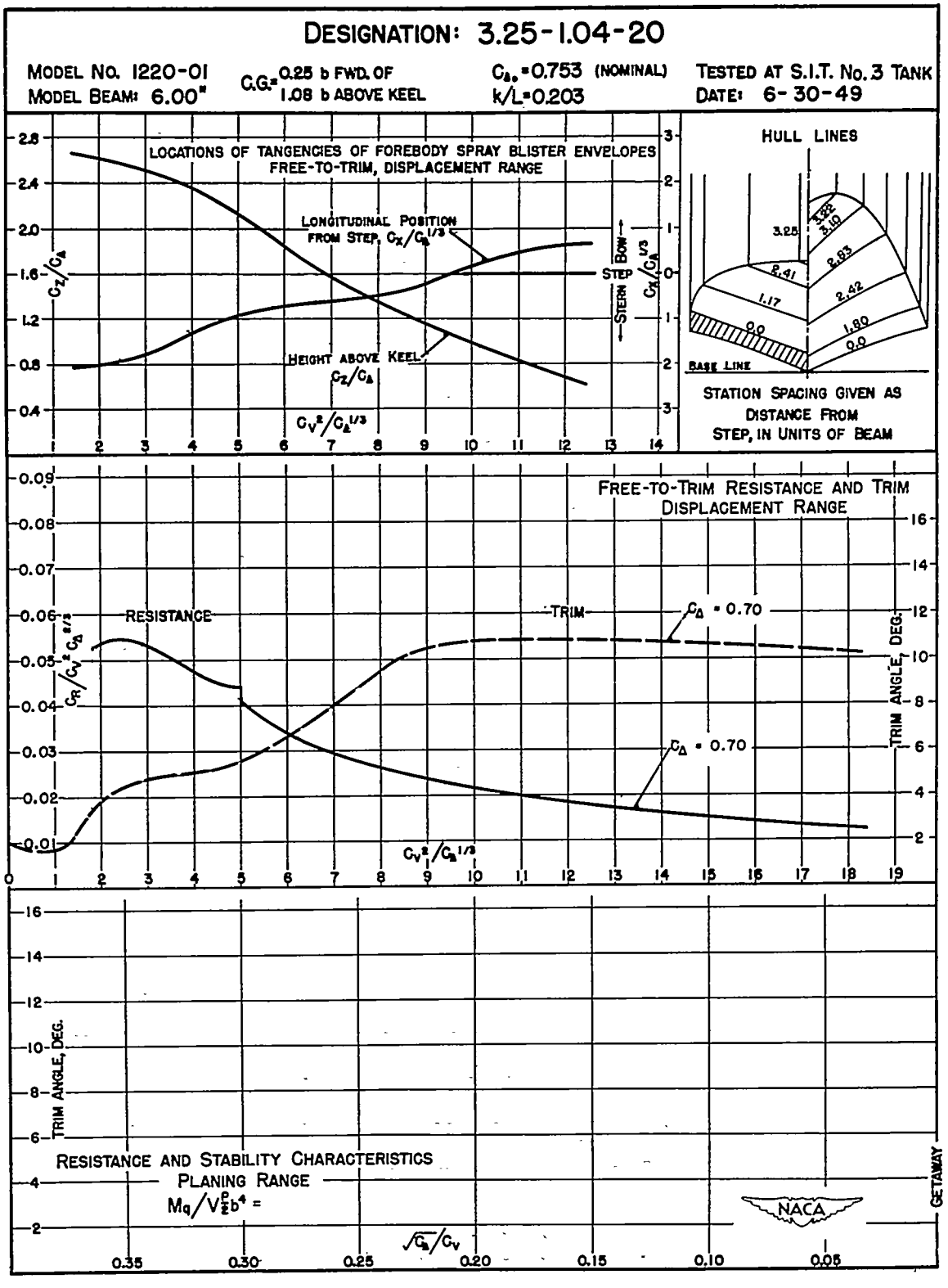
DESIGNATION: 3.25-1.04-20
MODEL NO. 1220-01
MODEL BEAM: 6.00"
C.G.: 0.25 b FWD. OF 1.08 b ABOVE KEEL
C_{Δ_o} = 0.753 (NOMINAL)
k/L = 0.203
TESTED AT S.I.T. No. 3 TANK
DATE: 6-30-49
LOCATIONS OF TANGENCIES OF FOREBODY SPRAY BLISTER ENVELOPES FREE-TO-TRIM, DISPLACEMENT RANGE
LONGITUDINAL POSITION FROM STEP, $C_x/C_\Delta^{1/3}$
HEIGHT ABOVE KEEL, C_z/C_Δ
C_z/C_Δ
$C_V^2/C_\Delta^{1/3}$
BOW
STEP
STERN
$C_x/C_\Delta^{1/3}$
HULL LINES
3.25
2.41
1.17
0.0
2.83
2.42
1.89
0.0
BASE LINE
STATION SPACING GIVEN AS DISTANCE FROM STEP, IN UNITS OF BEAM
FREE-TO-TRIM RESISTANCE AND TRIM DISPLACEMENT RANGE
RESISTANCE
TRIM
C_Δ = 0.70
C_Δ = 0.70
$C_R/C_V^2 C_\Delta^{2/3}$
TRIM ANGLE, DEG.
$C_V^2/C_\Delta^{1/3}$
TRIM ANGLE, DEG.
RESISTANCE AND STABILITY CHARACTERISTICS
PLANING RANGE
$Mq/V_z^2 b^4$ =
$\sqrt{C_\Delta}/C_V$
NACA
GETAWAY

Figure 41.

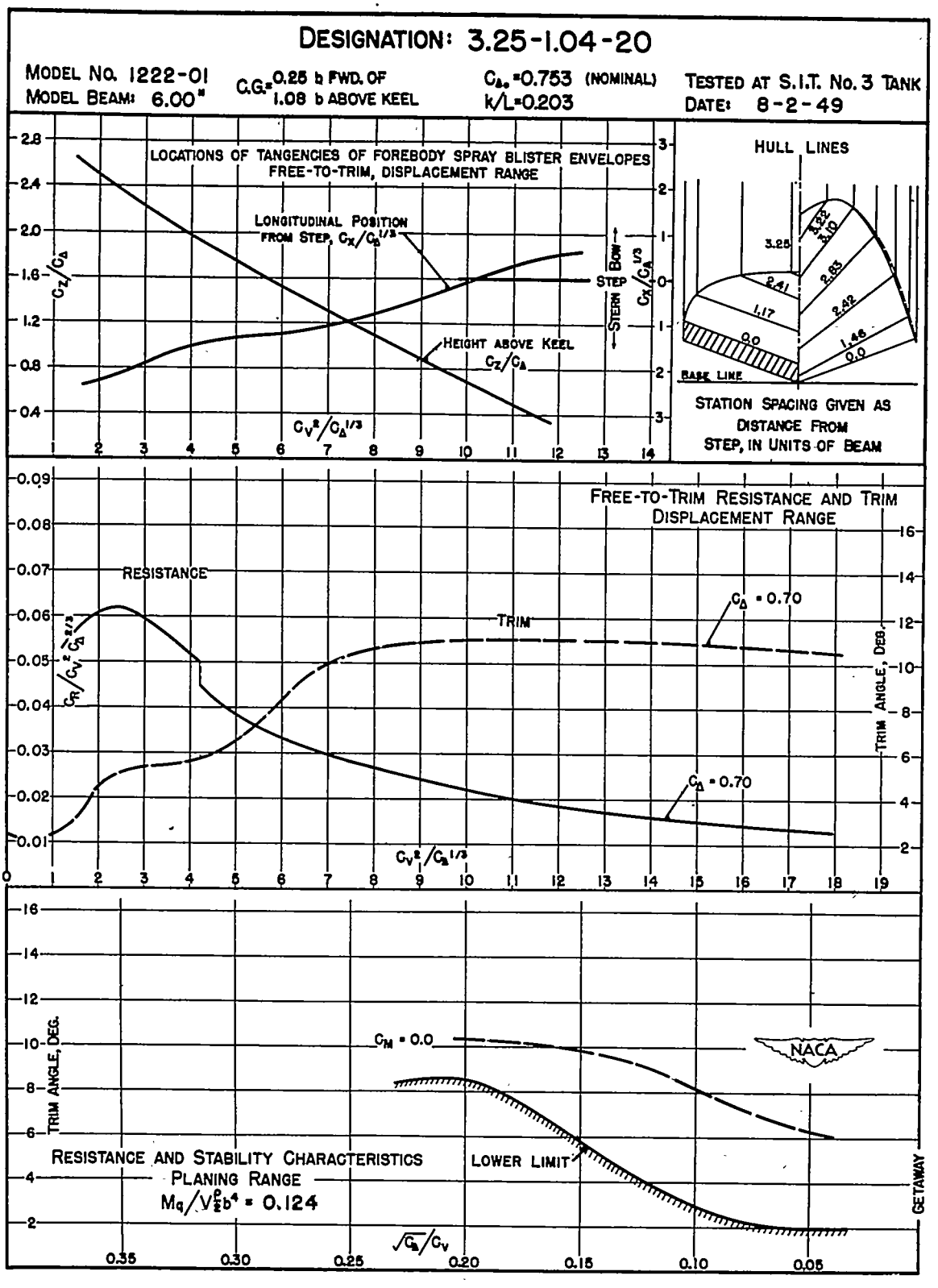
DESIGNATION: 3.25-1.04-20
MODEL NO. 1222-01
MODEL BEAM: 6.00"
C.G.=0.25 b FWD. OF 1.08 b ABOVE KEEL
C_{Δ_0}=0.753 (NOMINAL)
k/L=0.203
TESTED AT S.I.T. No. 3 TANK
DATE: 8-2-49
LOCATIONS OF TANGENCIES OF FOREBODY SPRAY BLISTER ENVELOPES FREE-TO-TRIM, DISPLACEMENT RANGE
LONGITUDINAL POSITION FROM STEP, $C_x/C_\Delta^{1/3}$
HEIGHT ABOVE KEEL C_z/C_Δ
C_z/C_Δ
$C_x/C_\Delta^{1/3}$
STEP
BOW
STERN
$C_V^2/C_\Delta^{1/3}$
HULL LINES
3.25
2.41
1.17
0.0
3.22
3.10
2.65
2.42
1.46
0.0
BASE LINE
STATION SPACING GIVEN AS DISTANCE FROM STEP, IN UNITS OF BEAM
FREE-TO-TRIM RESISTANCE AND TRIM DISPLACEMENT RANGE
RESISTANCE
TRIM
C_Δ = 0.70
C_Δ = 0.70
$C_R/C_V^2 C_\Delta^{2/3}$
TRIM ANGLE, DEG.
$C_V^2/C_\Delta^{1/3}$
TRIM ANGLE, DEG.
C_M = 0.0
NACA
RESISTANCE AND STABILITY CHARACTERISTICS
PLANING RANGE
$Mq/V\frac{\rho}{2}b^4$ = 0.124
LOWER LIMIT
GETAWAY
$\sqrt{C_\Delta}/C_V$

Figure 42.

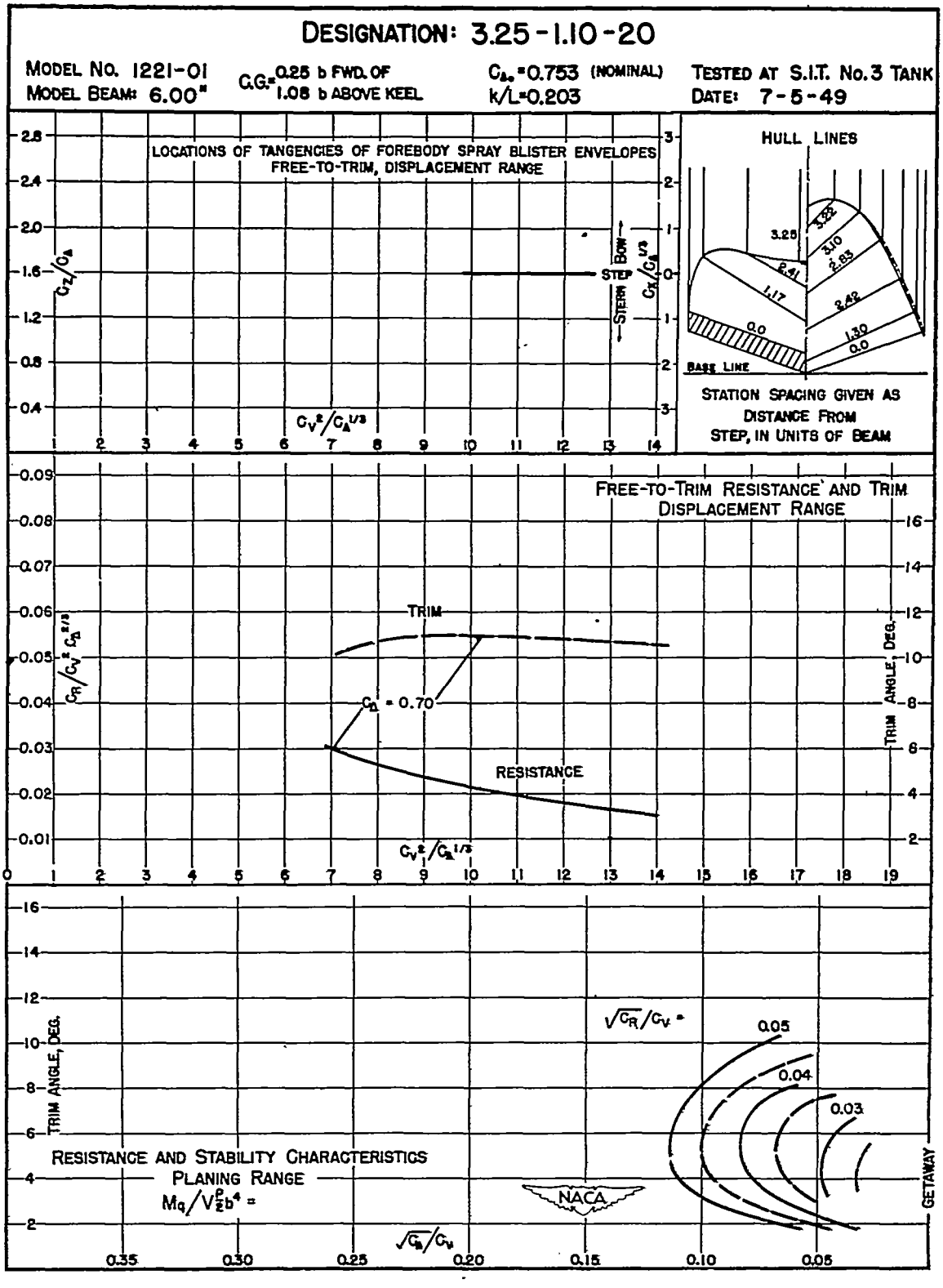
DESIGNATION: 3.25 - 1.10 - 20
MODEL NO. 1221-01
MODEL BEAM: 6.00"
C.G. 0.25 b FWD. OF 1.08 b ABOVE KEEL
C_{Δ_0} = 0.753 (NOMINAL)
k/L = 0.203
TESTED AT S.I.T. No. 3 TANK
DATE: 7-5-49
LOCATIONS OF TANGENCIES OF FOREBODY SPRAY BLISTER ENVELOPES FREE-TO-TRIM, DISPLACEMENT RANGE
C_Z/C_Δ
$C_V^2/C_\Delta^{1/3}$
STEP
BOW
STERN
C_X/C_Δ
HULL LINES
3.25
3.22
3.10
2.83
2.41
1.17
2.42
1.39
0.0
BASE LINE
STATION SPACING GIVEN AS DISTANCE FROM STEP, IN UNITS OF BEAM
FREE-TO-TRIM RESISTANCE AND TRIM DISPLACEMENT RANGE
$C_R/C_V^2 C_\Delta^{2/3}$
TRIM
C_Δ = 0.70
RESISTANCE
TRIM ANGLE, DEG.
RESISTANCE AND STABILITY CHARACTERISTICS
PLANING RANGE
$M_q/V\rho b^4$ =
$\sqrt{C_R}/C_V$ =
0.05
0.04
0.03
GETAWAY
NACA
$\sqrt{C_\Delta}/C_V$

Figure 43.

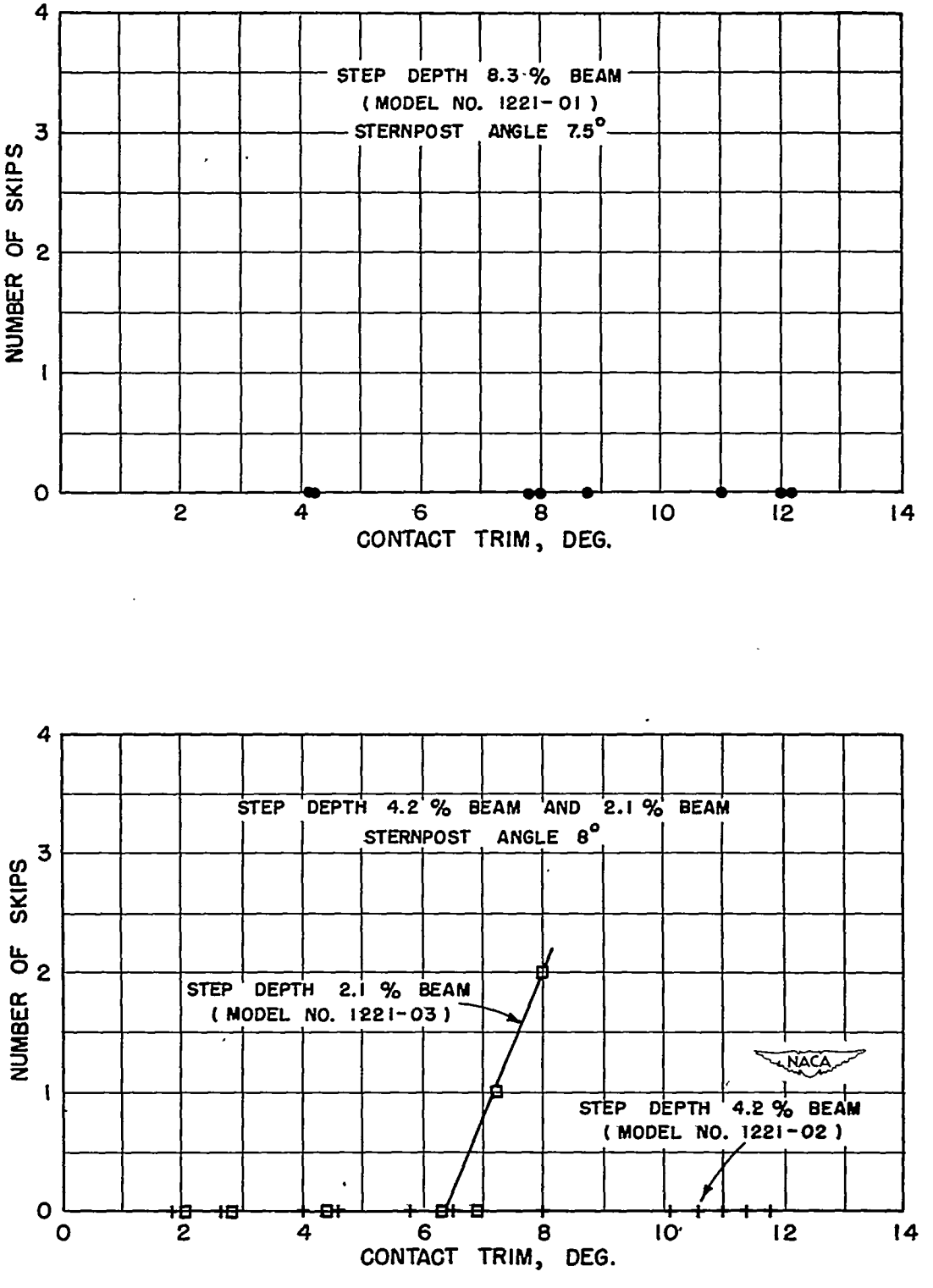

Figure 44.- Effect of step depth on number of skips encountered on landing. Warped-afterbody hulls; gross weight, 3000 pounds; wing loading, 14.5 pounds per square foot.

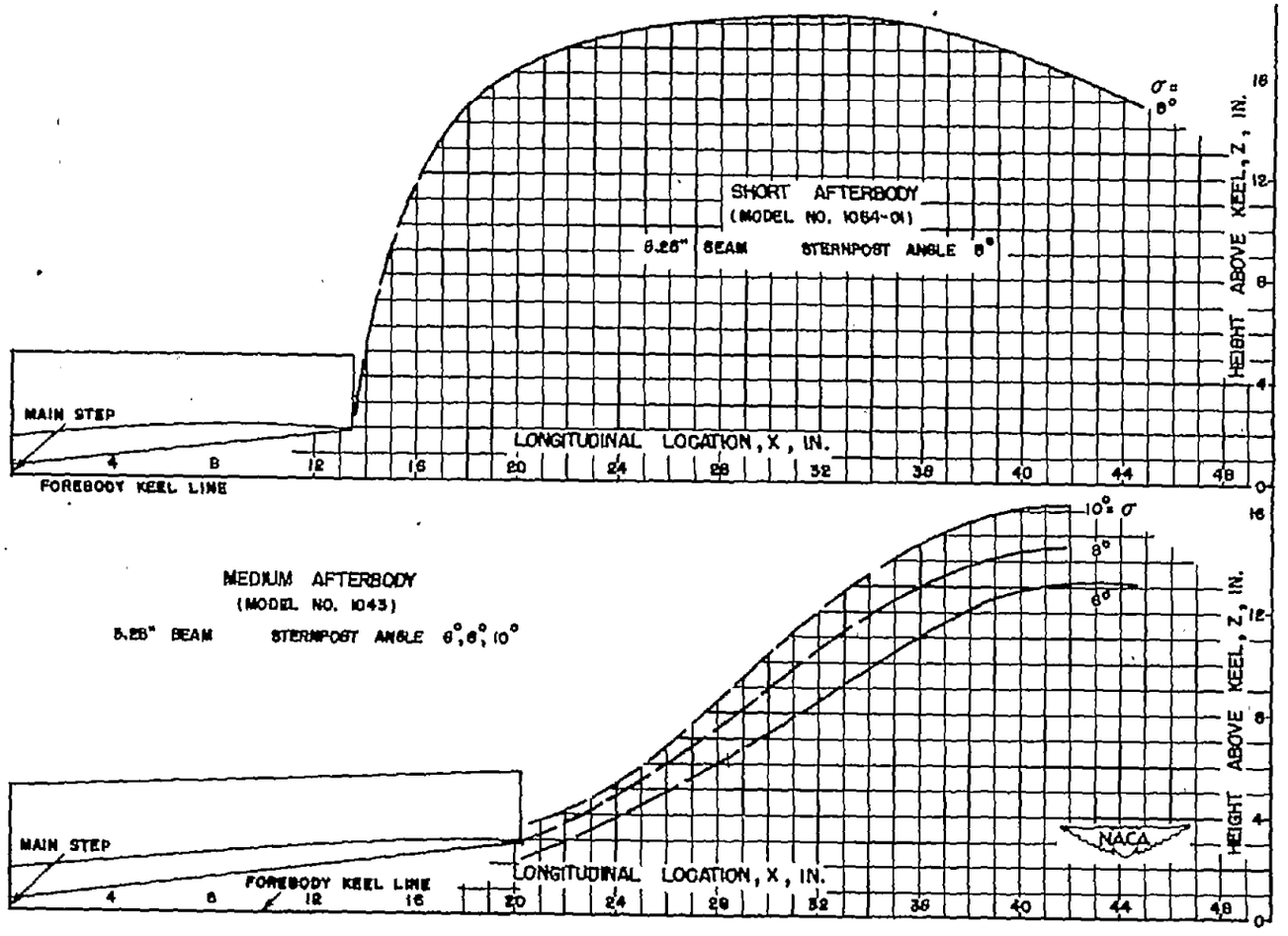

Figure 45.- Envelope of afterbody-roach profile. Constant-load comparison of free-to-trim tests at zero trimming moment for short-afterbody model no. 1054-01 and medium-afterbody model no. 1043.

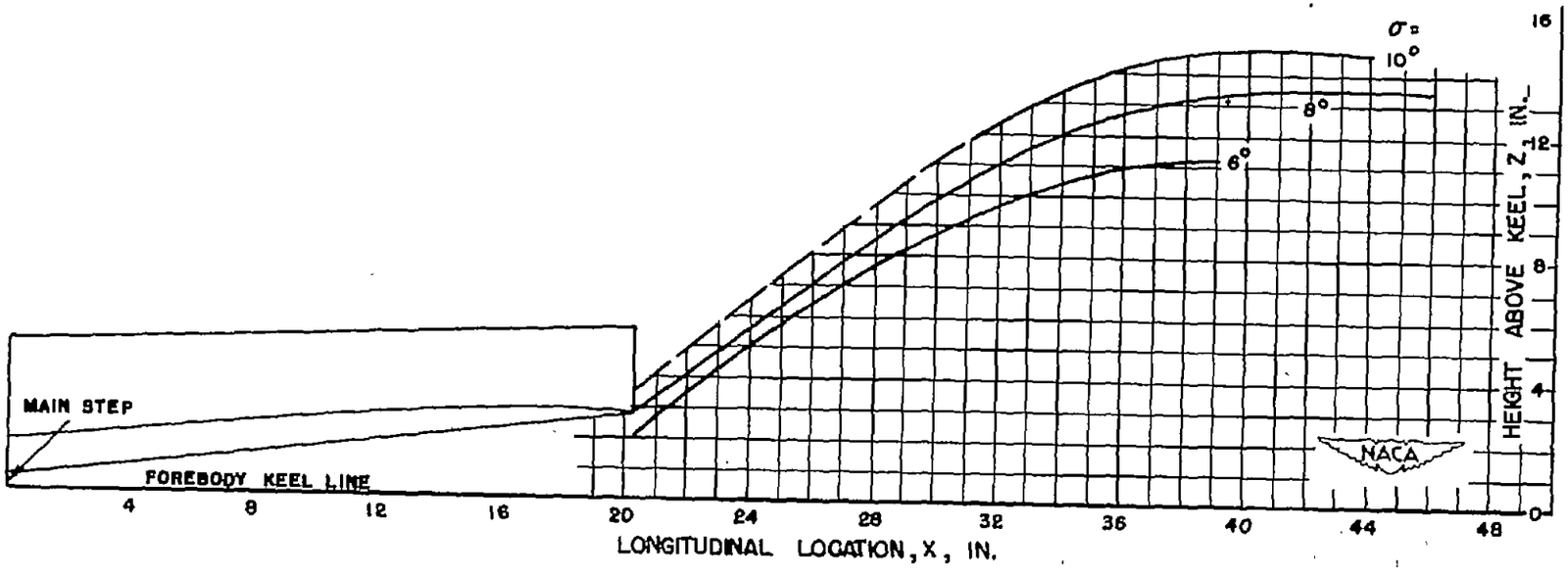

Figure 46.- Envelope of afterbody-roach profile. Constant-load comparison of free-to-trim tests at zero trimming moment for medium-afterbody model no. 1024 with 6-inch beam and a sternpost angle of 6°, 8°, and 10°.

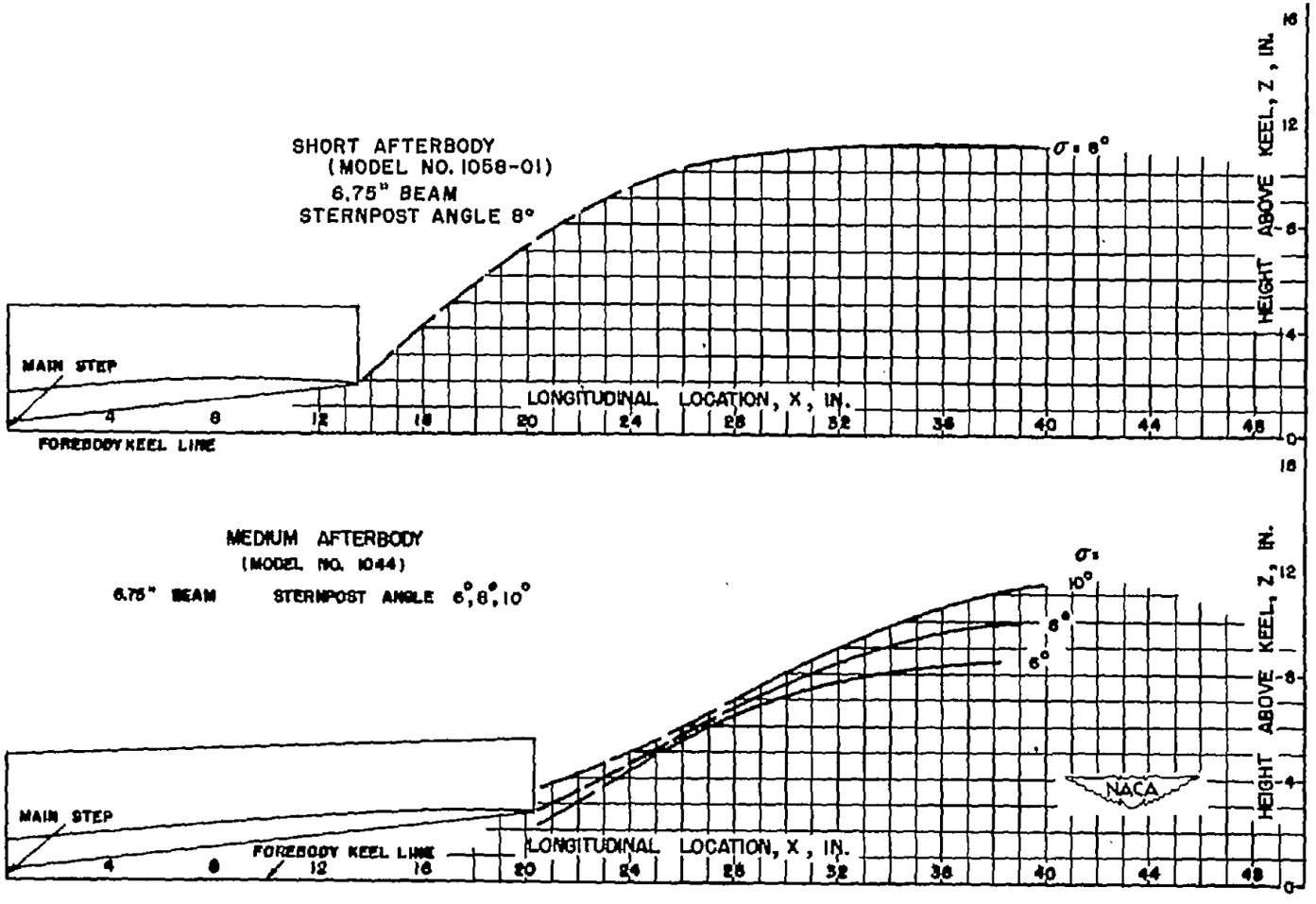

Figure 47.- Envelope of afterbody-roach profile. Constant-load comparison of free-to-trim tests at zero trimming moment for short-afterbody model no. 1058-01 and medium-afterbody model no. 1044.

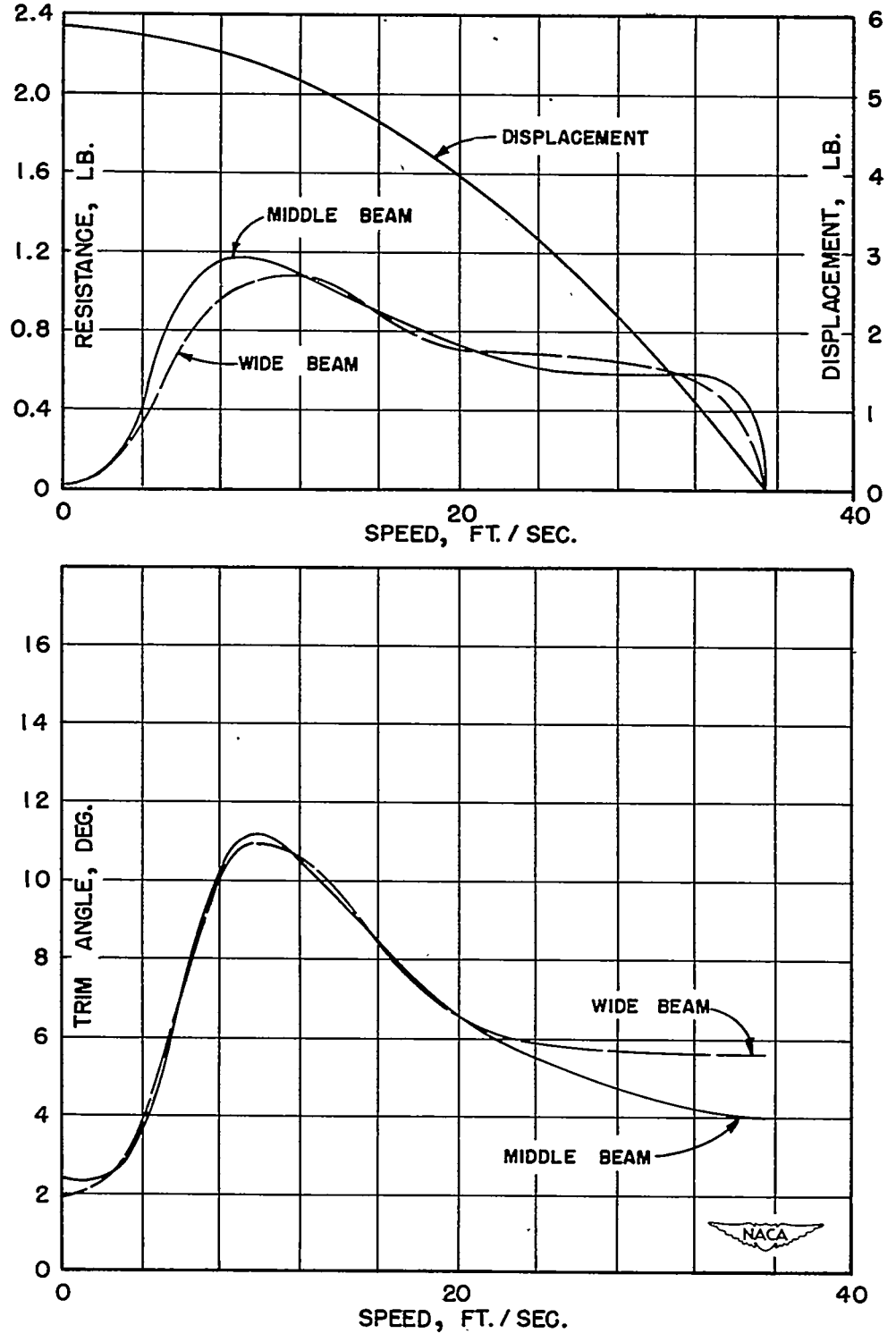

Figure 48.- Variation of resistance and trim with speed for models with a short afterbody and sternpost angle of 6°. Constant-load comparison; initial load, 5.86 pounds; take-off speed, 35.6 feet per second.

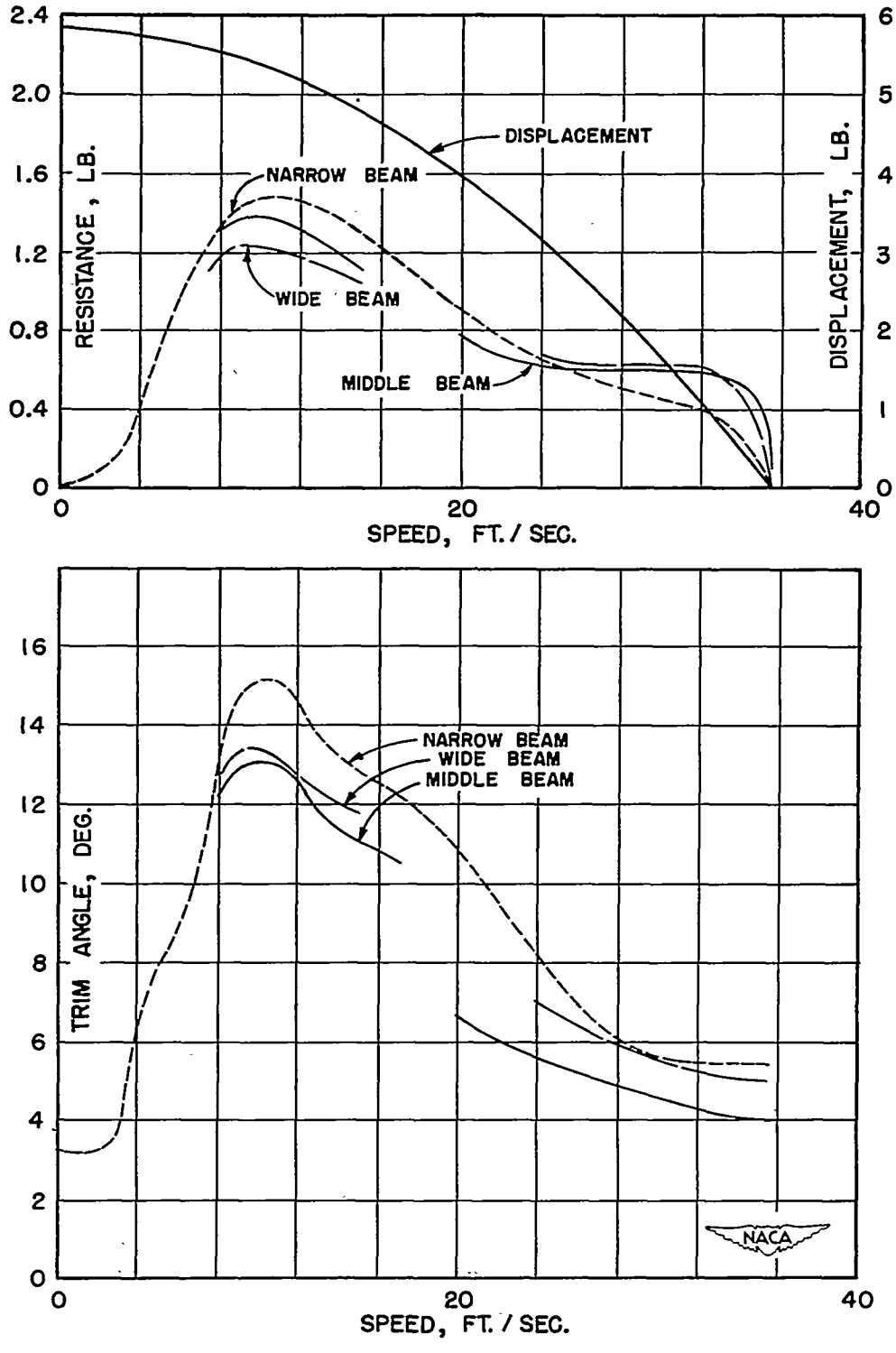

Figure 49.- Variation of resistance and trim with speed for models with a short afterbody and sternpost angle of 8°. Constant-load comparison; initial load, 5.86 pounds; take-off speed, 35.6 feet per second.

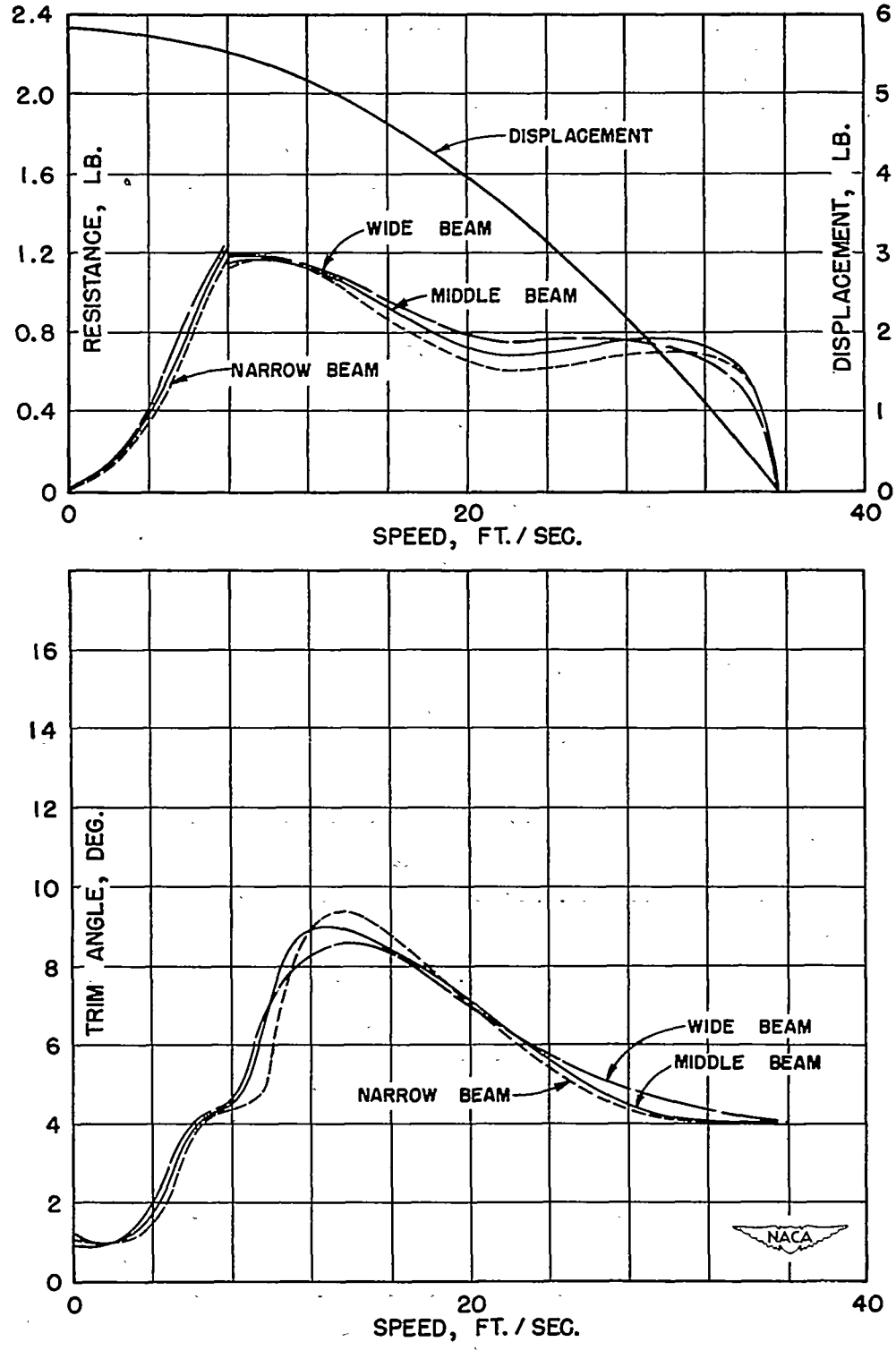

Figure 50.- Variation of resistance and trim with speed for models with a medium afterbody and sternpost angle of 6°. Constant-load comparison; initial load, 5.86 pounds; take-off speed, 35.6 feet per second.

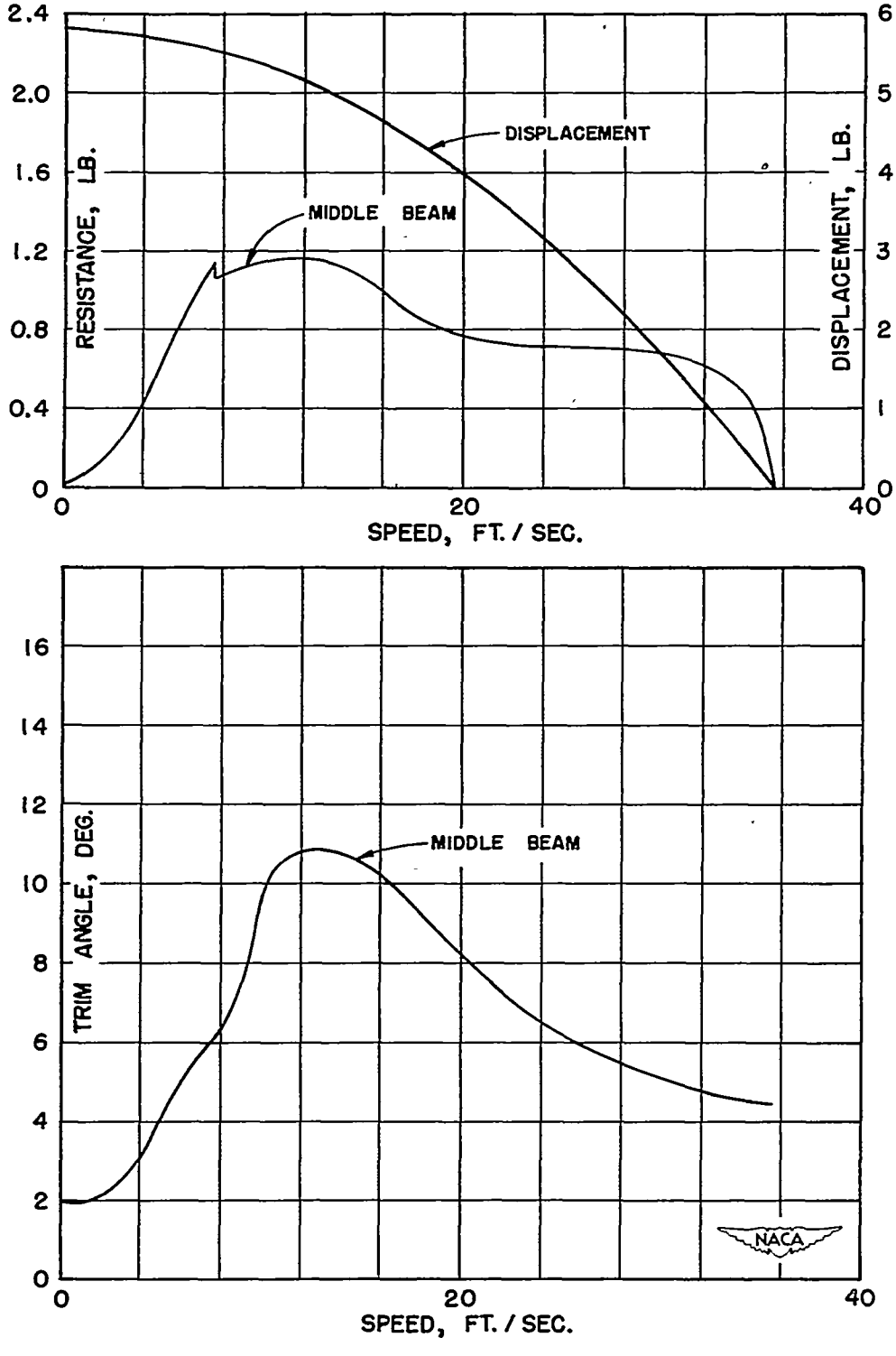

Figure 51.- Variation of resistance and trim with speed for model with a medium afterbody and sternpost angle of 8°. Constant-load comparison; initial load, 5.86 pounds; take-off speed, 35.6 feet per second.

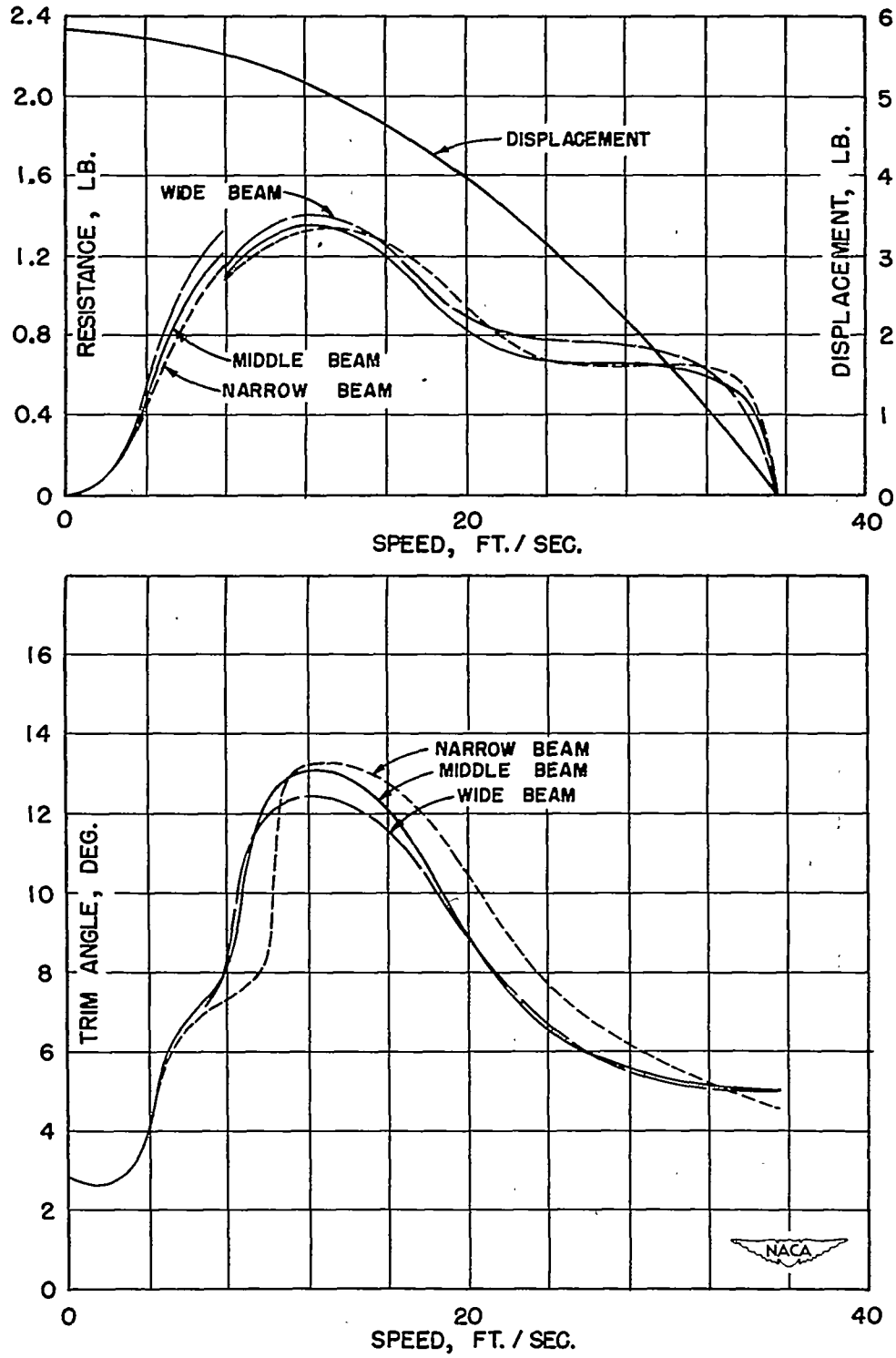

Figure 52.- Variation of resistance and trim with speed for models with a medium afterbody and sternpost angle of 10°. Constant-load comparison; initial load, 5.86 pounds; take-off speed, 35.6 feet per second.

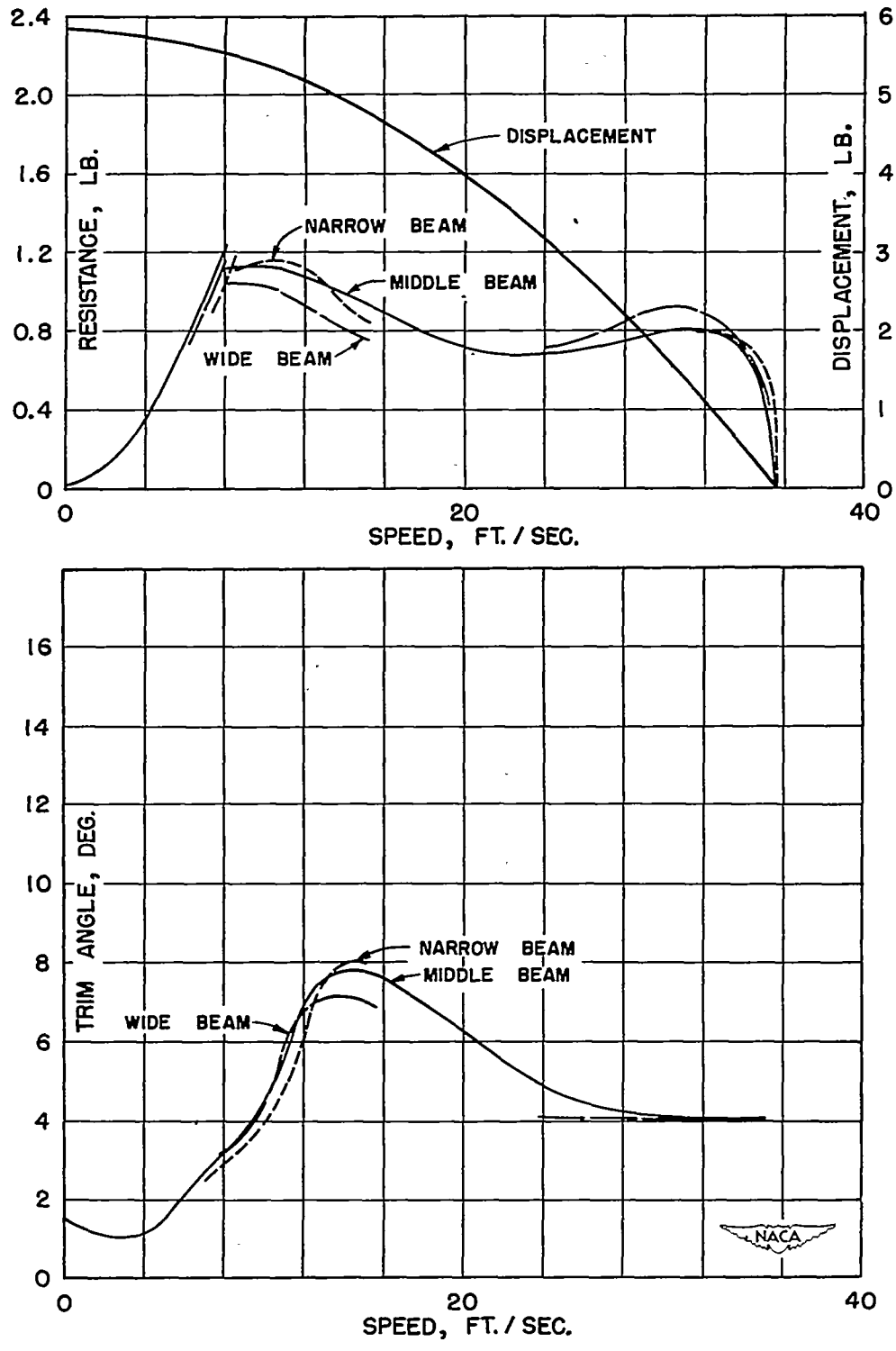

Figure 53.- Variation of resistance and trim with speed for models with a long afterbody and sternpost angle of 6°. Constant-load comparison; initial load, 5.86 pounds; take-off speed, 35.6 feet per second.

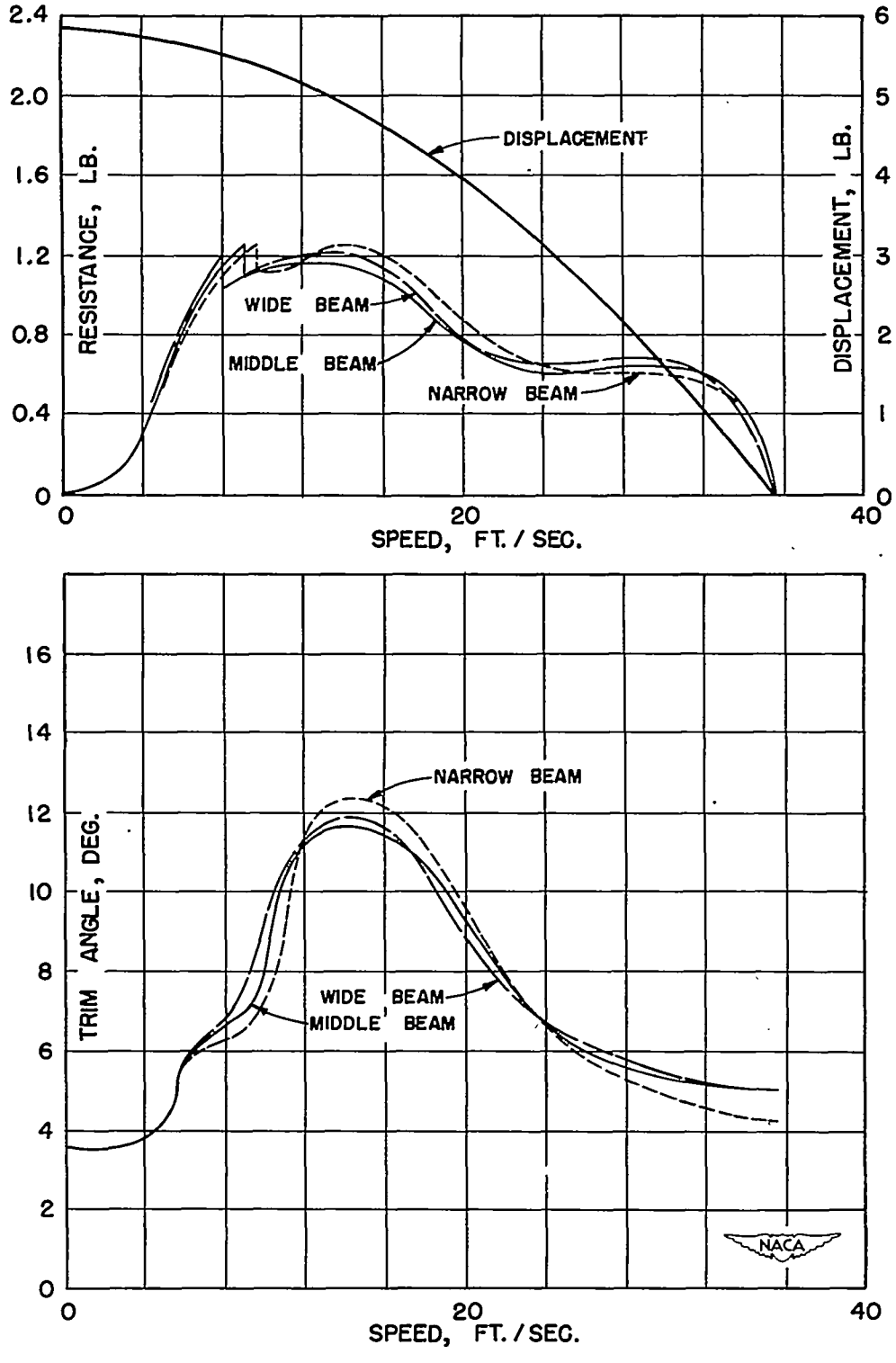

Figure 54.- Variation of resistance and trim with speed for models with a long afterbody and sternpost angle of 10°. Constant-load comparison; initial load, 5.86 pounds; take-off speed, 35.6 feet per second.

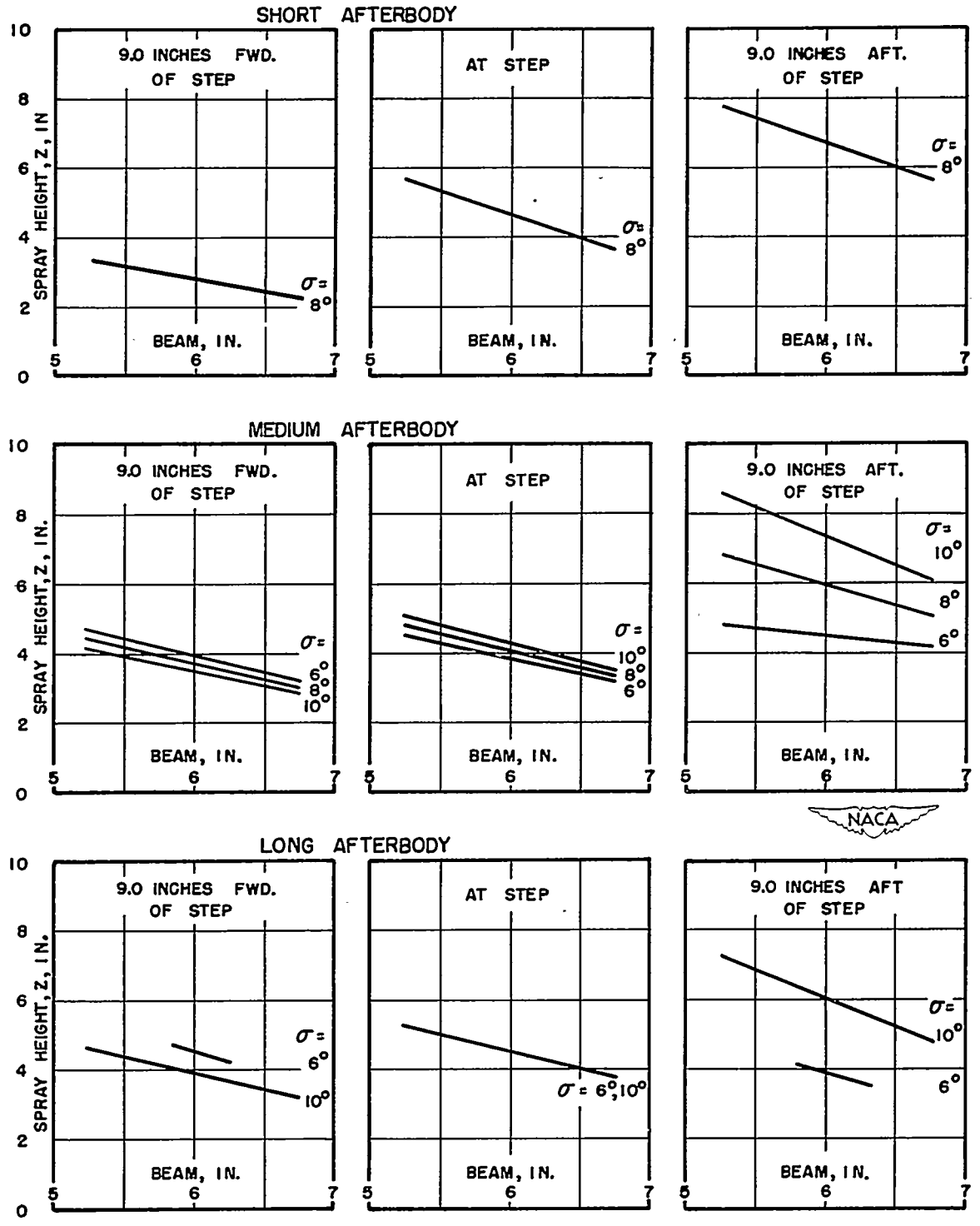

Figure 55.- Variation of model spray height with beam at three longitudinal locations along hull for free-to-trim tests at zero trimming moment. Constant-load comparison; initial load, 5.86 pounds; take-off speed, 35.63 feet per second.

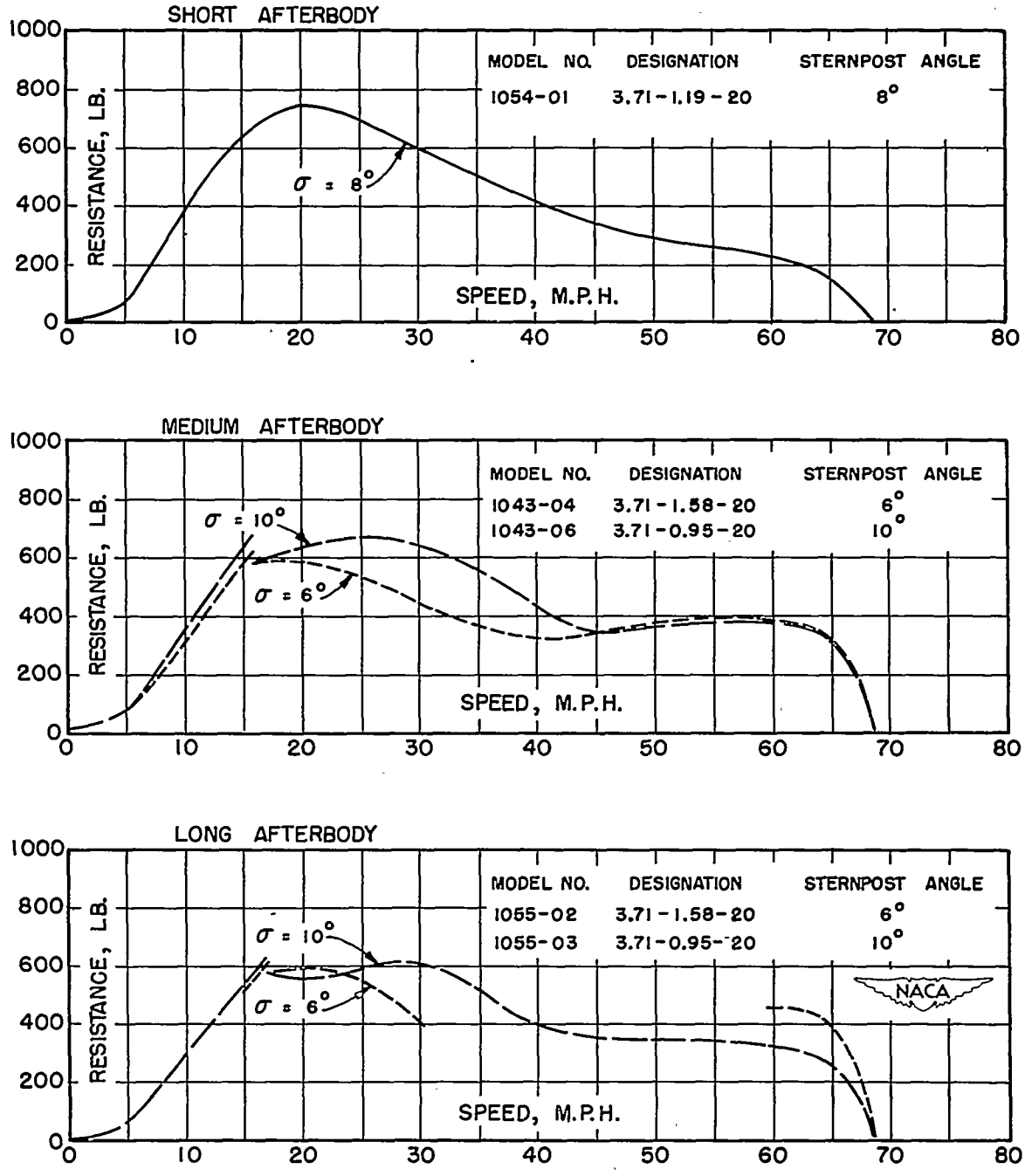

Figure 56.- Variation of resistance with speed for narrow-beam hulls. Comparison with constant forebody plan-form area; gross weight, 3000 pounds; take-off speed, 68.7 miles per hour.

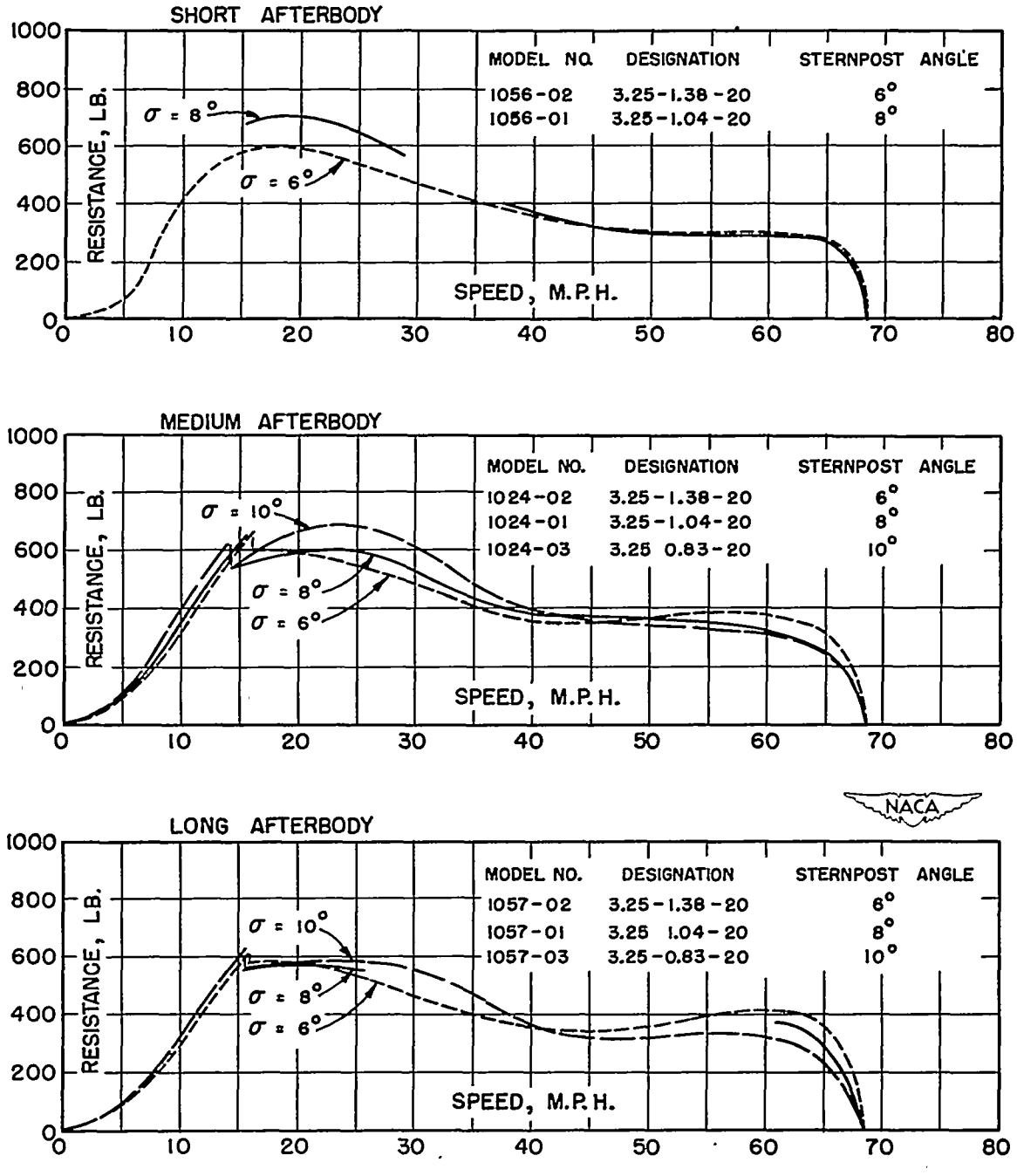

Figure 57.- Variation of resistance with speed for middle-beam hulls. Comparison with constant forebody plan-form area; gross weight, 3000 pounds; take-off speed, 68.7 miles per hour.

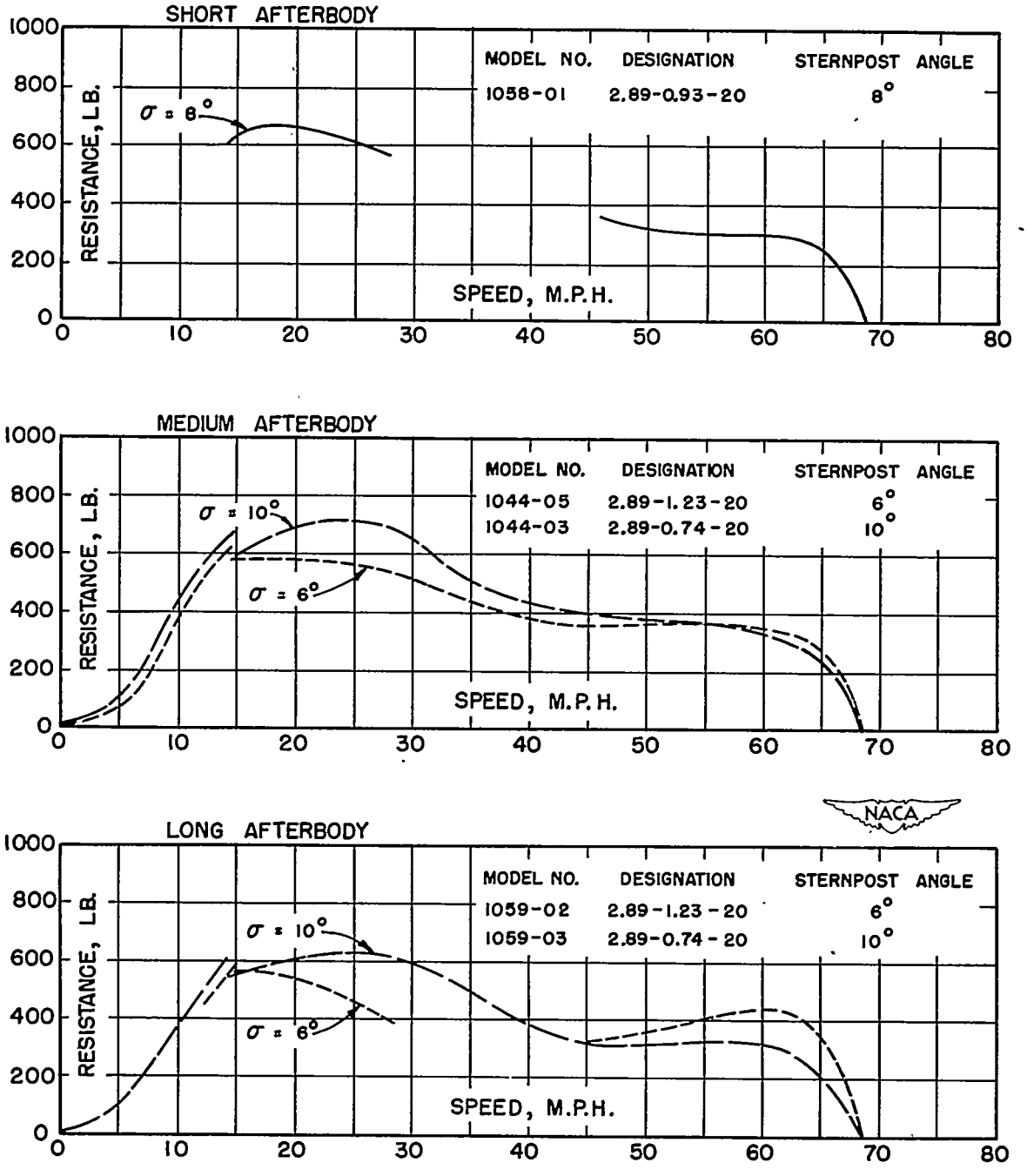

Figure 58.- Variation of resistance with speed for wide-beam hulls. Comparison with constant forebody plan-form area; gross weight, 3000 pounds; take-off speed, 68.7 miles per hour.

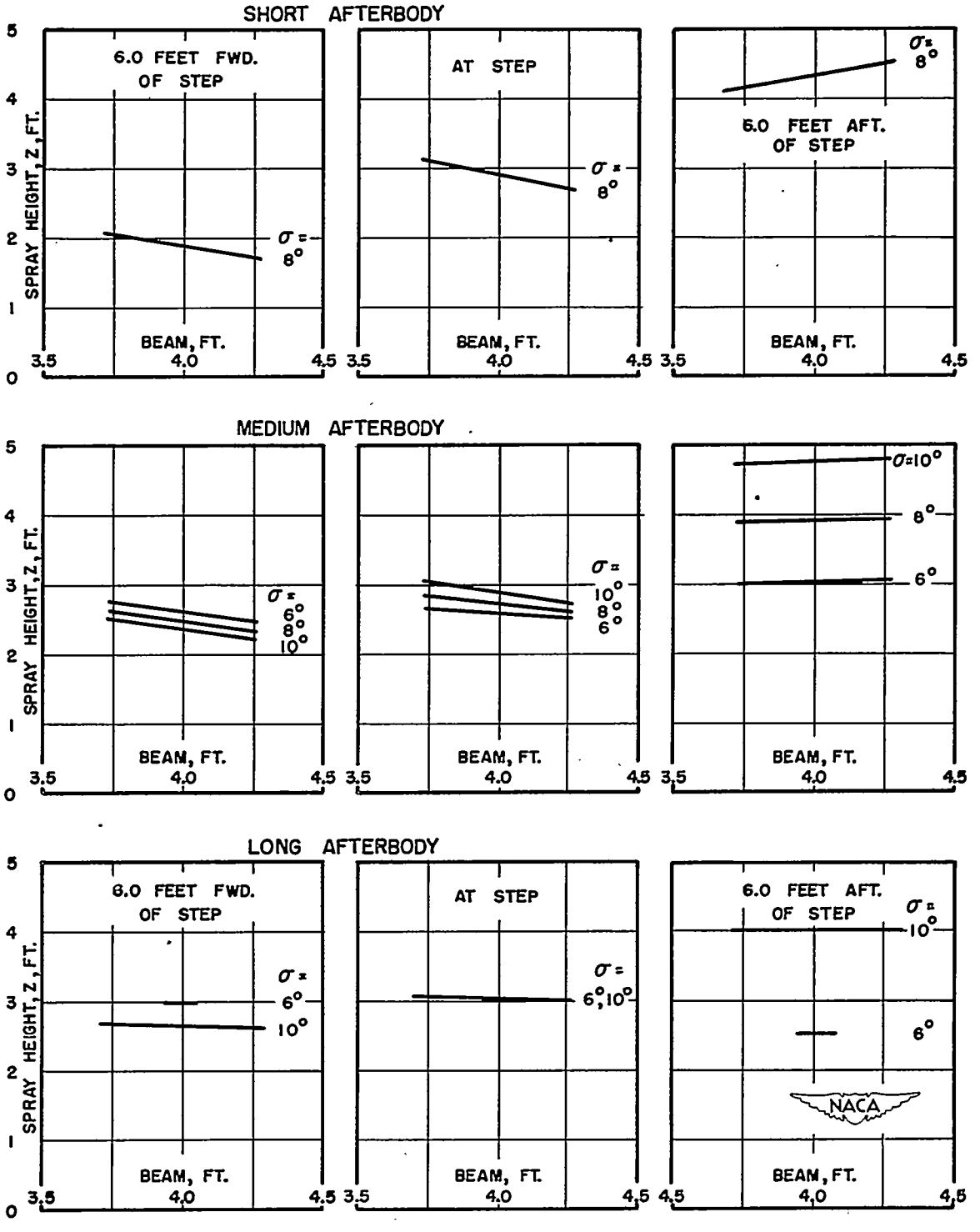

Figure 59.- Variation of spray height with beam at three longitudinal locations along hull. Comparison with constant forebody plan-form area for free-to-trim tests at zero trimming moment; gross weight, 3000 pounds; take-off speed, 68.7 miles per hour.

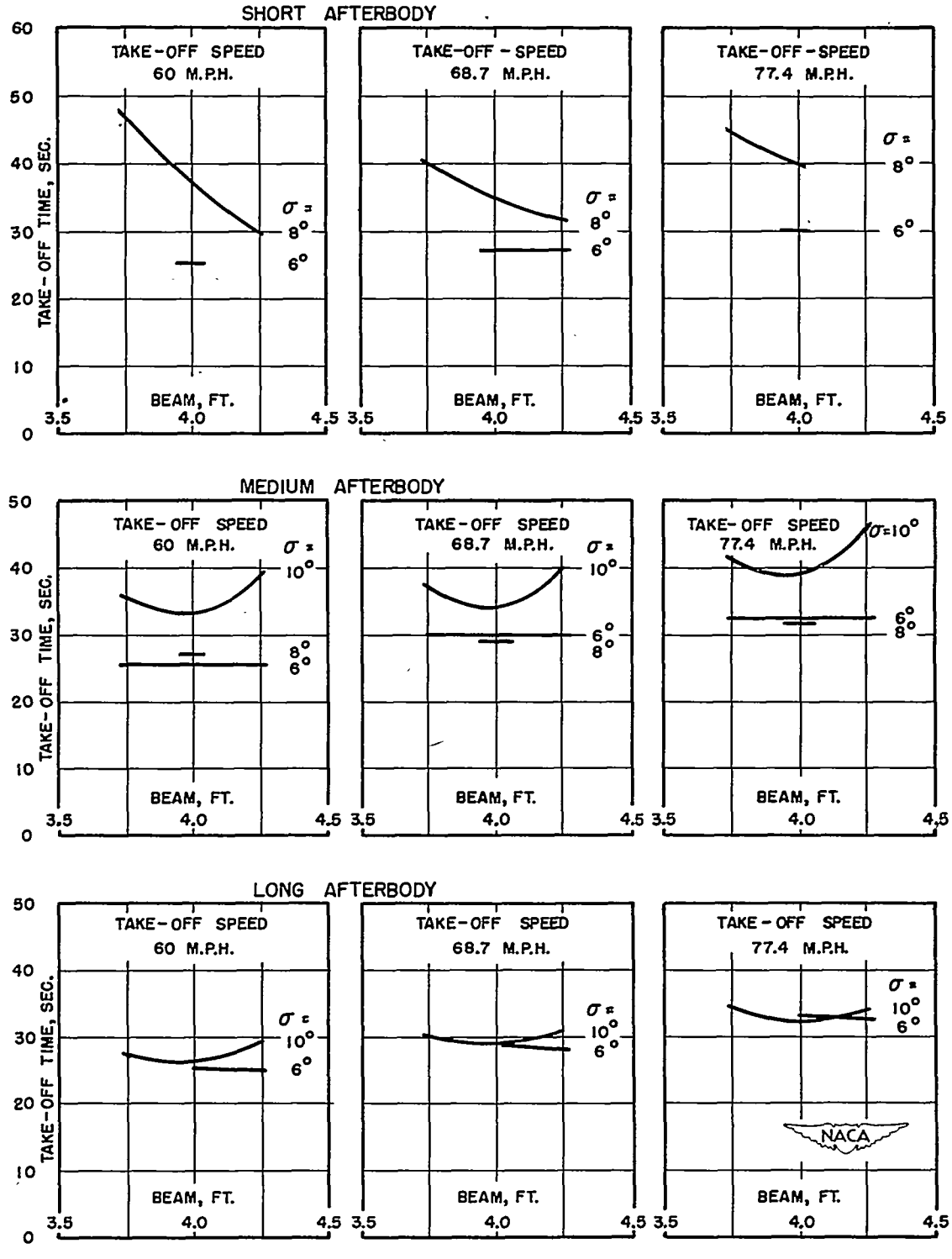

Figure 60.- Variation of take-off time with beam for three take-off speeds. Comparison with constant forebody plan-form area; gross weight, 3000 pounds.

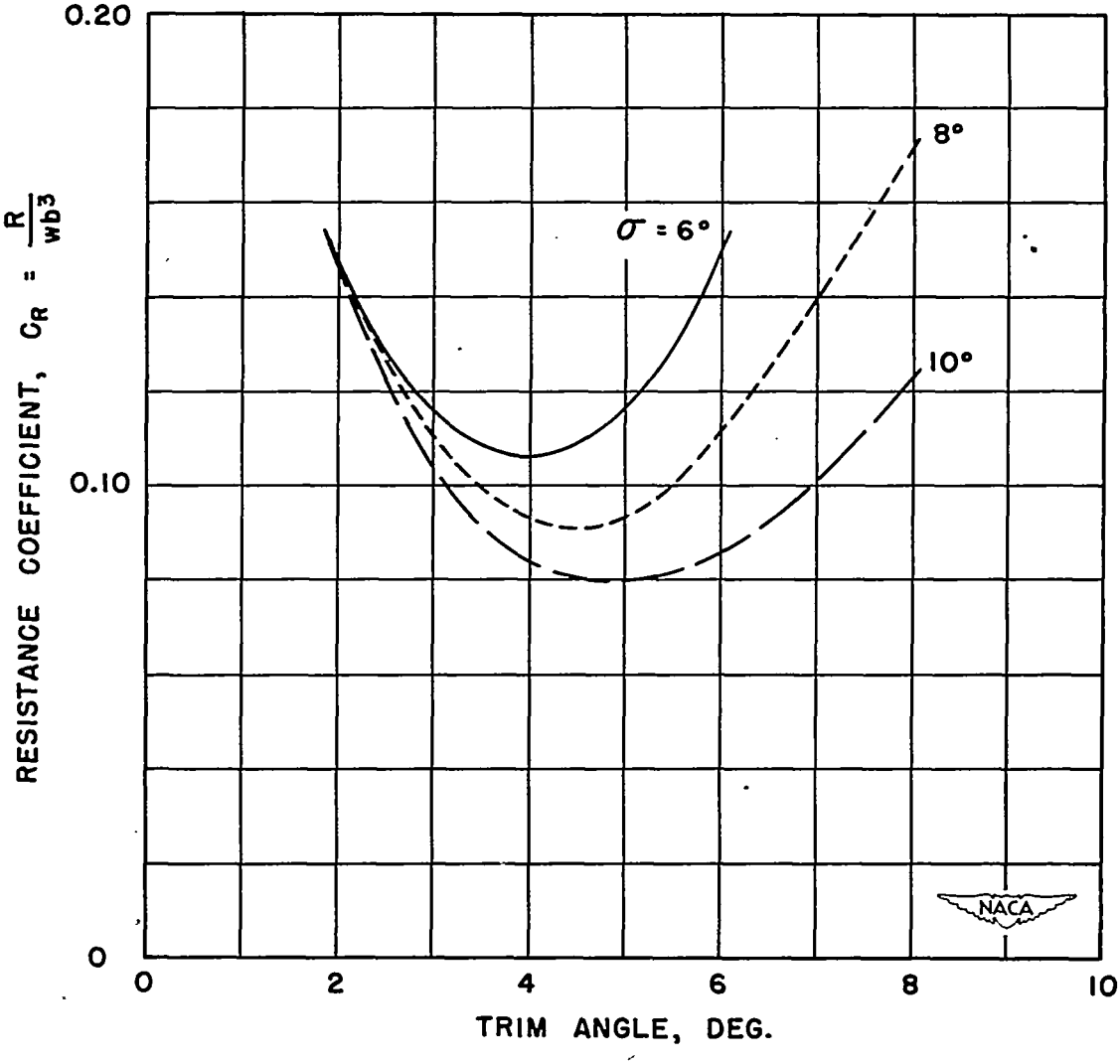

Figure 61.- Variation of resistance coefficient with trim angle at 90 percent of take-off speed of 68.7 miles per hour. Long-afterbody model no. 1057; C_V = 7.99; C_Δ = 0.143.

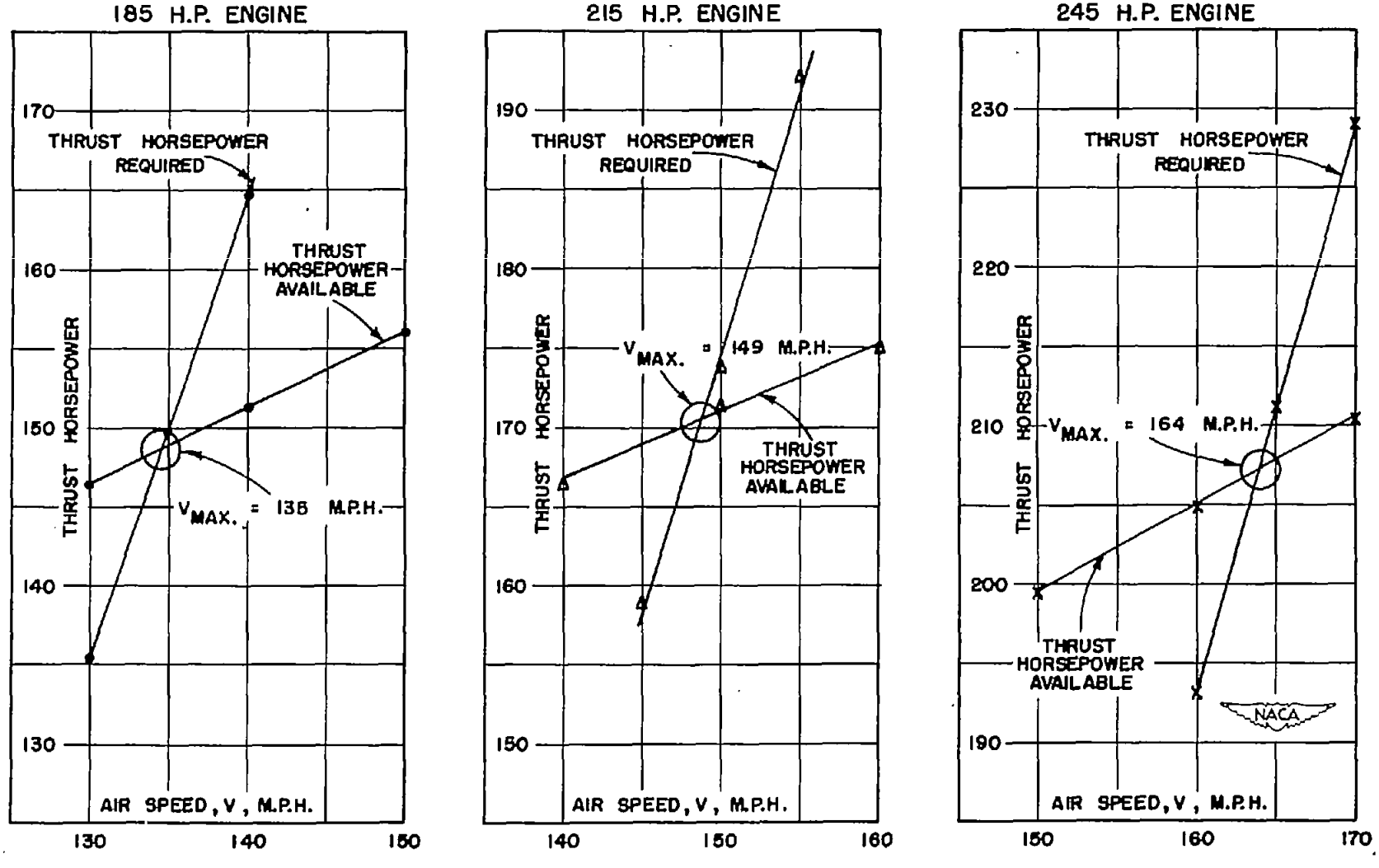

Figure 62.- Curves of power available and power required.

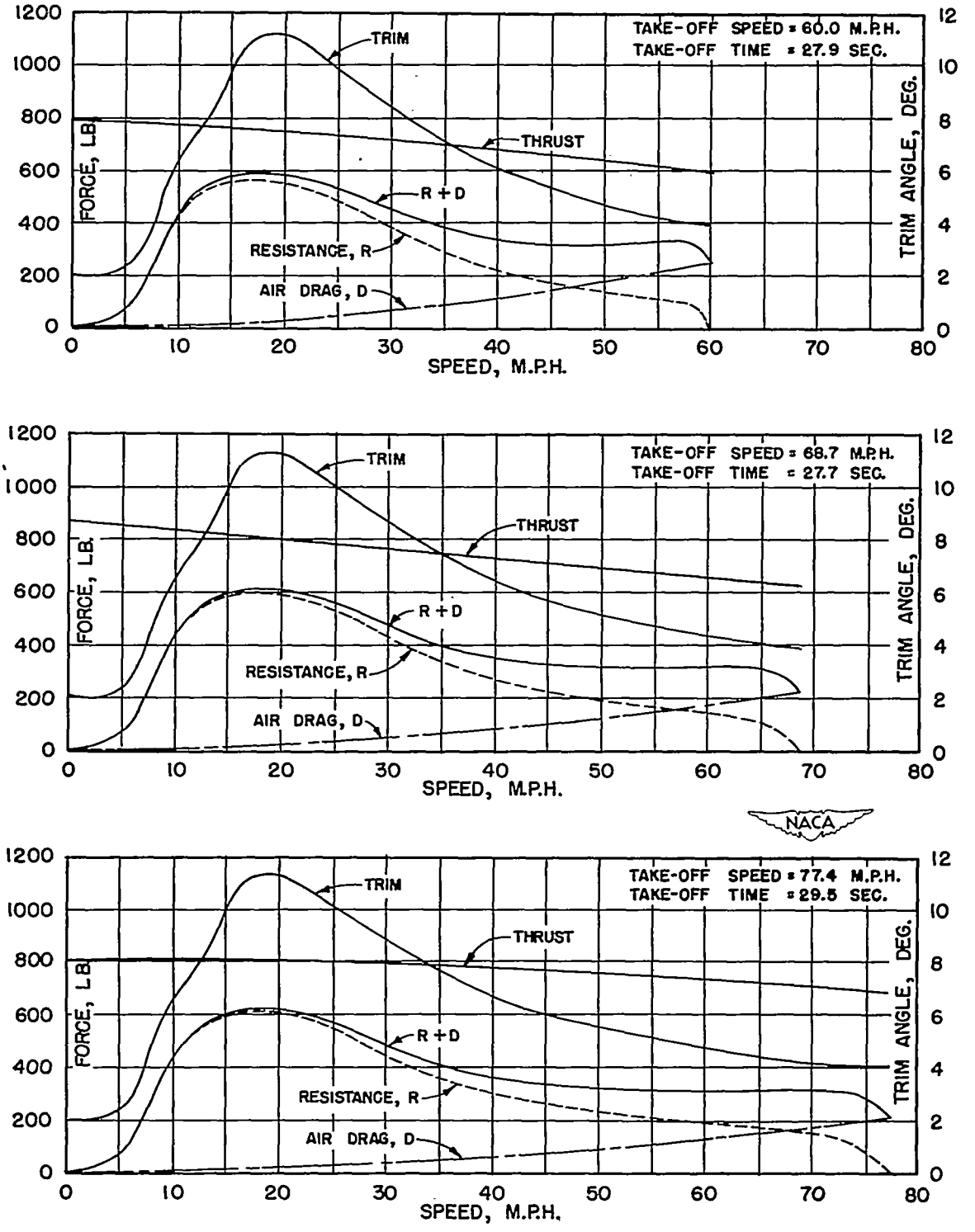

Figure 63.- Curves for determining take-off times of short-afterbody hull. Model no. 1056-02; gross weight, 3000 pounds.

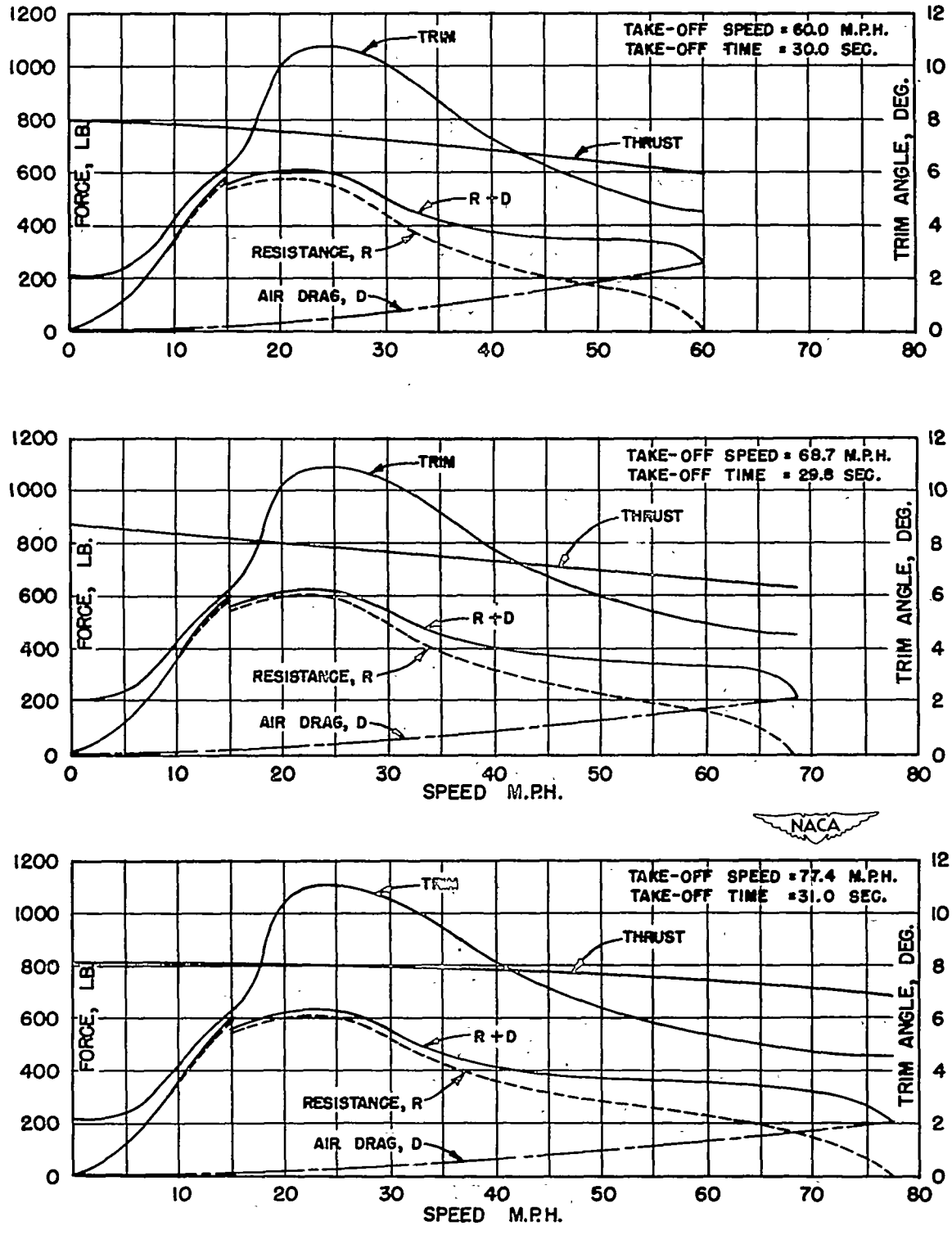

Figure 64.- Curves for determining take-off times of medium-afterbody hull. Model no. 1024-01; gross weight, 3000 pounds.

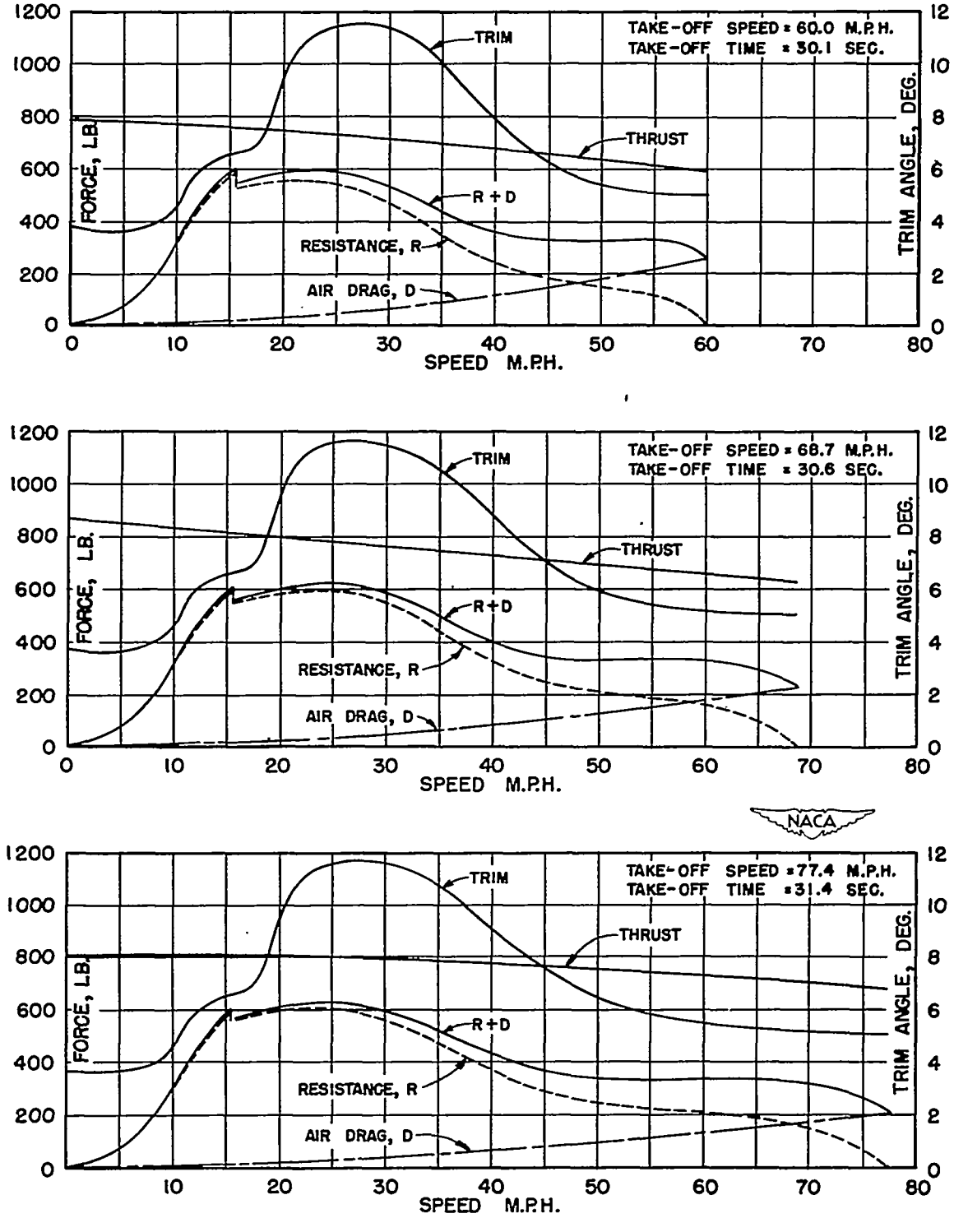

Figure 65.- Curves for determining take-off times of long-afterbody hull. Model no. 1057-03; gross weight, 3000 pounds.

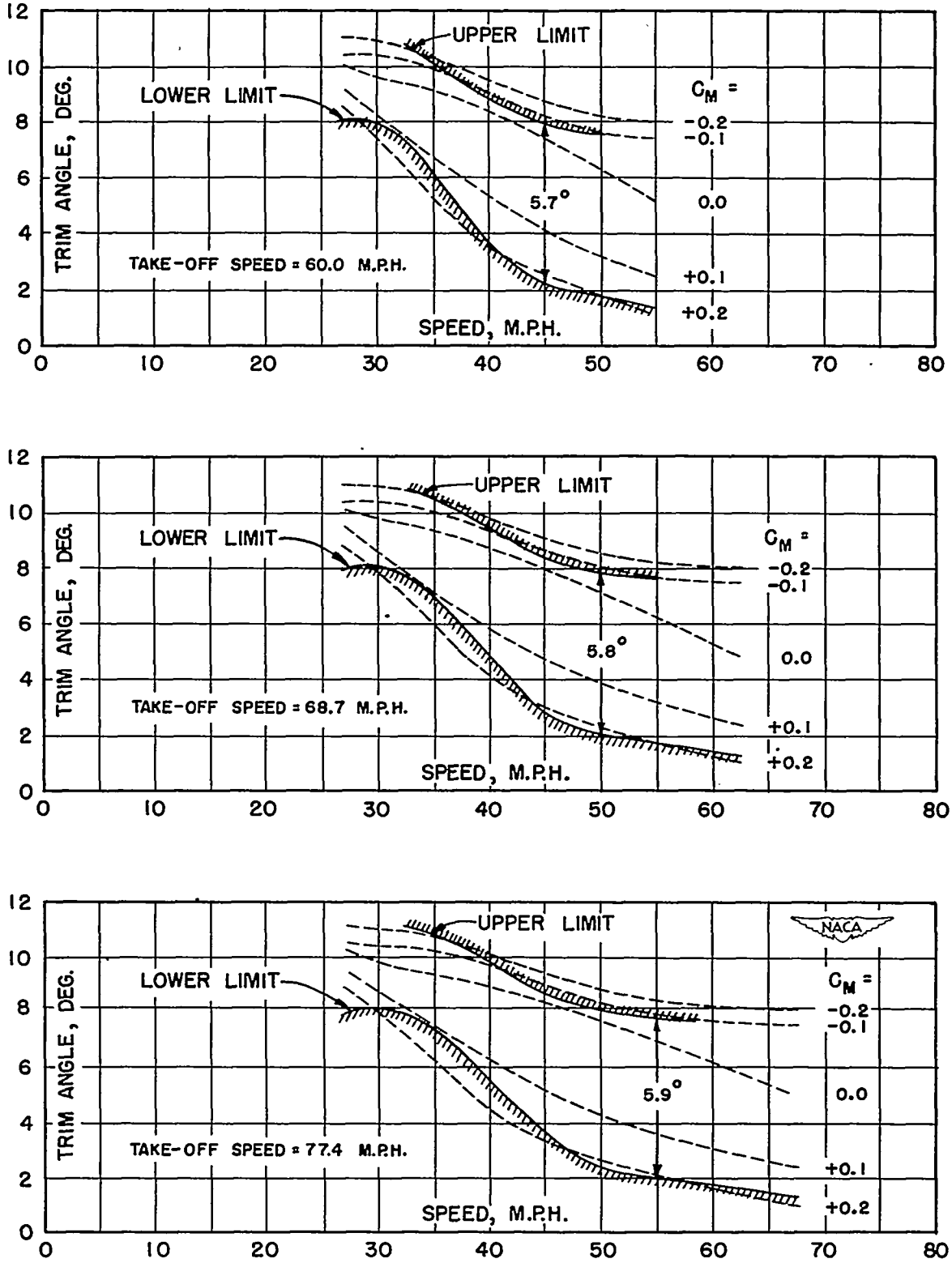

Figure 66.- Longitudinal stability characteristics of short-afterbody hull. Model no. 1056-02; gross weight, 3000 pounds.

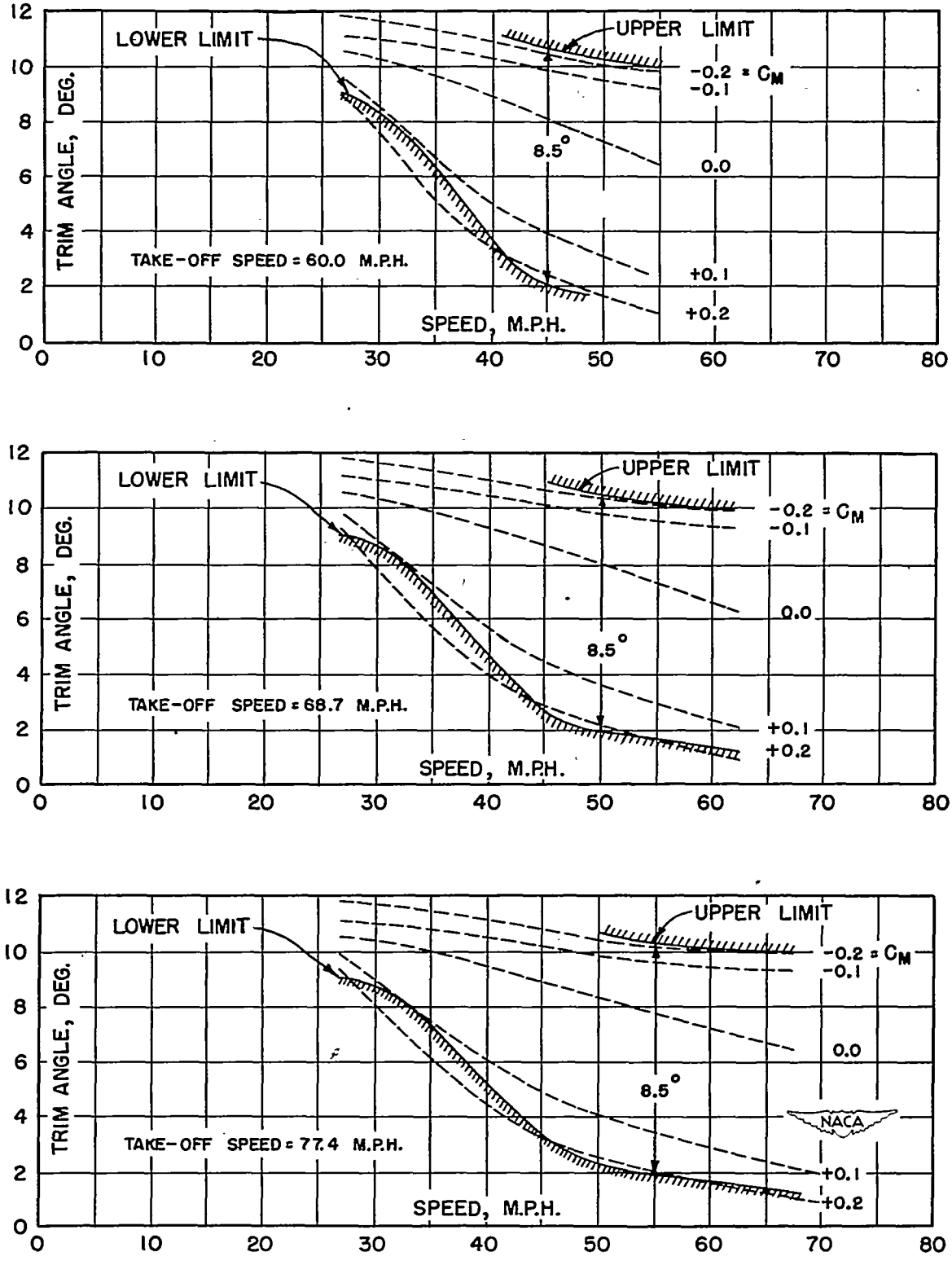

Figure 67.- Longitudinal stability characteristics of medium-afterbody hull. Model no. 1024-01; gross weight, 3000 pounds.

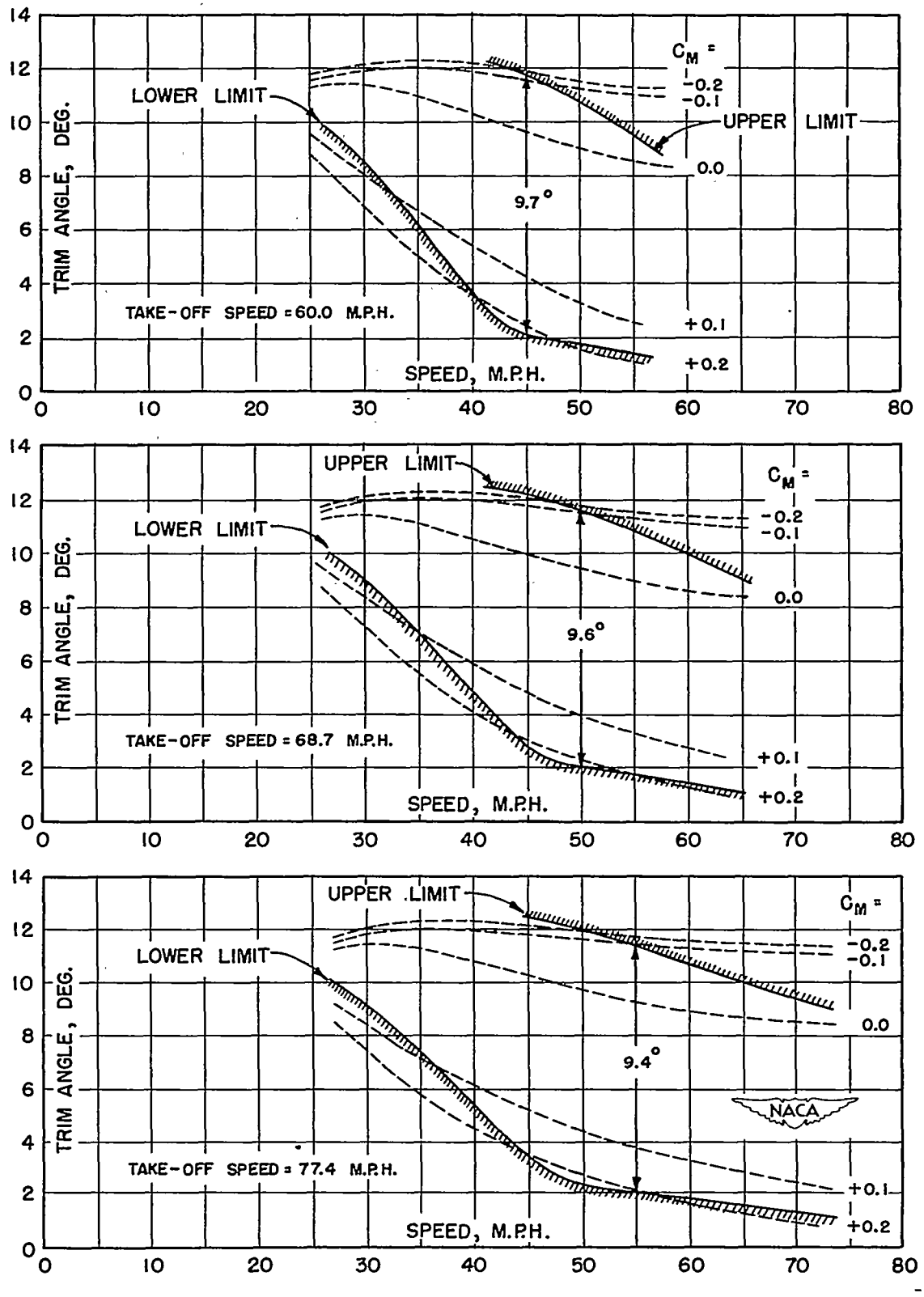

Figure 68.- Longitudinal stability characteristics of long-afterbody hull. Model no. 1057-03; gross weight, 3000 pounds.

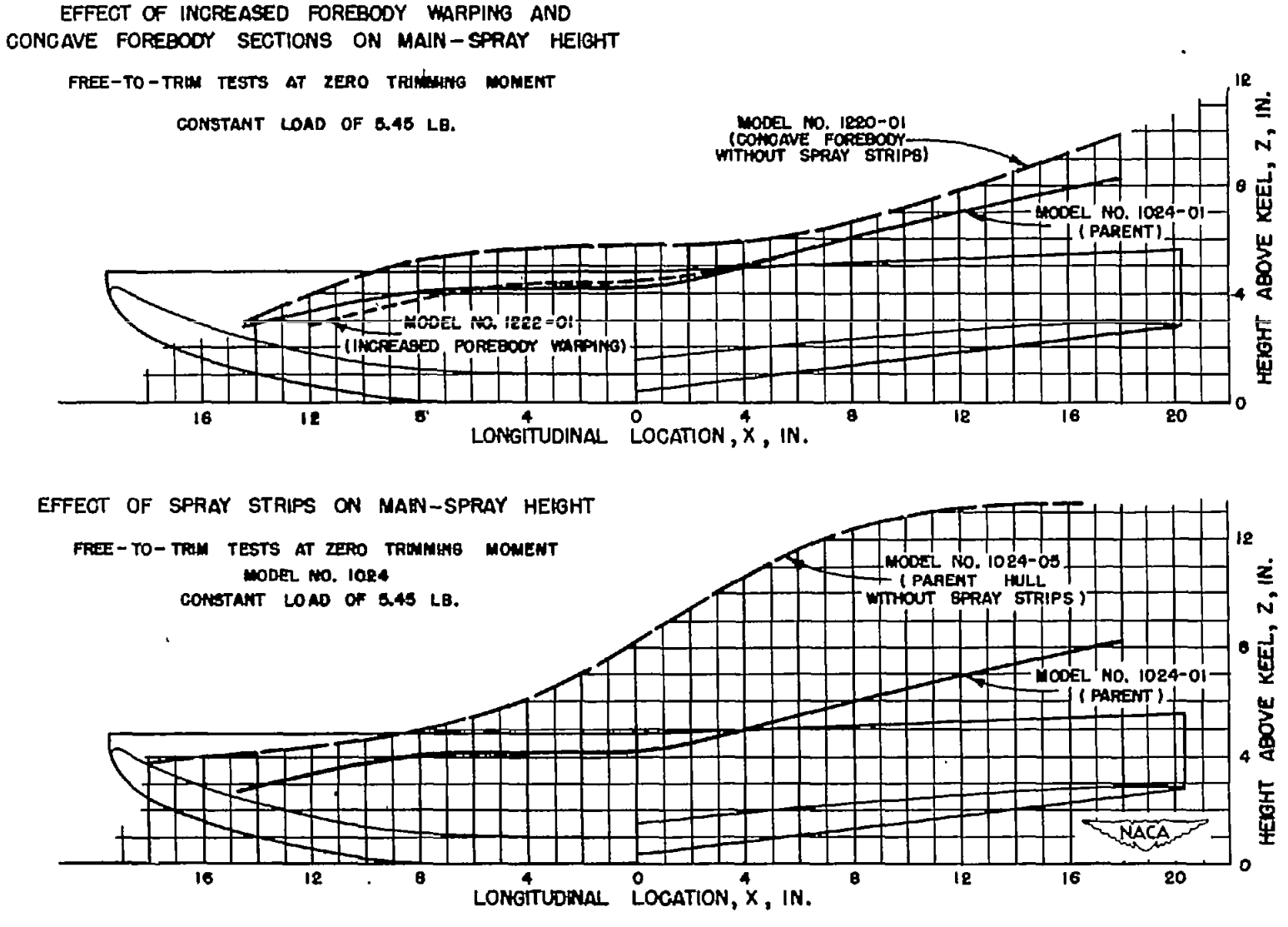

Figure 69.- Effect of various factors on main-spray height.

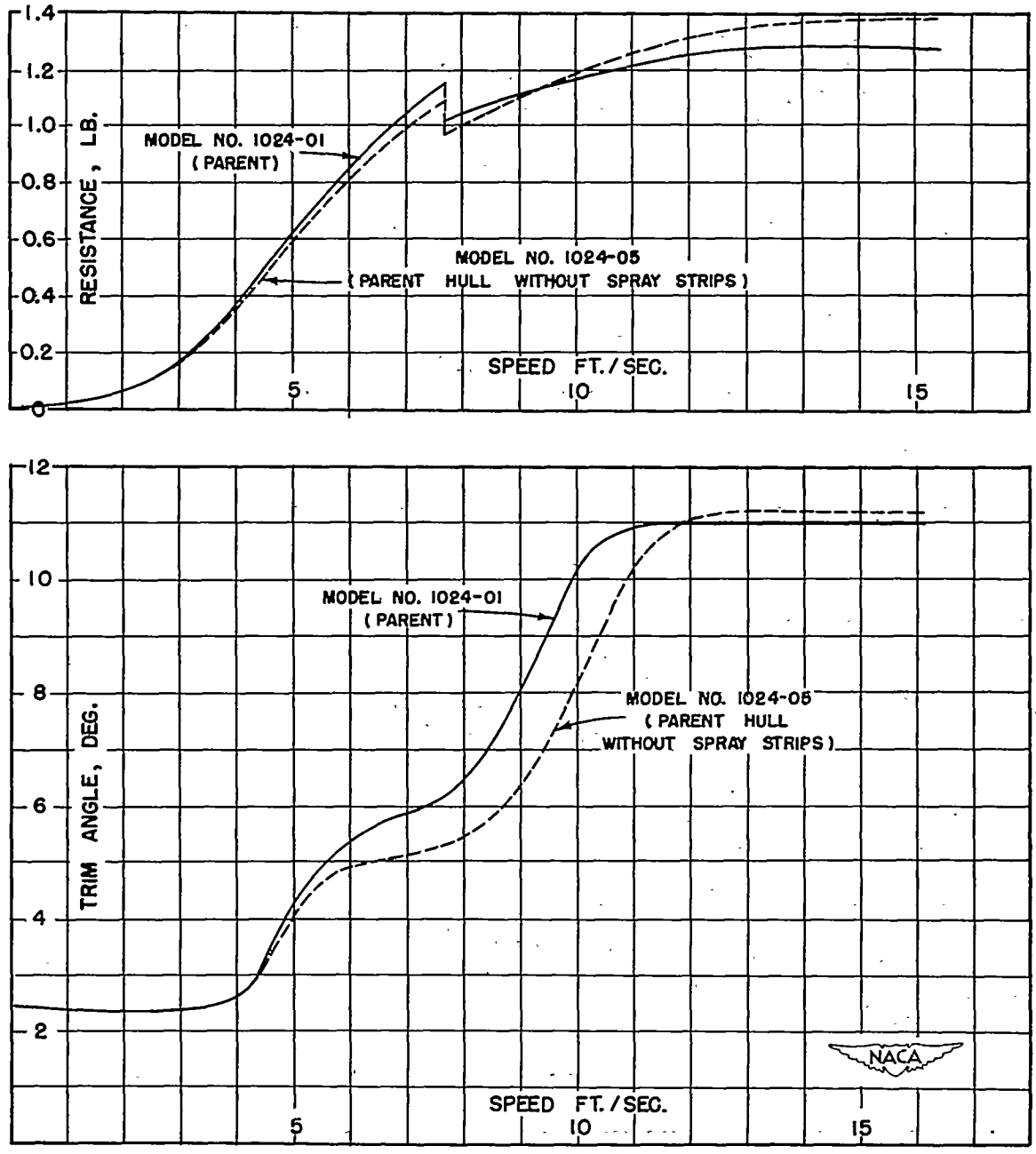

Figure 70.- Effect of spray strips on resistance and trim in displacement speed range. Free-to-trim tests at zero trimming moment of model no. 1024 with a constant load of 5.45 pounds.

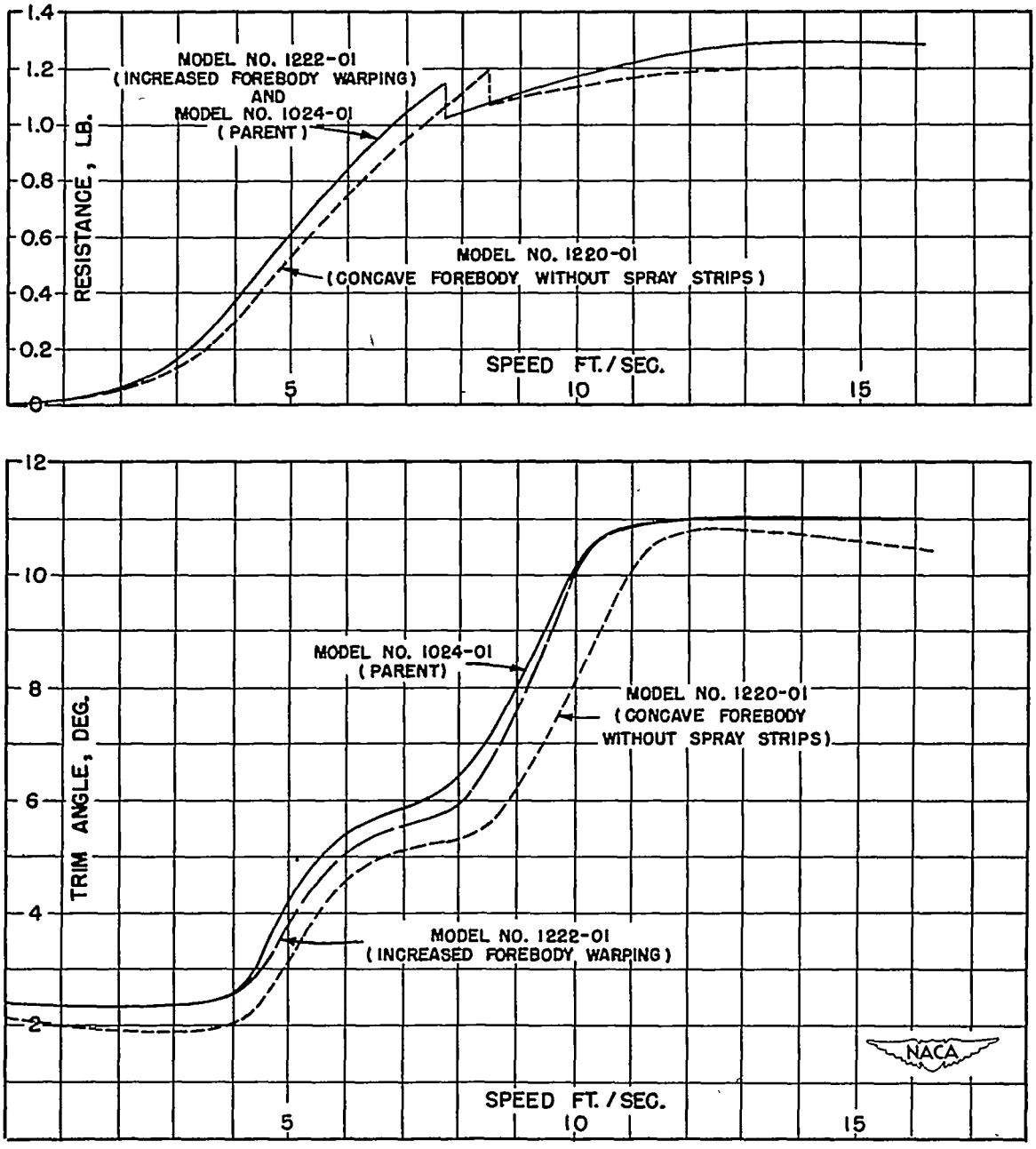

Figure 71.- Effect of increased forebody warping and concave forebody sections on resistance and trim in displacement range. Free-to-trim tests at zero trimming moment with a constant load of 5.45 pounds.

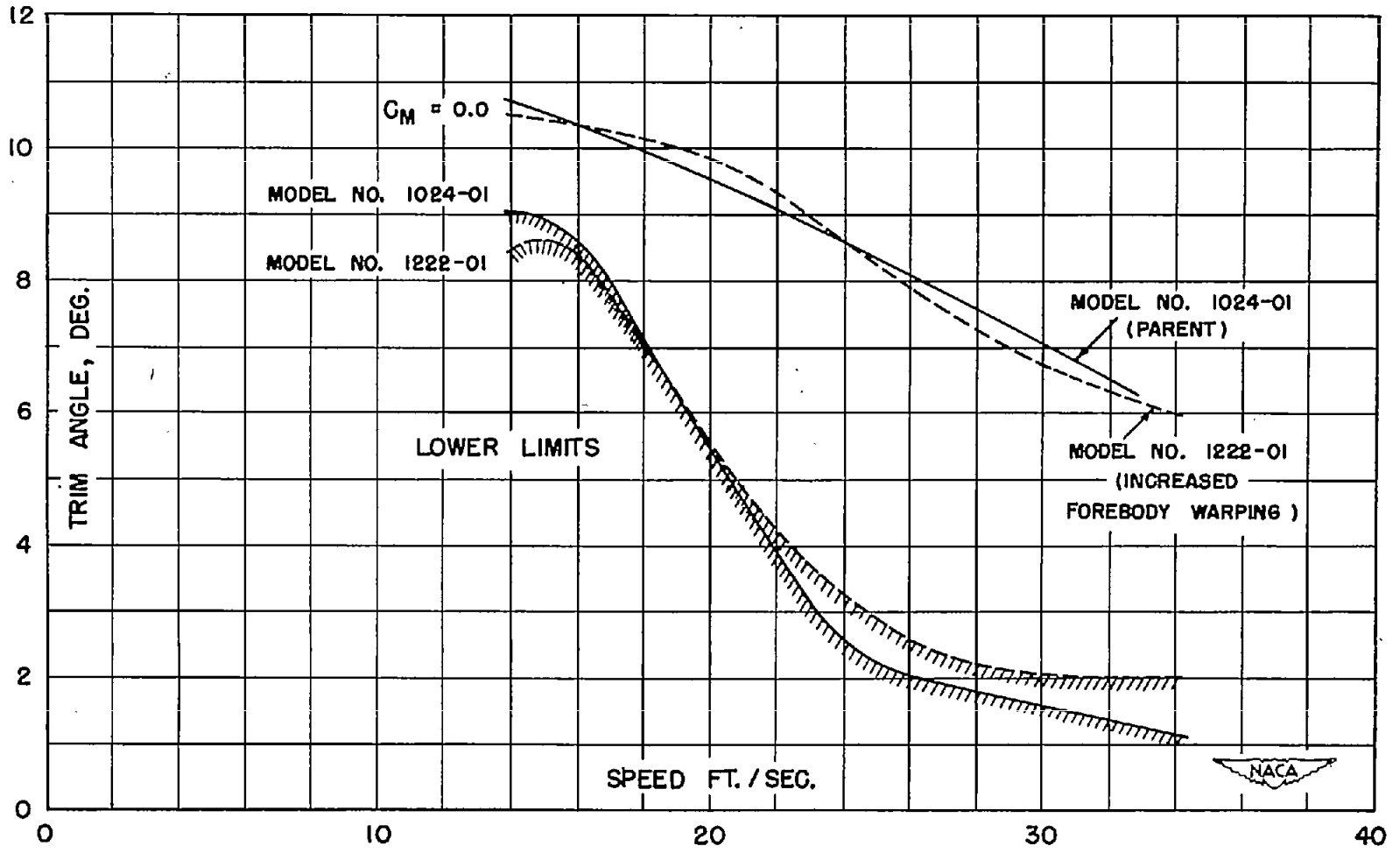

Figure 72.- Effect of increased forebody warping on lower trim limit of stability. Initial load, 5.86 pounds.

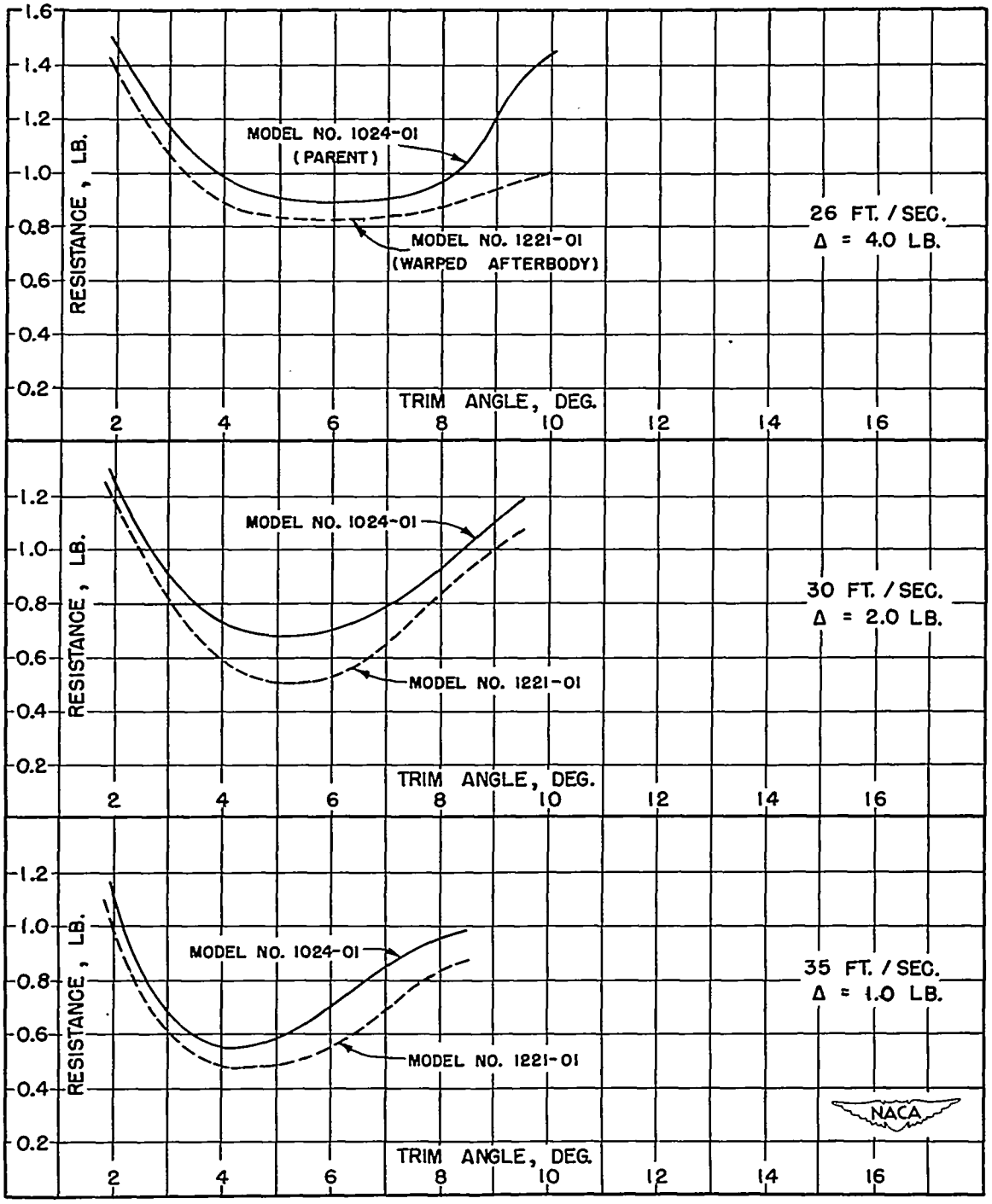

Figure 73.- Effect of afterbody dead-rise warping on high-speed resistance characteristics. Fixed-trim test; model no. 1024-01, sternpost angle, 8.0°; model no. 1221-01, sternpost angle, 7.5°.

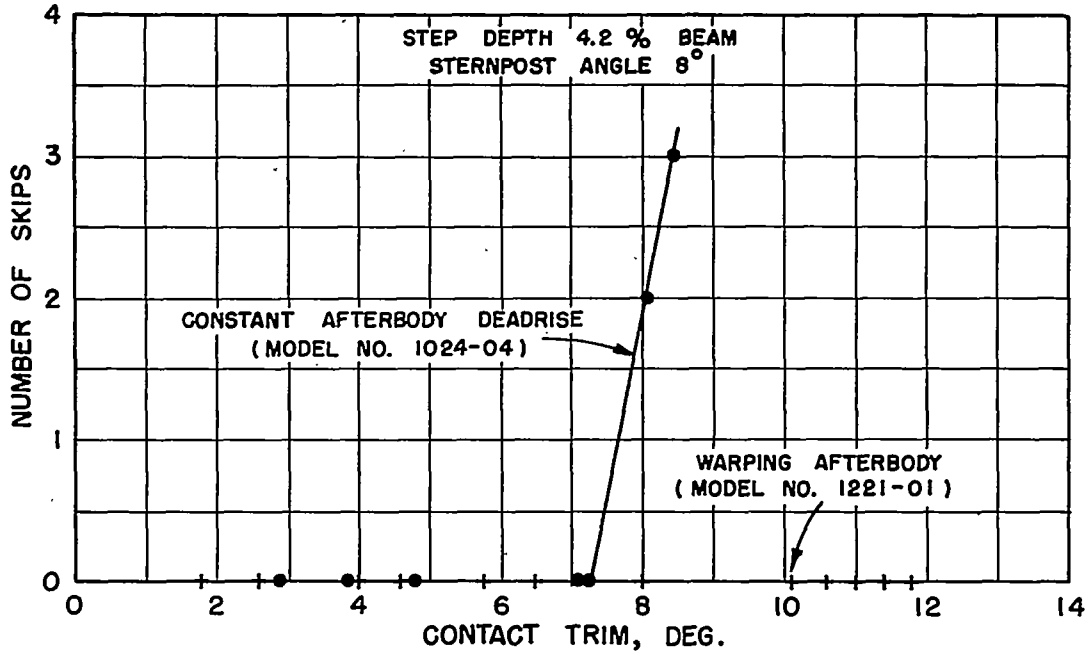

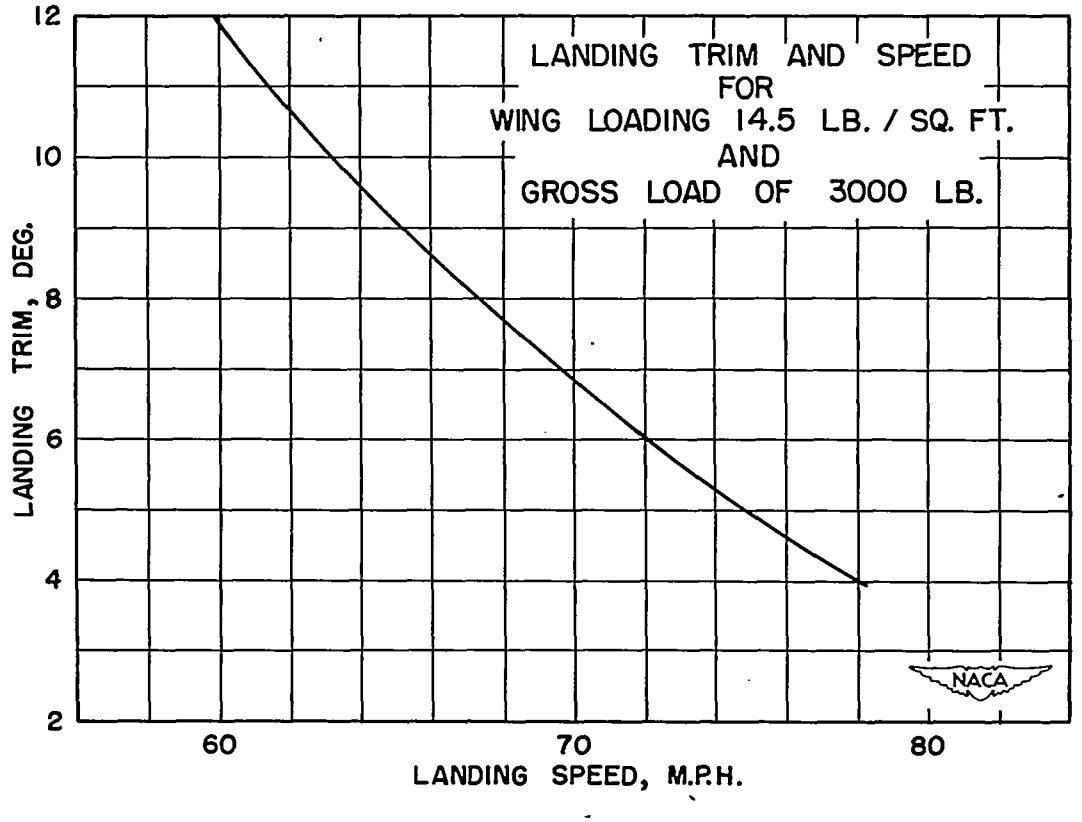

Figure 74.- Effect of afterbody dead-rise warping on number of skips encountered on landing. Gross weight, 3000 pounds; wing loading, 14.5 pounds per square foot.

UNDERWATER PHOTOGRAPH OF FOREBODY AND AFTERBODY WETTED AREA

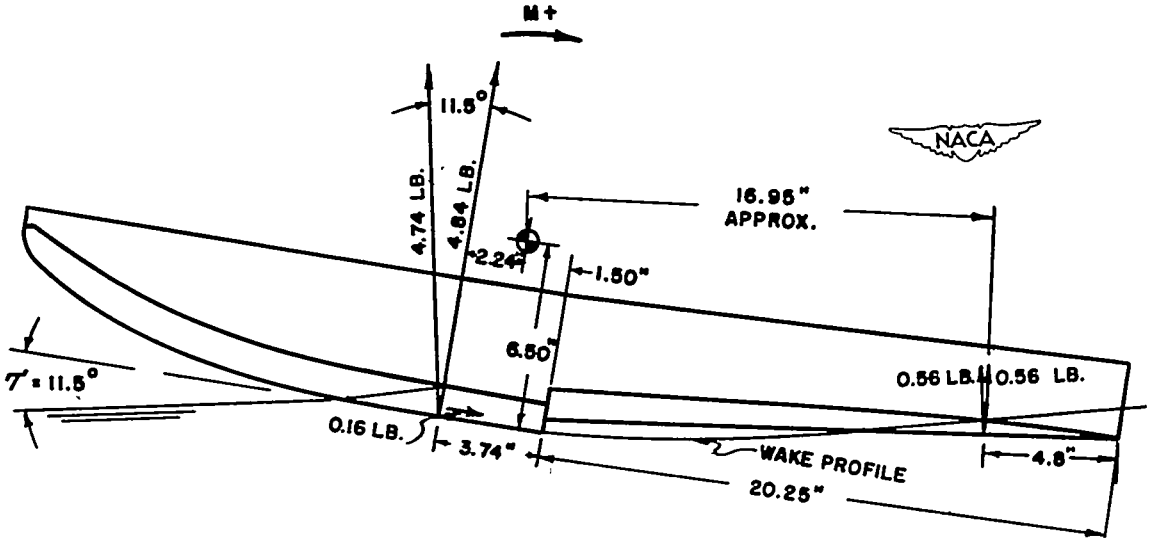

Figure 75.- Forces on a flying-boat hull model in two-step planing. Model no. 1024-05 (parent with forebody spray strips removed). Actual test conditions: load, 5.33 pounds; speed, 12 feet per second; and trim, 11.5°.

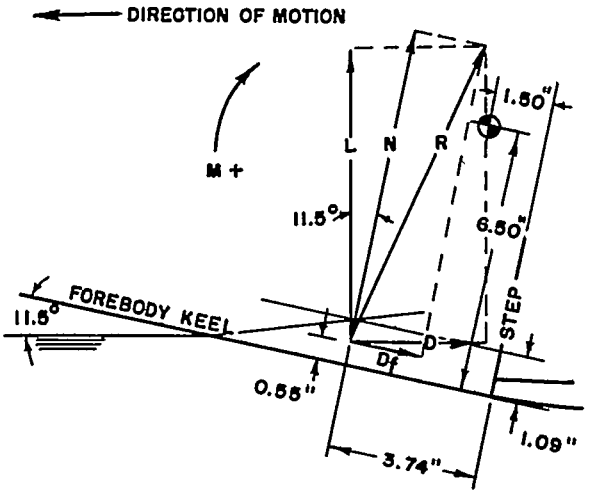

FORCE DIAGRAM FOR FOREBODY

Forebody:

L = 4.74 lb. (reference 18)

$N = \frac{4.74}{\cos 11.5^\circ} = 4.84$ lb. (approx.)

$D_f = 0.16$ lb. (reference 18)

$N = \frac{4.74 + 0.16 \sin 11.5^\circ}{\cos 11.5^\circ} = 4.87$ (actual)

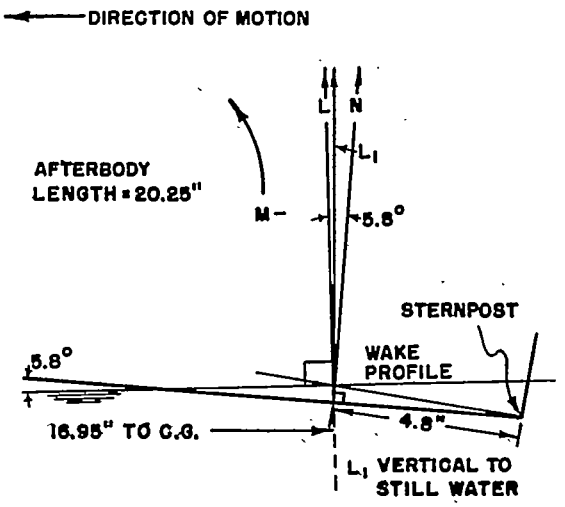

FORCE DIAGRAM FOR AFTERBODY

Afterbody:

L = 0.56 lb. (reference 18)

$L_1 \approx L$

$N = \frac{0.56}{\cos 5.8^\circ} = 0.56$ lb. (approx.)

D_f = negligible

Because angles concerned are small, moment arm ≈ 20.25 + 1.50 − 4.8 = 16.95 in.

Moment due to forebody forces = 4.87 x 2.24 − 0.16 x 5.95 = 9.96 in.lb.

Moment due to afterbody forces = −0.56 x 16.95 = −9.49 in.lb.

Lift on forebody = 4.74 lb.
Lift on afterbody = .56 lb.
Total = 5.30 lb.

Figure 76.- Forces and moments on a flying-boat hull model in two-step planing. Model no. 1024-05 (parent with forebody spray strips removed). Actual test conditions: Load, 5.33 pounds; speed, 12 feet per second; trim, 11.5°.

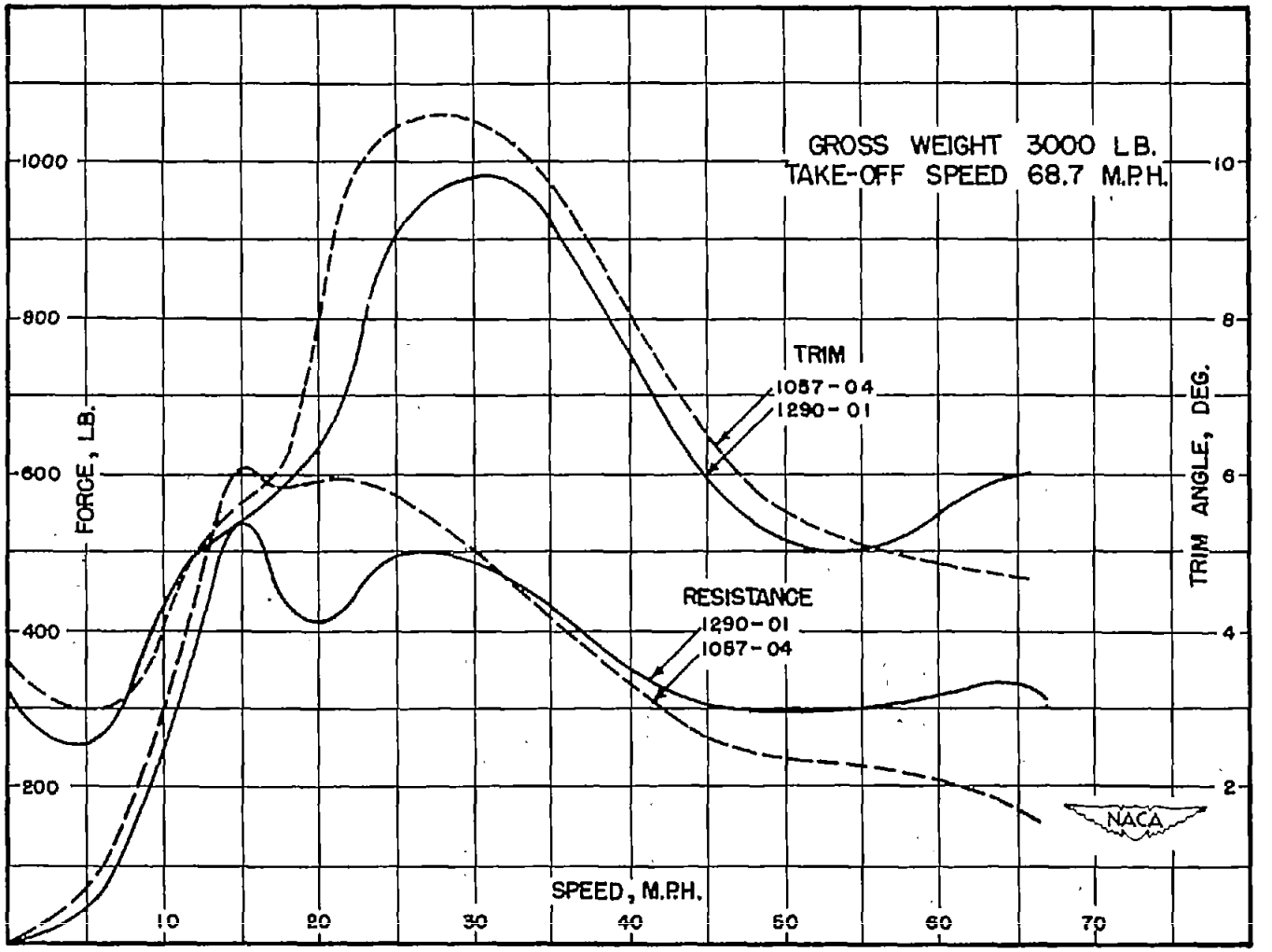

Figure 86.- Comparison of trim and resistance characteristics of NACA 40BE design (model no. 1290-01) and E.T.T. design (model no. 1057-04).

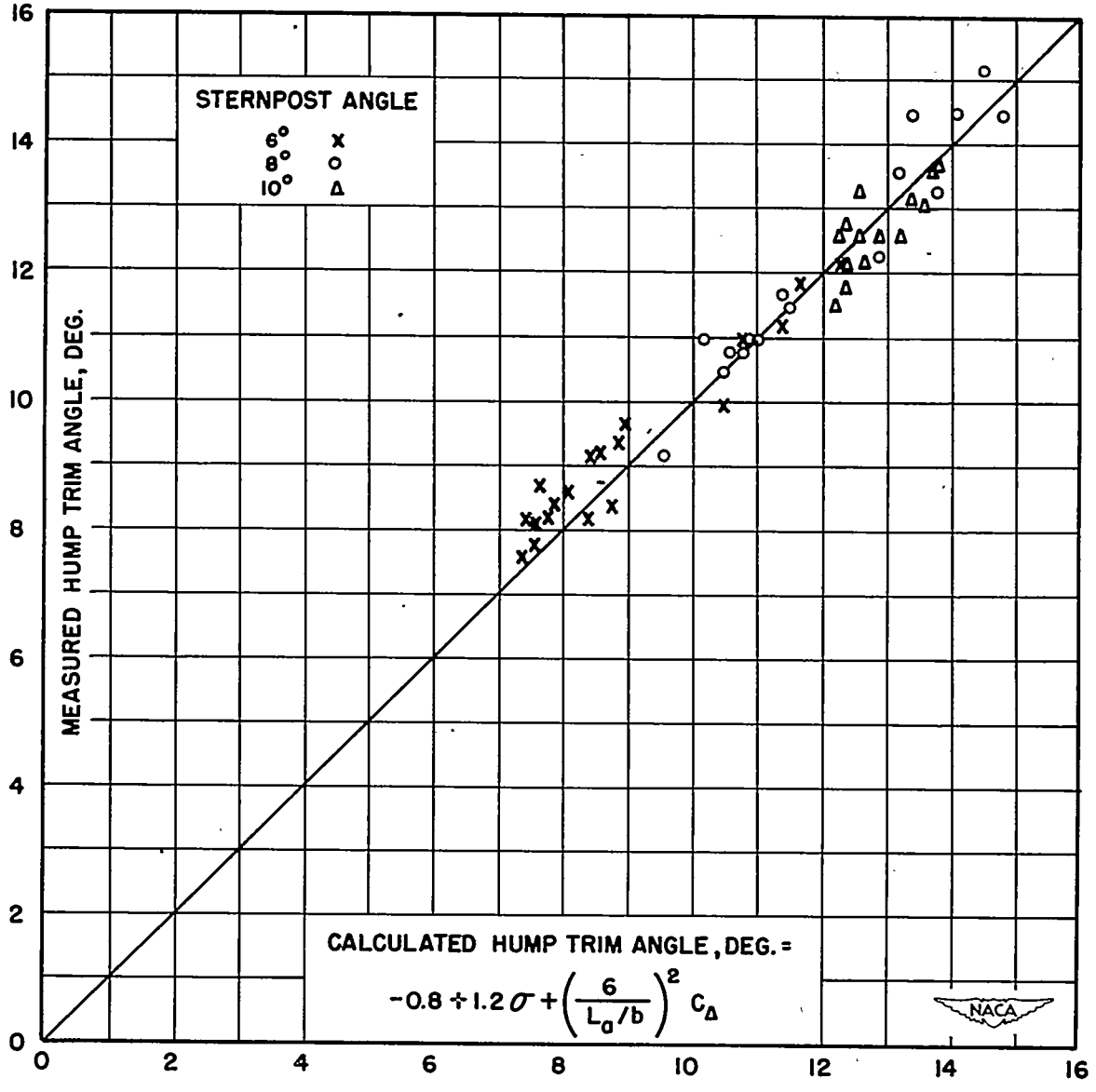

Figure 77.- Comparison of measured and calculated hump trim angle.

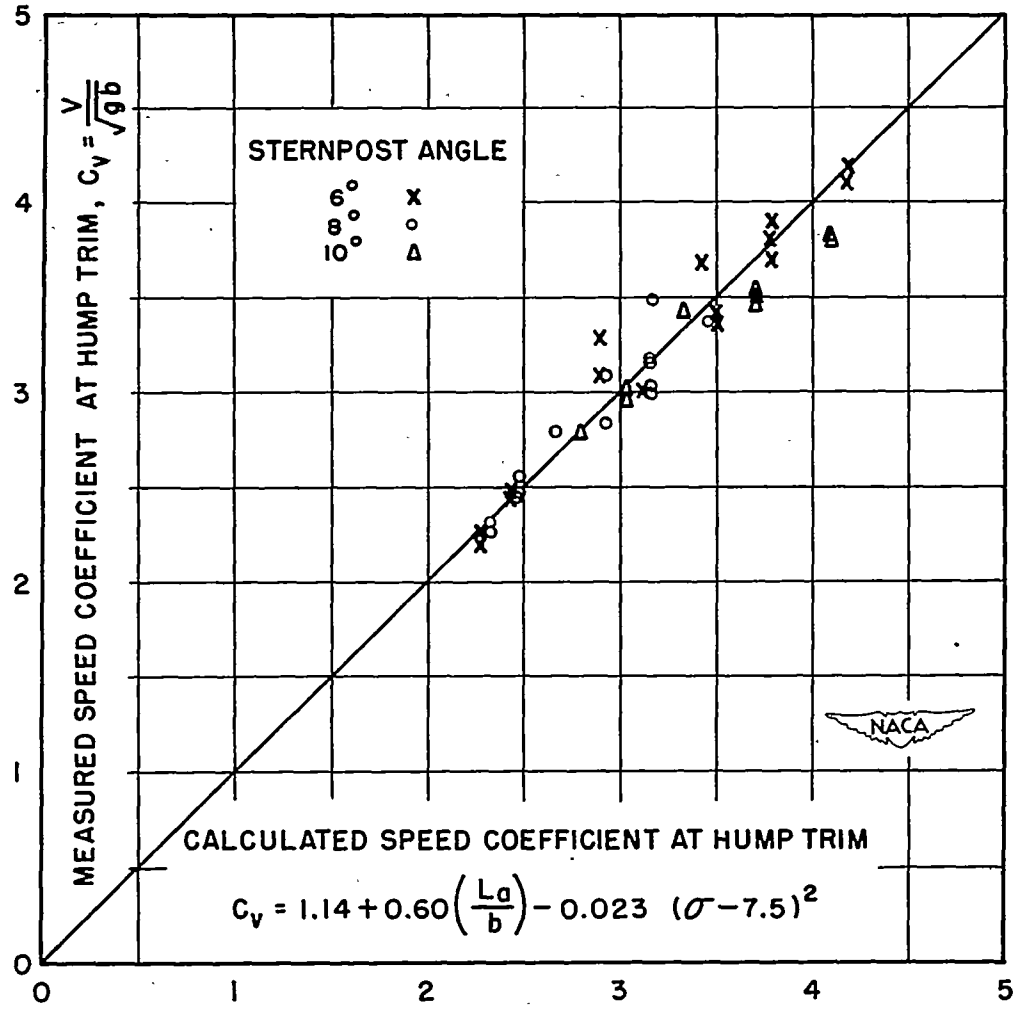

Figure 78.- Comparison of measured and calculated speed coefficient at hump trim angle.

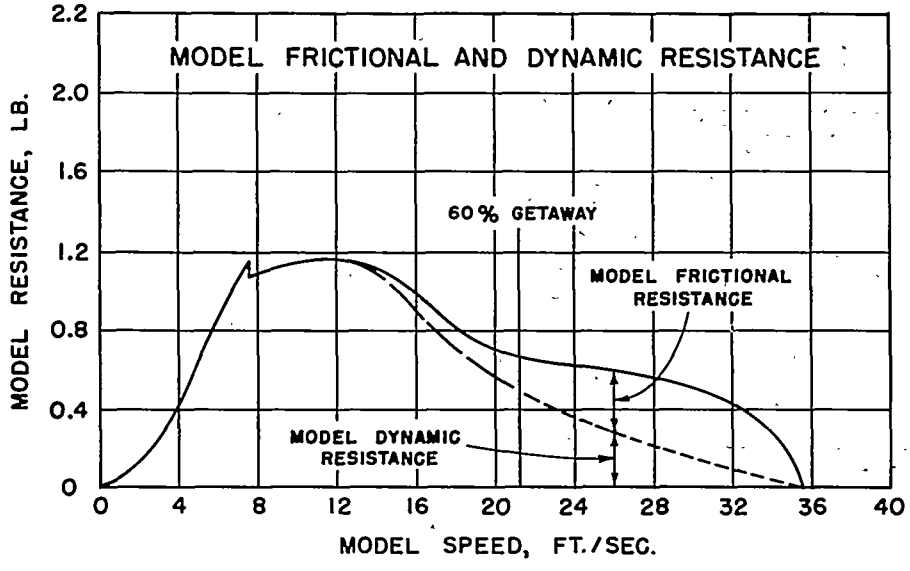

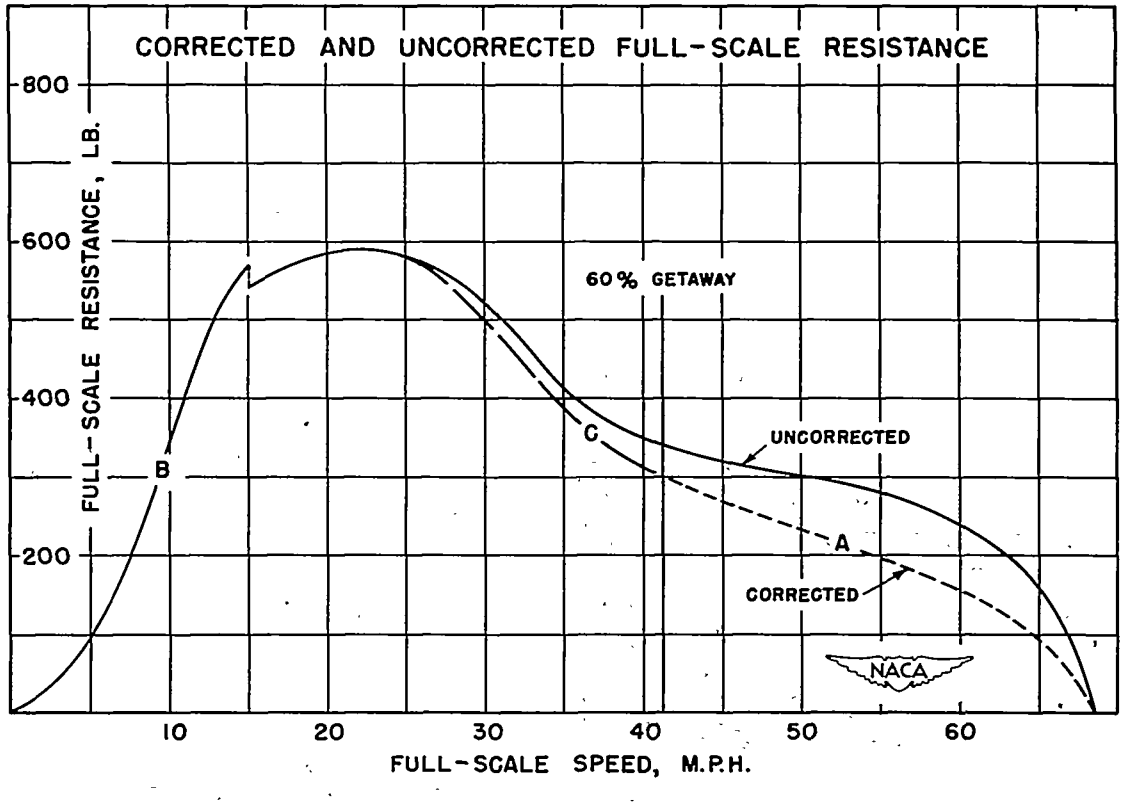

Figure 79.- Model and full-scale resistance.

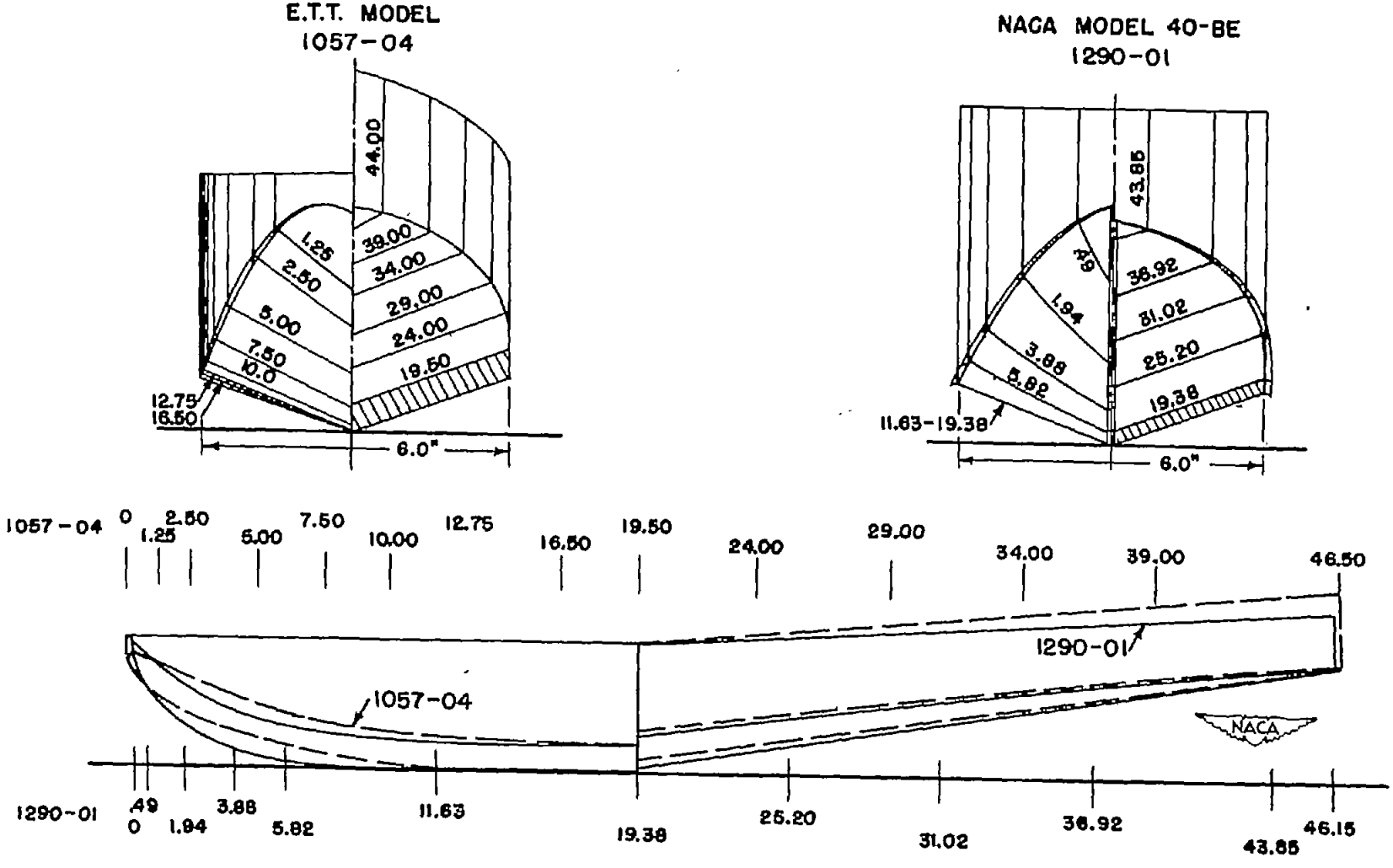

Figure 80.- Comparison of hull lines of NACA 40BE design (model no. 1290-01) and E.T.T. design (model no. 1057-04). Dimensions are in inches.

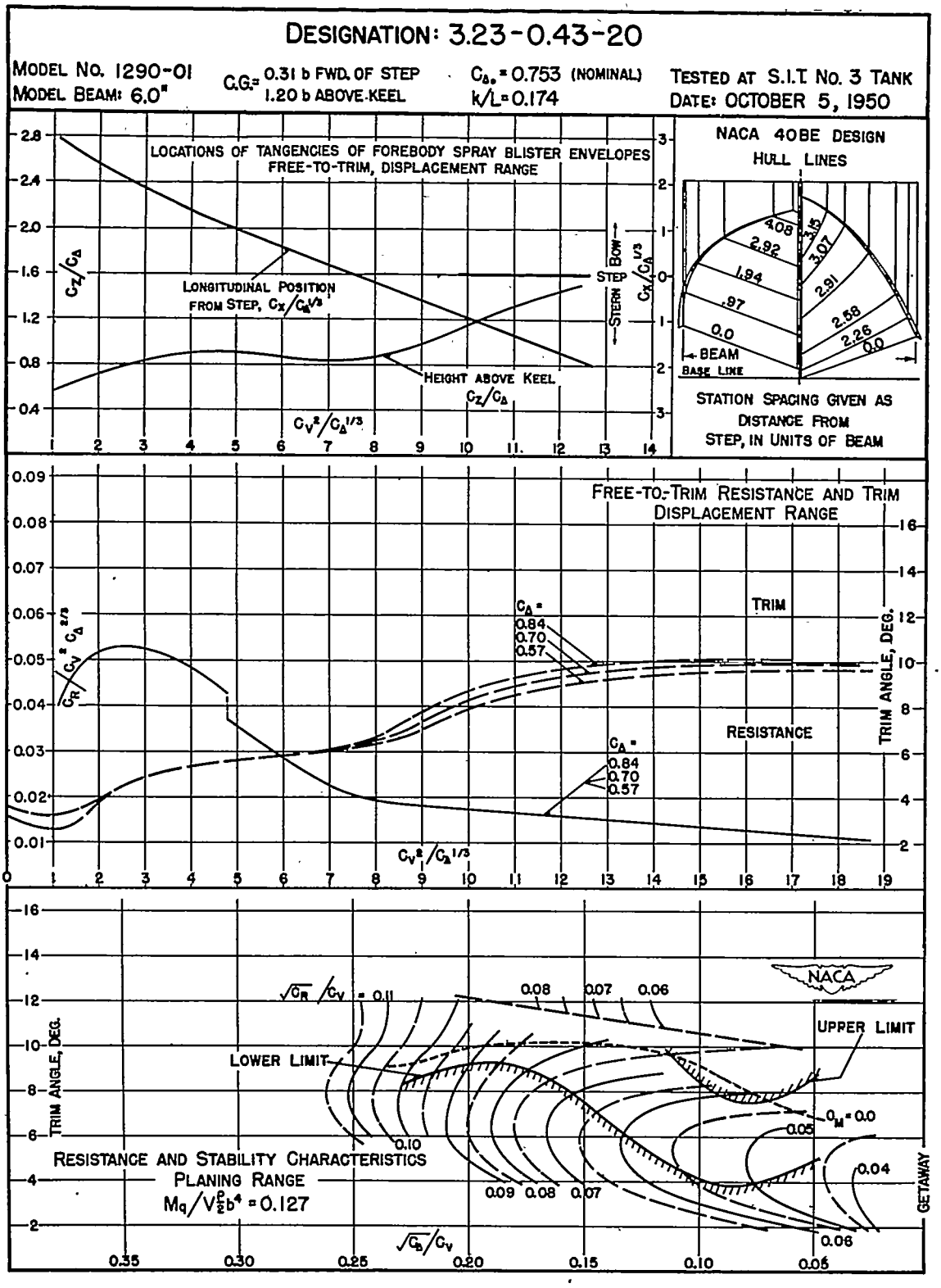
DESIGNATION: 3.23-0.43-20
MODEL NO. 1290-01
MODEL BEAM: 6.0"
C.G.= 0.31 b FWD. OF STEP
1.20 b ABOVE KEEL
C_{Δ_0} = 0.753 (NOMINAL)
k/L = 0.174
TESTED AT S.I.T. NO. 3 TANK
DATE: OCTOBER 5, 1950
LOCATIONS OF TANGENCIES OF FOREBODY SPRAY BLISTER ENVELOPES FREE-TO-TRIM, DISPLACEMENT RANGE
LONGITUDINAL POSITION FROM STEP, $C_x/C_\Delta^{1/3}$
HEIGHT ABOVE KEEL C_z/C_Δ
BOW
STEP
STERN
C_z/C_Δ
$C_x/C_\Delta^{1/3}$
$C_V^2/C_\Delta^{1/3}$
NACA 40BE DESIGN HULL LINES
4.08
3.45
3.07
2.92
2.91
1.94
.97
0.0
2.58
2.26
0.0
BEAM
BASE LINE
STATION SPACING GIVEN AS DISTANCE FROM STEP, IN UNITS OF BEAM
FREE-TO-TRIM RESISTANCE AND TRIM DISPLACEMENT RANGE
$C_R/C_V^2 C_\Delta^{2/3}$
C_Δ = 0.84 0.70 0.57
TRIM
RESISTANCE
TRIM ANGLE, DEG.
$C_V^2/C_\Delta^{1/3}$
RESISTANCE AND STABILITY CHARACTERISTICS
PLANING RANGE
$Mq/V\frac{\rho}{2}b^4 = 0.127$
$\sqrt{C_R}/C_V$ = 0.11
0.08 0.07 0.06
NACA
UPPER LIMIT
LOWER LIMIT
0_M = 0.0
0.05
0.04
0.10
0.09 0.08 0.07
0.06
GETAWAY
TRIM ANGLE, DEG.
$\sqrt{C_B}/C_V$

Figure 81.

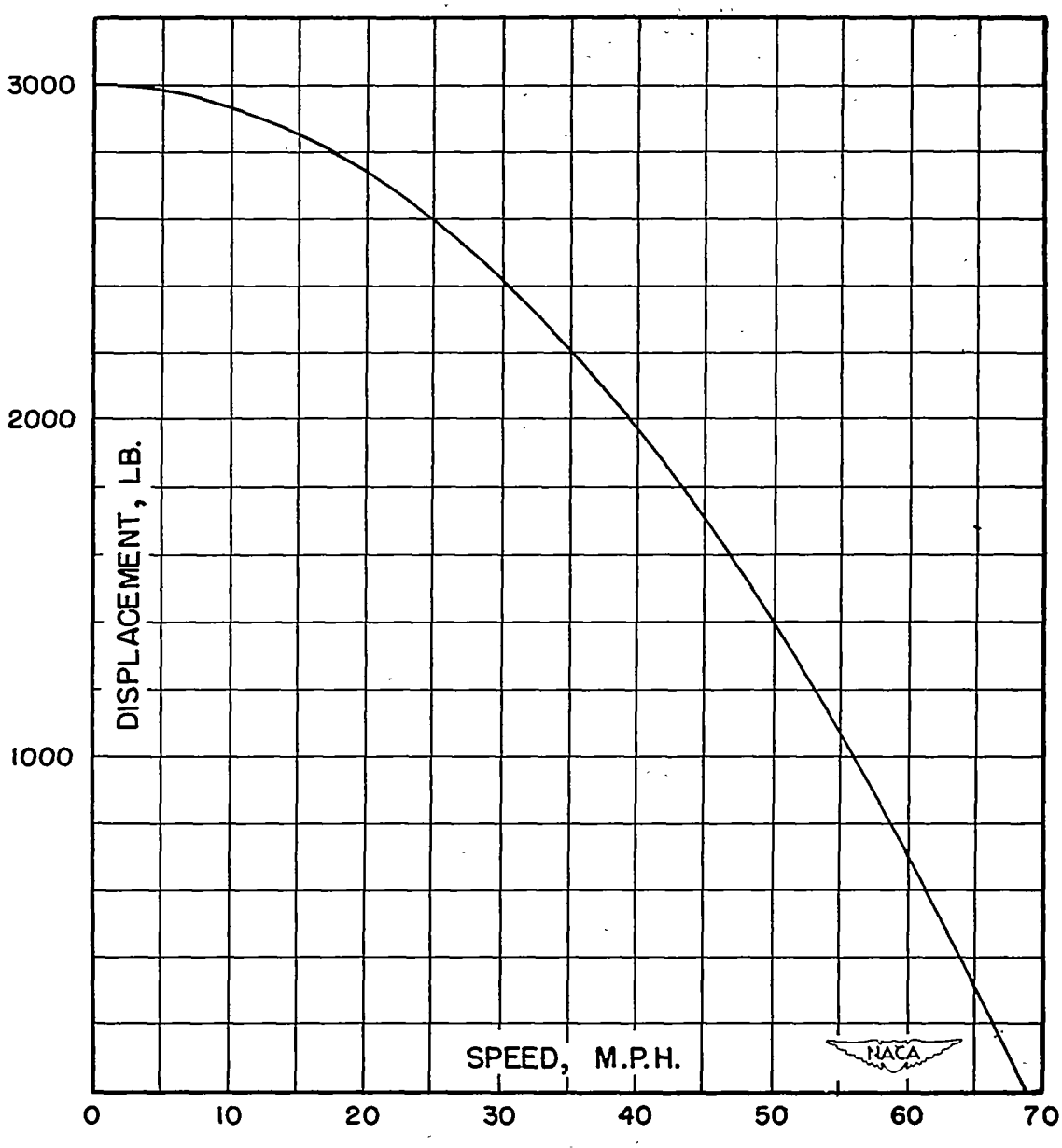

Figure 82.- Load fall-off curve for comparison of NACA 40BE design (model no. 1290-01) and E.T.T. design (model no. 1057-04).

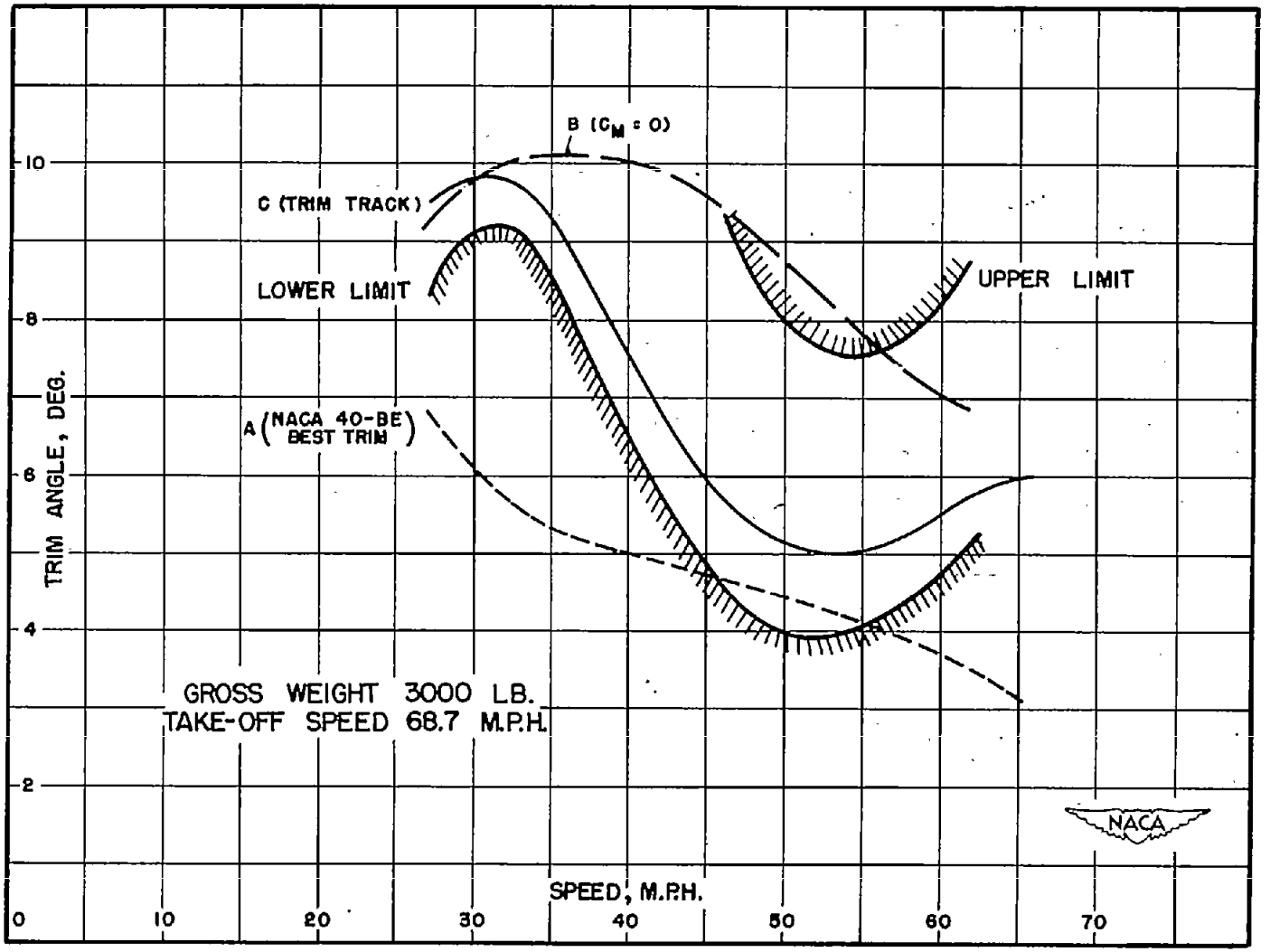

Figure 83.- Longitudinal stability characteristics of NACA 40BE design (E.T.T. model no. 1290-01).

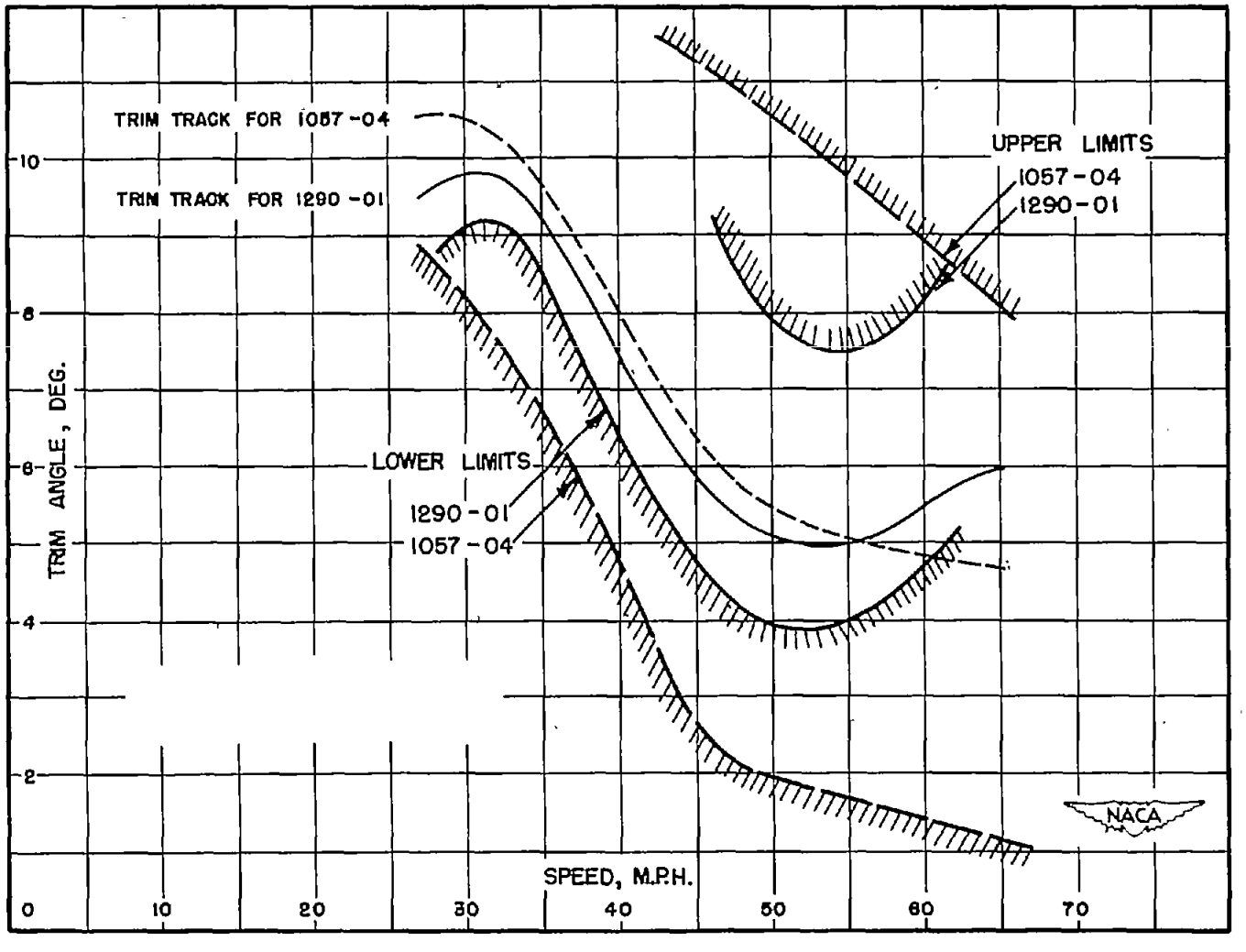

Figure 84.- Comparison of longitudinal stability characteristics of NACA 40BE design (model no. 1290-01) and E.T.T. design (model no. 1057-04).

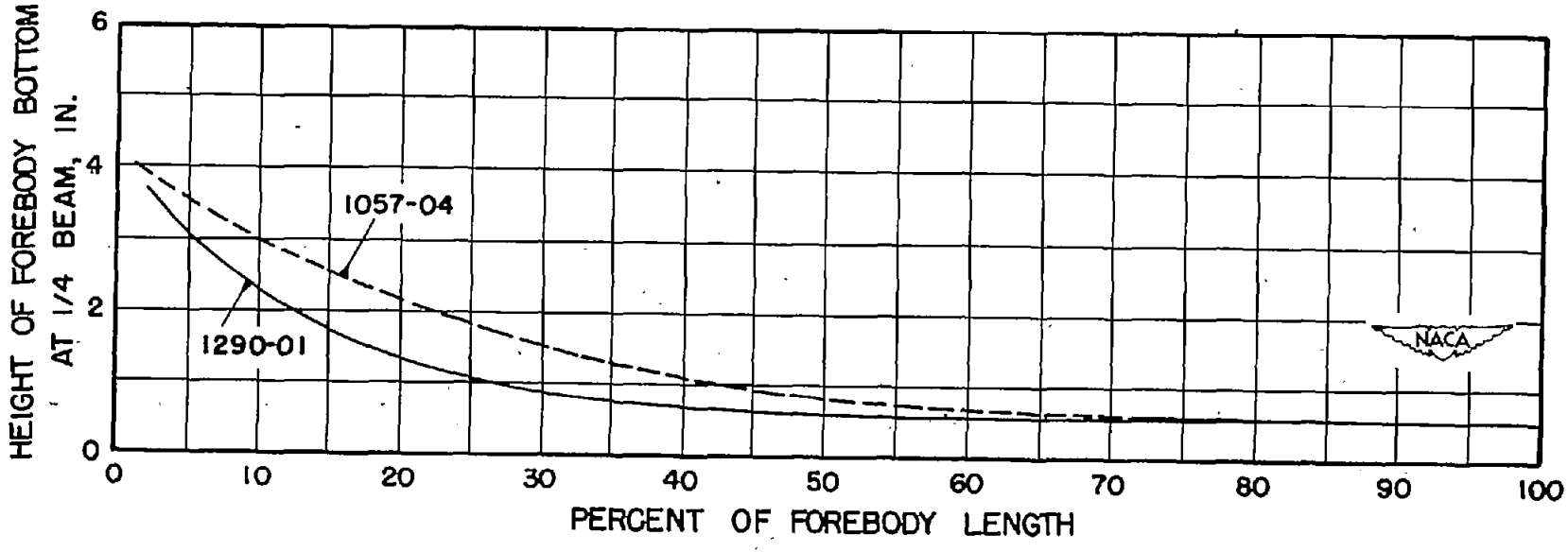

Figure 85.- Comparison of forebody-bottom heights of NACA 4OBE design (model no. 1290-01) and E.T.T. design (model no. 1057-04) at 1/4 beam width.

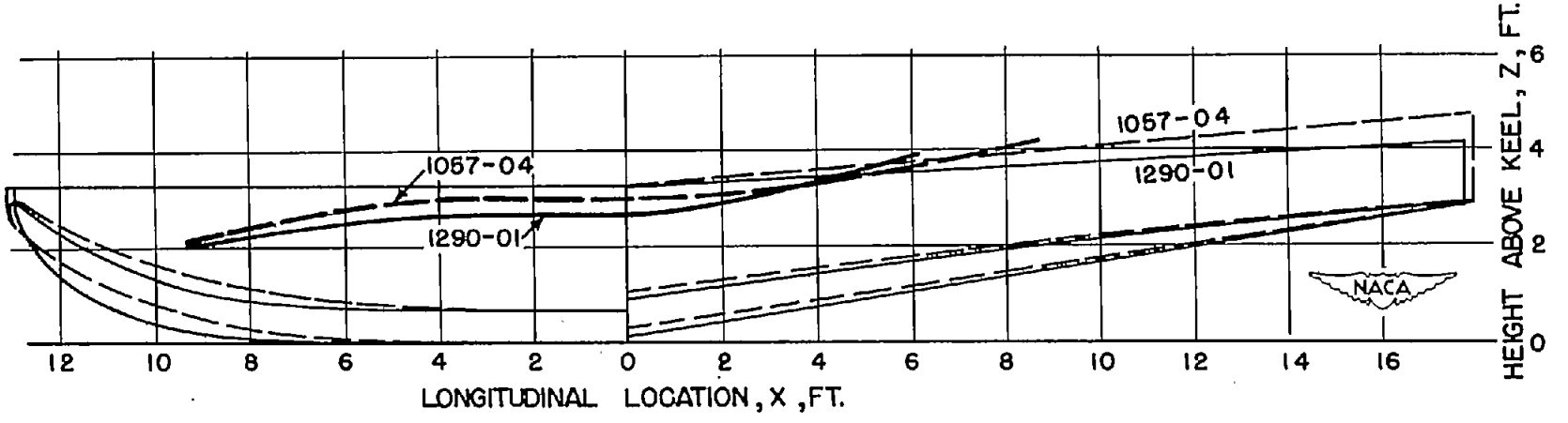

Figure 87.- Comparison of spray heights of NACA 4OBE design (model no. 1290-01) and E.T.T. design (model no. 1057-04). Gross weight, 3000 pounds; take-off speed, 68.7 miles per hour.